N71-17259

NASA CR-72805

DEVELOPMENT OF A
NON-MAGNETIC, STABLE, CADMIUM ELECTRODE
FOR SILVER-CADMIUM CELLS

by

S. Lerner and S. Charlip

GULTON INDUSTRIES, INC.

Prepared For

NATIONAL AERONAUTICS AND SPACE ADMINISTRATION

NASA Lewis Research Center

CONTRACT NAS 3-11829

William J. Nagle, Project Manager

NOTICE

NASA CR-72805

FINAL REPORT

DEVELOPMENT OF A NON-MAGNETIC, STABLE, CADMIUM ELECTRODE FOR SILVER-CADMIUM CELLS

by

S. Lerner and S. Charlip

GULTON INDUSTRIES, INC.
Battery & Power Sources Division
212 Durham Avenue
Metuchen, N. J. 08840

Prepared For

NATIONAL AERONAUTICS AND SPACE ADMINISTRATION

January 31, 1971

CONTRACT NAS 3-11829

NASA Lewis Research Center
Cleveland, Ohio
William J. Nagle, Project Manager
Space Power Systems Division

FOREWORD

The work described herein, which was conducted by the Gulton Industries Battery & Power Sources Division, was performed under NASA contract NAS 3-11829 with Mr. W. Nagle, of NASA/Lewis Research Center, as Project Manager.

The authors wish to acknowledge their gratitude to Dr. R. Bolton and Mr. R. Casciano, of Gulton Industries Microceramics Division, for their help in performing the particle size measurements.

DEVELOPMENT OF A NON-MAGNETIC, STABLE, CADMIUM ELECTRODE FOR SILVER-CADMIUM CELLS

by

S. Lerner and S. Charlip

ABSTRACT

The objectives of this program were the development of a non-magnetic, cadmium electrode, which has stable capacity features during cycling, for use in a silver-cadmium cell.

Several fabricating techniques were used including pasting, pressing, and impregnating cadmium salts into sintered silver plaques. The raw materials under investigation were commercial cadmium oxide and Gulton produced cadmium hydroxide. The electrode combination which gave the best results was a compound of teflon and cadmium hydroxide which had been heat cured and pressed onto a silver screen. Initial utilization of these electrodes, on early cycles, yielded better than 80% of theoretical capacity. This utilization stabilized to approximately 65% on continued cycling. This value compares with less than 40% for cadmium electrodes presently in use in the silver-cadmium system.

Silver-cadmium cells, of 5 Ah capacity, were fabricated from the teflonated cadmium hydroxide electrodes and placed on a cycling regime of 24 hour orbit (22.8 hour charge and 1.2 hour discharge) at 50% depth of discharge. Ten cells have completed an average of 362 cycles (five at 342 and five at 382) as of the end of the program.

TABLE OF CONTENTS

PAGE NO.

LIST OF TABLES

LIST OF FIGURES

LIST OF FIGURES - Continued

I. SUMMARY

The objectives of this program were the development of a non-magnetic, cadmium electrode which has stable capacity features during cycling, for use in a silver-cadmium cell.

Several fabricating techniques were used, including pasting, pressing, and impregnating cadmium salts into sintered silver plaques. The raw materials under investigation were commercial cadmium oxide and Gulton produced cadmium hydroxide.

Preliminary testing of these electrodes in negative limiting nickel-cadmium cells eliminated further evaluation of pasted electrodes, due to poor mechanical strength and difficulties in fabrication.

Further evaluation of electrodes in silver-cadmium cells showed that the $Cd(OH)_2$ impregnated sintered silver electrode was not a practical negative, since cells could not be made positive limiting and failed early in cycling due to severe silver migration.

The electrode combination which gave the best results was a compound of Teflon and cadmium hydroxide which had been heat cured and pressed onto a silver screen. Initial utilization of these electrodes, on early cycles, yielded better than 80% of theoretical capacity. This utilization stabilized to approximately 65% on continued cycling. This value compares with less than 40% for cadmium electrodes presently in use in the silver-cadmium system.

Silver-cadmium cells of 5 Ah capacity were fabricated from the teflonated cadmium hydroxide electrodes and placed on a cycling regime of 24 hour orbit (22.8 hour charge and 1.2 hour discharge) at 50% depth of discharge. Ten cells have completed an average of 362 cycles (five at 342 and five at 382) as of the end of the program.

II. INTRODUCTION

Silver-cadmium batteries have been successfully used in many aerospace applications. The silver-cadmium battery has an advantage over other batteries used in similar applications in its ability to deliver higher capacities per unit of weight. It has good cycle life capabilities under moderate conditions of use. It can operate in the sealed condition and can be constructed from non-magnetic materials, a prerequisite for many space programs.

The two main disadvantages of the silver-cadmium system have to do with the negative electrode. The first has to do with the manufacturing quality and reliability, which cannot always be obtained from non-uniformly vendor produced cadmium oxide (CdO). The latter leads to negative limiting cells which reduce the cell's capacity after a number of cycles. In addition to reducing the capacity, this fading phenomenon often contributes to catastrophic battery failure due to hydrogen evolution in the negative limiting cells.

The objectives of this program were the development of a stable cadmium electrode with the following properties:

1. Produced from non-magnetic materials
2. To have stable capacity features, with little fading beyond the initial drop-off.
3. To be capable of being reproduced with manufacturing techniques.

These electrodes, once developed, will be used in the construction of non-magnetic silver-cadmium cells for aerospace applications.

Prior to the start of this program, cadmium electrodes existed. The state-of-the-art of such electrodes in the battery industry can be summarized as follows:

Pocket and Tubular Electrodes - The earliest cadmium electrodes, developed by Junger, were electrodeposited. After Edison entered the storage battery field, he invented the tubular electrode. The pocket electrode and the tubular electrodes both utilize iron or steel to contain the active material. These electrodes are, of course, magnetic.

Sintered Electrodes - The sintered plate nickel-cadmium cell utilizes this kind of electrode. Nickel powder is sintered onto a grid. The nickel sinter ranges from 70% to 80% porous. Cadmium salts are impregnated into the pores of the sinter and converted to $Cd(OH)_2$. These electrodes are capable of high rate discharge, but are magnetic because of the nickel, and have a low ampere-hour per unit volume because 50% of the electrode is inactive sinter.

Pasted Electrodes - This electrode is manufactured by pasting a slurry, consisting of cadmium oxide or hydroxide, silver and binders onto a conductive substrate with subsequent pressing to the desired thickness and density. The utilization of such electrodes is fairly low compared to the sinters, but the theoretical capacity per unit volume is sufficiently great to compensate for the low utilization. However, these electrodes exhibit the effects of severe capacity fading as cycle life progresses.

Pressed Electrodes - The pressed electrode is produced by dry pressing a mixture of cadmium oxide or hydroxide, silver and binders onto a conductive substrate.

At the start of the contract, the standard Gulton non-magnetic electrode was of the pressed type. The active material was a mixture of CdO and $Cd(OH)_2$ in the ratio of 3:1 with 5% silver powder. The $Cd(OH)_2$ acts as an active binder which eliminates the need for inactive organic binders. The utilization of theoretical capacity is initially the same as the pasted electrode. Its green strength is better than the pasted electrode and it fades much less on cycling.

To achieve a stable non-magnetic electrode, we investigated standard types of pressed electrodes, pasted electrodes, and electrodes in which the cadmium hydroxide is impregnated into a porous sintered silver body, and pressed electrodes with a Teflon inorganic binder.

III. EXPERIMENTAL PROCEDURES, RESULTS, & DISCUSSION

A. PRELIMINARY EVALUATION

The preliminary evaluation consisted of fabricating sets of electrodes by four (4) different techniques and determining the capacity utilization and degradation as a function of five "C" rate charge and discharge cycles.

1. Pasted Electrodes

a. Fabrication and Testing

Three sets of pasted electrodes (two each of the A $\left[3CdO:Cd(OH)_2\right]$, B $\left[CdO:Cd(OH)_2\right]$, and C $\left[CdO:3Cd(OH)_2\right]$ formulations) were fabricated from water slurries of the above mixes. The slurries were pasted onto silver substrates and then pressed at 1.8 tons/sq. in. They were then dried and weighed to obtain their theoretical capacities. Upon drying, the B and C plates appeared to be almost completely converted to $Cd(OH)_2$, since they had become almost completely white in color, while the A plates became very light in color.

X-ray diffraction analysis confirmed the fact that the color changes were due to the hydrolysis of the CdO to $Cd(OH)_2$. The rate of this hydrolysis was found to be dependent upon the amount of hydroxide present in the original paste mixture and could be accelerated by additions of KOH. This causes some problem in ascertaining the theoretical capacities, since the hydrolysis reactions make it difficult to determine the actual ratio of $CdO:Cd(OH)_2$. Theoretical capacity was then calculated as if the active materials were all $Cd(OH)_2$.

The electrodes were given a formation cycle of 200 mA charge for 34 hours, followed by a 400 mA discharge to 0.0 volts against a charged NiOx reference. They were then put through five C/1 rate charge/discharge cycles to determine Cd utilization. Tables I and II show the formation cycle data and C rate utilization data respectively.

TABLE I. - FORMATION CYCLE DATA (Pasted Plates)

ELECTRODE	CAPACITY (Ah)	THEORETICAL CAP. (Ah)	PERCENT OF THEORETICAL
A-7	.760	1.48	51.3
A-8	.723	1.40	51.6
B-7	1.20	2.36	50.8
B-8	.717	1.74	41.2
C-7	1.00	2.02	49.6
C-8	1.28	2.44	52.7

TABLE II. - Cd UTILIZATION DATA (Pasted Plates)

CYCLE NO.	PERCENT THEORETICAL CAPACITY					
	A-7	A-8	B-7	B-8	C-7	C-8
1	17.5	30.9	23.9	----	24.2	20.9
2	15.8	30.9	23.9	21.6	23.8	16.6
3	15.0	33.4	22.5	20.0	22.5	16.6
4	14.1	33.4	22.5	19.2	21.6	15.9
5	14.1	31.6	21.6	18.3	21.6	15.9

b. Shedding Test

Shedding tests were performed by placing an electrode between two porous plates in a beaker of KOH and cycling five times at the C/1 rate. After cycling the electrolyte was filtered and the residue dried and weighed. Table III gives the results for the pasted electrodes.

TABLE III. - SHEDDING TEST DATA (Pasted Electrodes)

RATIO OF $CdO : Cd(OH)_2$	NUMBER OF TESTS	PERCENT MATERIAL LOSS
3 : 1	2	24.2%
1 : 1	2	34.3%
1 : 3	2	37.1%

The pasted electrodes which were tested up to this point did not seem to hold much promise. Their fabrication could not be closely controlled, their green strength was poor, and they exhibited low capacity utilization. The loss of materials due to shedding made any future testing needs unnecessary.

2. Pressed Electrodes

a. Fabrication & Testing

Six pressed powder electrodes were fabricated--two each of the formulations $3CdO : Cd(OH)_2$ (A type); $CdO:Cd(OH)_2$ (B type); and $CdO : 3Cd(OH)_2$ (C type). Each electrode had 5% Ag powder as a conductive diluent.

The electrodes were pressed at 7 tons/in^2.

The formation procedure consisted of a 200 mA charge (~ C/10) for 34 hours and a 400 mA discharge to 0.0 volts, using a NiOx reference electrode. The results are shown in Table IV.

TABLE IV. - FORMATION CYCLE DATA (Pressed Electrodes)

ELECTRODE	CAPACITY (Ah/Elec.)	THEORETICAL CAP. (Ah)	PERCENT OF THEORETICAL	GREEN STRENGTH
A	1.24	2.59	47.8	Good
B	1.32	2.51	52.5	Fair
C	1.68	2.43	69.1	Poor

After formation, the three types of electrodes were given five C-rate cycles; i.e., a C rate charge for 70 minutes and a C-rate discharge to 0.0 V against the NiOx reference electrode. These results are shown in Table V.

TABLE V. - C-RATE UTILIZATION (Pressed Electrodes)

CYCLE NO.	PERCENT UTILIZATION					
	A_1	A_2	B_1	B_2	C_1	C_2
1	35.1	36.8	36.4	41.3	44.4	44.4
2	33.5	37.3	34.7	38.5	42.7	42.7
3	--	--	--	--	--	--
4	34.4	36.8	--	--	41.2	41.2
5	33.4	33.1	33.1	38.5	42.7	42.7

On the basis of these results, the "C" type $[CdO : 3Cd(OH)_2]$ electrodes were chosen for further study. These electrodes were stable over the 5 cycle test at the C/1 rate and yielded about 40% utilization.

b. Shedding Test

The shedding tests were performed as previously described. Table VI indicates the results of these tests.

TABLE VI. - SHEDDING TEST DATA (Pressed Electrodes)

RATIO OF $CdO : Cd(OH)_2$	NUMBER OF TESTS	PERCENT MATERIAL LOSS
3 : 1	3	7.3%
1 : 1	4	10.0%
1 : 3	6	5.7%

Compared with the pasted electrodes, the shedding losses were minimal.

c. Additional Evaluation

Since the preliminary investigations indicated promising results, further evaluations were carried out.

(1) Utilization As A function of Pressure

Three sets of two electrodes were fabricated. Each set was pressed at a different pressure. The electrodes were then given a formation cycle, after which the C/1 rate Cd utilization tests were run. Tables VII and VIII give the formation cycle data and Cd utilization data, respectively.

TABLE VII. - FORMATION CYCLE DATA (Pressed Plates)

ELECTRODE	CAPACITY (Ah)	THEORETICAL CAP. (Ah)	PERCENT OF THEORETICAL	PRESSURE TONS/SQ. IN.
6-1	1.52	2.44	62.3	3
6-2	1.49	2.51	59.6	3
15-1	1.48	2.53	58.5	7 Standard
15-2	1.46	2.42	60.3	7
22-1	1.44	2.47	58.3	10
22-2	1.40	2.31	60.6	10

TABLE VIII. - Cd UTILIZATION DATA (Pressed Plates

f(Pressure)

CYCLE NO.	PERCENT THEORETICAL CAPACITY					
	6-1	6-2	15-1	15-2	22-1	22-2
1	33.6	27.7	28.4	28.8	27.4	32.0
2	32.7	27.0	25.9	28.0	27.4	32.0
3	31.9	27.0	24.3	25.9	25.9	31.1
4	31.9	25.9	20.3	27.0	25.9	31.1
5	31.1	26.1	18.6	27.9	23.2	30.2

The results of these tests indicate that the ultimate utilization of the electrode is not significantly affected by any of the electrode fabrication pressures used.

(2) Utilization As A Function of Silver Powder Quantity

Pressed powder electrodes were made with varying quantities of silver powder. The silver powder acts as a conductive diluent and also aids in oxygen recombination. Three sets of three "C" electrodes each were made, having 5.0, 7.5, and 10.0% silver powder respectively (Handy & Harmon Silpowder 150). The "C" type electrodes have CdO and $Cd(OH)_2$ in the ratio of 1:3.

The electrodes were given the normal formation cycle and then the Cd utilization tests were run at the C/1 rate.

Tables IX and X give the formation cycle and Cd utilization data respectively.

TABLE IX. - FORMATION CYCLE DATA (% Ag Powder)

ELECTRODE	CAPACITY (Ah)	THEORETICAL CAP. (Ah)	% OF THEORETICAL	% Ag POWDER
S-1	1.51	2.32	64.5	5.0
S-2	1.49	2.32	64.3	5.0
S-3	1.20	2.32	51.7	5.0
S-4	1.30	2.25	57.7	7.5
S-5	1.39	2.25	61.8	7.5
S-6	1.46	2.25	64.8	7.5
S-7	1.43	2.19	65.3	10.0
S-8	1.50	2.19	68.5	10.0
S-9	1.44	2.19	65.6	10.0

TABLE X - Cd UTILIZATION DATA (Ag Powder)

CYCLE NO.	C RATE CYCLING PERCENT THEORETICAL CAPACITY								
	S_1	S_2	S_3	S_4	S_5	S_6	S_7	S_8	S_9
1	37.5	36.7	30.8	31.6	35.0	35.0	36.0	35.2	35.2
2	40.8	39.2	30.8	32.5	36.7	37.5	36.9	36.9	37.7
3	40.8	40.8	30.0	32.5	37.5	39.2	38.5	39.4	39.4
4	40.8	40.8	29.0	31.6	36.7	39.2	39.4	40.2	40.2
5	39.2	40.8	28.3	30.8	36.7	39.2	39.4	41.0	40.2

These results indicate that the utilization is not dependent on the amount of silver powder used as the conductive diluent in this experiment. Indeed, it may be possible to eliminate the silver in cells where oxygen recombination is not a factor (vented cells).

(3) Use Of A Soluble Fugitive

In an attempt to increase the utilization of the pressed electrodes in excess of the 40% at the C/1 discharge rate, an attempt was made to increase porosity. In order to increase the porosity of the pressed electrodes, various percentages of crystalline KOH were added to the electrode formulations.

Three groups consisting of three electrodes per group were fabricated using the ratio of CdO : 3Cd(OH)$_2$. The first group of three contained 5% crystalline KOH; the second group 10%; and the third group 15%. The electrodes also contained 10% silver powder.

The electrodes were formed by charging at 200 mA for 34 hours and discharging at 500 mA to 0.0 V versus a nickel oxide reference electrode. The formation data are shown in Table XI.

TABLE XI. - ELECTRODE COMPOSITION, THEORETICAL CAPACITY & FORMATION CAPACITY

ELECTRODE	% KOH	THEORETICAL CAP. (Ah)	FORMATION CAP. (Ah)	PERCENT UTILIZATION
A	5	2.43	1.54	63.5
B	5	2.43	1.55	63.8
C	5	2.43	1.58	65.0
D	10	2.26	1.54	68.0
E	10	2.26	1.52	67.3
F	10	2.26	1.53	67.7
G	15	2.14	1.54	71.0
H	15	2.14	1.54	71.0
J	15	2.14	1.54	71.0

After the formation cycle, the electrodes were given five C/1 rate cycles; i.e., a 2.3 A charge for 70 minutes and a 2.3 A discharge to 0.0 V, versus a nickel oxide reference electrode. These data are shown in Table XII.

TABLE XII. - CYCLING DATA

C RATE

ELECTRODE	% UTILIZATION FOR CYCLE				
	1	2	3	4	5
A	47.0	45.4	39.0	35.5	37.0
B	43.5	43.5	39.0	39.0	38.2
C	43.3	37.4	37.5	35.5	35.8
D	45.6	42.0	40.3	40.3	39.4
E	44.6	43.6	40.3	40.3	39.4
F	44.6	44.6	40.3	39.5	39.4
G	39.2	37.4	37.4	35.5	34.5
H	44.5	46.2	40.7	41.5	40.2
J	39.2	38.4	35.5	31.3	31.7

The data shows a first cycle utilization of from 4 to 7% greater (except for two electrodes) than the same electrodes without KOH. However, by the third cycle, the utilization has dropped to the level of the pressed plate without KOH. In addition, a physical examination showed that the electrode material had poor adhesion to the substrate.

No further use was made of the soluble fugitive method for increasing electrode porosity.

3. $Cd(OH)_2$ Impregnated Sintered Silver Electrodes

a. Fabrication of Porous Sinters

The use of sintering was employed using silver powder to produce a non-magnetic porous carrier which could be impregnated with cadmium salts.

Silver powder was compacted in a mold with an expanded silver substrate in the center and heated to a point of agglomeration of silver particles. Controlling porosity levels was considered a major step in this development.

Initial tests consisted of compacting a silver powder in a mold to a density of 4.0 to 5.0 gm/cc, then sintering at 1200°F in a continuous feed sintering furnace. The resultant sinters were found to be too dense for use as carriers.

The level of porosity of the sinter was determined by saturating the sinter with toluene. Toluene was used because of its moderate boiling point, low surface tension and low viscosity. These properties permit rapid penetration into small pores and a slow rate of evaporation.

Subsequent attempts were made using organic extenders mixed in with the silver powder. A composition of 25 to 30% paraffin wax with silver powder, when sintered, produced consistent and continuous electrodes with porosities ranging between 68 and 74%. The wax was pyrolyzed during sintering.

b. Impregnation

Sintered silver plaques of the desired porosity were prepared by firing a mixture of silver and wax at the sintering temperature of silver. The pyrolysis of the wax left the desired porosity.

The sintered plaques were vacuum impregnated with $Cd(NO_3)_2$ solution and converted with cold KOH to the hydroxide. The amount of $Cd(OH)_2$ pickup ranged from 2.8 g (1 ampere-hour) to 3.5 g ($\sim$ 1.25 Åh). Nine such electrodes were prepared and tested.

c. Testing

The nine electrodes were formed by charging at 150 mA for 24 hours and subsequent discharging at 500 mA. The formation capacities are shown in Table XIII.

TABLE XIII - FORMATION CYCLE DATA

ELECTRODE	THEORETICAL CAP. (Ah)	FORMATION CAP. (Ah)	PERCENT UTILIZATION
N-1	1.07	.75	69.5
N-2	1.15	.59	51.2
N-3	1.00	.75	75.0
N-4	1.05	.58	55.3
N-5	1.13	.86	76.5
N-6	1.25	.90	72.0
N-7	1.00	.79	79.0
N-12	1.17	.89	75.5
N-13	1.14	.66	58.0

After formation, the electrodes were cycled at the C/1 rate to an end of discharge voltage of 0.0 V versus a NiOx reference electrode. These data are shown in Table XIV.

TABLE XIV. - CYCLING DATA - C/1 RATE

CYCLE	PERCENT UTILIZATION								
	N-1	N-2	N-3	N-4	N-5	N-6	N-7	N-12	N-13
1	33.0	48.6	37.0	47.6	45.0	45.0	46.7	43.0	50.9
2	34.0	47.0	43.0	51.5	49.0	49.0	38.0	40.0	52.5
3	--	46.0	--	48.6	41.0	44.0	--	--	53.5
4	--	40.0	--	48.6	38.0	43.0	--	--	49.1
5	--	44.5	--	46.6	--	--	--	--	49.1

As evidenced by Table XIV, the utilization of the impregnated sintered silver electrode is greater than that of the pressed electrodes. Because of the weight and volume of the silver sinter, the capacity per unit weight and volume is less than for the pressed plates. However, these electrodes were still of sufficient interest to carry them into the next phase of the evaluation.

4. Development of Teflonated $Cd(OH)_2$ Electrodes

Original experimentation of pressed electrodes indicated that pure CdO would not adhere to a substrate. It was, at that time, that $Cd(OH)_2$ was admixed with the CdO as an active binder. As use of Teflon in fabrication of zinc oxide electrodes was successful in this laboratory, it was decided to investigate this method with the non-magnetic cadmium electrode.

a. Method of Fabrication

The requisite amount of $Cd(OH)_2$ was weighed out, to which was added silver powder to the extent of 5% by weight. To the $Cd(OH)_2$, Ag powder was added, 5% by weight of Dupont P-30 Teflon emulsion (60.7% solids). The mix was formed into a paste by adding distilled water. The paste was thoroughly mixed and then dried at 70°C. After drying, the mix was cured at 275°C for 20 minutes. After curing, the mix was sieved through a 40 mesh screen and then pressed into electrodes.

b. Testing

(1) 5% Ag - 5% Teflon

Three electrodes were fabricated; each had a theoretical capacity of 2.26 Ah. Formation consisted of a C/10 charge for 24 hours and a 500 mA discharge. These results are shown in Table XV. After formation, the cells were subjected to five C/1 rate cycles; i.e., a C/1 rate charge for 70 minutes and a C rate discharge. These results are shown in Table XVI.

TABLE XV. - FORMATION CYCLE

ELECTRODE	MEASURED CAPACITY (Ah)	% UTILIZATION
8	1.85	82.0
9	2.00	89.0
10	2.16	96.0

TABLE XVI. - C/1 RATE CYCLING

CYCLE	PERCENT UTILIZATION		
	8	9	10
1	64.0	70.0	71.0
2	69.0	67.0	69.0
3	58.0	65.0	63.0
4	60.0	65.0	65.0
5	60.0	65.0	65.0

After the high rate cycles were complete, two additional low rate discharge cycles were performed. In each case, the discharge rate was 500 mA; however, the charge rate differed. In the first case it was C/10 for 24 hours and in the second it was C/1 for 70 minutes. These results are shown in Table XVII.

TABLE XVII. - LOW RATE DISCHARGES (500 mA)

ELECTRODE	C/10 CHARGE		C/1 CHARGE	
	CAPACITY	% UTILIZATION	CAPACITY	% UTILIZATION
8	1.66	74.0	1.50	67.0
9	1.66	74.0	1.50	67.0
10	1.50	67.0	1.52	68.0

These results clearly indicated that the teflonated $Cd(OH)_2$ electrodes were far superior to any other electrodes prepared under this program. In fact, utilization data as determined by the preliminary testing indicated that their utilization is on a par with $Cd(OH)_2$ impregnated nickel sinter electrodes as used in hermetically sealed nickel-cadmium cells. Because of this, their ampere-hour capacity per unit weight and volume exceed that of the nickel sinter electrodes.

A typical discharge at the 2 hour rate is shown in Figure 1.

Because of the highly promising results obtained so far, further experimentation was initiated to determine the effects of varying the silver and Teflon binder contents.

(2) 10% Ag - 5% Teflon

Four electrodes were fabricated, each with a theoretical capacity of 2.12 Ah. Formation consisted of a C/10 charge for 24 hours and a 500 mA discharge. These results are shown in Table XVIII. After formation, the cells were subjected to five C rate cycles; i.e., a C rate charge for 70 minutes and a C rate discharge. These results are shown in Table XIX.

TABLE XVIII. - FORMATION CYCLE

ELECTRODE	MEASURED CAPACITY (Ah)	% UTILIZATION
11	1.92	90.5
12	1.93	91.1
13	1.91	90.1
14	1.87	88.2

TABLE XIX. - C RATE CYCLING

CYCLE NO.	% UTILIZATION			
	11	12	13	14
1	76.0	74.5	74.5	74.5
2	74.5	74.5	74.5	74.5
3	67.0	67.0	67.0	64.4
4	67.5	67.5	67.5	67.5
5	65.5	64.2	65.5	62.3

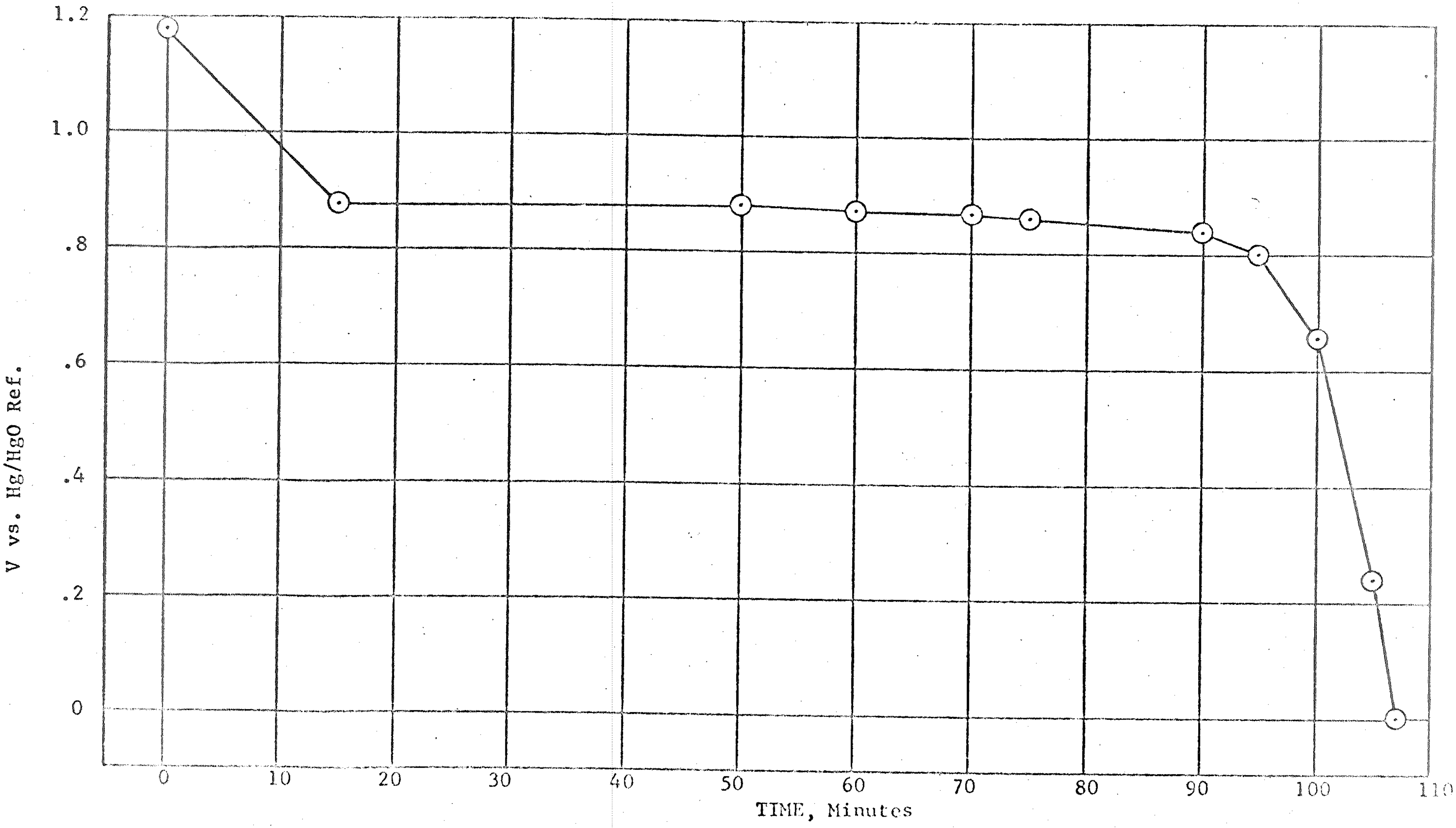

FIGURE 1.

REFERENCE DISCHARGE TEFLONATED CD(OH)$_2$ ELECTRODE
C/2 DISCHARGE - FORMATION CYCLE
THEORETICAL CAPACITY = 4.29 Ah
DELIVERED CAPACITY = 3.56 Ah
UTILIZATION = 85%

4-2691

The results indicate that initially the C/1 rate utilization is higher with 10% silver than with 5%; the ultimate utilization is about the same. Therefore, the 5% Ag would be preferred, since, for the same weight and utilization, the electrode's capacity is greater and there appears to be less trend for the capacity to decrease over the 5 cycles at the C/1 rate after formation.

(3) 15% Ag - 5% Teflon

Three electrodes were fabricated; each had a theoretical capacity of 2.01 Ah. Formation consisted of a C/10 charge for 24 hours and a 500 mA discharge. These results are shown in Table XX. After formation, the cells were subjected to five C rate cycles; i.e., a C rate charge for 70 minutes and a C rate discharge. These results are shown in Table XXI.

TABLE XX. - FORMATION CYCLE

ELECTRODE	MEASURED CAPACITY (Ah)	% UTILIZATION
15	1.79	89.1
16	1.85	92.3
17	1.87	93.2
18	1.79	89.1

TABLE XXI. - C RATE CYCLING

CYCLE NO.	% UTILIZATION			
	15	16	17	18
1	73.3	74.6	76.7	73.3
2	74.6	74.6	78.5	74.6
3	67.8	67.8	67.8	67.8
4	69.4	69.4	69.4	69.4
5	63.8	65.6	67.8	65.6

The results mirror those of electrodes with 10% silver, in that the extra silver powder over 5% does not achieve anything except lower capacity and higher cost.

(4) 5% Ag - 2-1/2% Teflon

A mixture of $Cd(OH)_2$, 5% Ag and 2-1/2% Teflon was prepared. This mixture was not adherent to the substrate at normal fabricating pressures.

The results of the preceding experiments indicated that the most favorable composition, from a cost and performance viewpoint, was the 5% silver, 5% Teflon emulsion combination.

On the basis of the data obtained in the preliminary evaluation phase of the work, three types of electrodes, the standard pressed $[3CdO : 1Cd(OH)_2]$, the $Cd(OH)_2$ impregnated silver sinters, and the teflonated $Cd(OH)_2$ were chosen for the next level of experimentation which consisted of fabricating and cycling negative limited nickel-cadmium cells.

B. EVALUATION OF NEGATIVE ELECTRODE MATERIALS IN NICKEL-CADMIUM CELLS

1. Cell Fabrication

In this phase of the program, ten cells of each of the cadmium electrode types which appeared to be the most promising, from the preliminary evaluation, were fabricated into negative limited nickel-cadmium cells. The electrode types chosen were:

a. Teflonated $Cd(OH)_2$
b. $Cd(OH)_2$ impregnated silver sinters
c. The mixture $3Cd(OH)_2 : 1CdO$
d. The mixture $1Cd(OH)_2 : 3CdO$ - The Gulton "Standard" Electrode

2. Cell Testing

The cells were placed on a cycling regime with a 90 minute orbit for 200 cycles or until failure.

Five cells of each type were cycled at 50% depth-of-discharge and the remaining five were cycled at 75% depth-of-discharge.

a. Formation Procedure

The formation procedure consisted of a C/10 charge for 24 hours and a C/2 discharge to 0.9 V per cell.

(1) Cells With Teflonated $Cd(OH)_2$ Electrodes

The ten cells fabricated (Nos. 1-10) were of VO-6 size (standard Gulton nickel-cadmium sealed cell), approximately 2" x 2" electrode size. Each positive was 0.030" thick and each negative was 0.050" thick.

The theoretical negative capacity was calculated at 4.5 Ah.

(2) Cells With $Cd(OH)_2$ Impregnated Sintered Silver Electrodes

Ten cells (Nos. 11-20) were fabricated using $Cd(OH)_2$ impregnated sintered silver electrodes with an electrode size of 1-3/16" x 2" and a theoretical capacity of 3 Ah. The positive electrodes were the same sintered nickel, VO-6 size (2" x 2").

(3) Cells With Pressed Electrodes of Composition $3Cd(OH)_2 : CdO$

The ten cells (Nos. 21-30) were fabricated using electrodes of the formulation $3Cd(OH)_2/CdO$. The electrodes were of VO-6 size, approximately 2" x 2". The positive electrodes were standard sintered nickel oxide electrodes. Each positive was 0.030" thick and each negative was 0.040" thick. The theoretical capacity of the negative electrodes was calculated at 5.4 Ah.

(4) Cells With Pressed Electrodes of Composition $Cd(OH)_2 : 3CdO$

The ten cells (Nos. 31-40) were fabricated using standard Gulton pressed cadmium electrodes $[Cd(OH)_2 : 3CdO]$. The electrode sizes and thickness were the same as cells 21-30. Theoretical capacity of the negative electrodes was 5.7 Ah.

The average formation capacity for each group of cells is given in Table XXII.

TABLE XXII - AVERAGE FORMATION CAPACITIES

ELECTRODE TYPE	CELL NO.	AVERAGE CAP., Ah	THEORETICAL CAP., Ah	AVERAGE UTILIZATION
Teflonated $Cd(OH)_2$	1-10	3.74	4.5	83%
$Cd(OH)_2$ Sintered Silver	11-20	1.85	3.0	62%
$3Cd(OH)_2 : CdO$	21-30	2.78	5.4	52%
$Cd(OH)_2 : 3CdO$	31-40	2.67	5.7	48%

The formation data show that the utilization of the teflonated $Cd(OH)_2$ electrodes is twice as high as that of the "standard" $[3CdO : Cd(OH)_2]$ electrode and at least 50% better than any of the other electrode types tested.

b. Cycling Procedure

The cycling orbit used was of 90 minute duration, 30 minutes of discharge followed by 60 minutes of charge.

Each group of ten cells was divided into two sub-groups of five cells each. The first group was cycled at 50% depth of discharge (C/1 discharge, 115% reinsertion on charge) while the second group was cycled at 75% depth of discharge (1.5 C discharge, 115% reinsertion on charge). The discharge rates were determined from the formation capacities.

The charge and discharge rates used for each type of cell are shown in Table XXIII.

TABLE XXIII. - CHARGE & DISCHARGE RATES

ELECTRODE TYPE	CELL NO.	PERCENT DOD	DISCHARGE RATE (30 Min.)	CHARGE RATE (60 Min.)
Teflonated $Cd(OH)_2$	1-5	50	3.5 A	2.1 A
" "	6-10	75	5.2 A	3.1 A
$Cd(OH)_2$-Sintered Silver	11-15	50	1.5 A	1.1 A
" " "	16-20	75	2.3 A	1.6 A
$3Cd(OH)_2 : CdO$	21-25	50	2.0 A	1.2 A
" "	26-30	75	3.0 A	1.8 A
$Cd(OH)_2 : 3CdO$	31-35	50	2.4 A	1.4 A
" "	36-40	75	3.6 A	2.1 A

All cells were continuously monitored during cycling and failure was considered to have occurred when the cell voltage fell below 0.6 V at the end of the discharge portion of the cycle.

Table XXIV gives the cycle of which the failure point was revealed for each of the cells.

TABLE XXIV. - CYCLE OF FAILURE

Cells 1 - 10 - Teflonated $Cd(OH)_2$
Cells 11-20 - $Cd(OH)_2$ Impregnated Silver Sinters
Cells 21-30 - $3Cd(OH)_2 : CdO$
Cells 31-40 - $Cd(OH)_2 : 3CdO$

CELL NO.	% DOD	CYCLE FAILED	CELL NO.	% DOD	CYCLE FAILED	CELL NO.	% DOD	CYCLE FAILED
1	50	41	16	75	6	31	50	≤ 14
2		48	17		7	32		≤ 14
3		45	18		7	33		≤ 14
4		30	19		13	34		≤ 14
5		52	20		14	35		≤ 14
6	75	12	21	50	≤ 14	36	75	≤ 14
7		6	22		48	37		≤ 14
8		6	23		48	38		≤ 14
9		15	24		≤ 14	39		≤ 14
10		18	25		≤ 14	40		≤ 14
11	50	65	26	75	≤ 14			
12		32	27		≤ 14			
13		64	28		≤ 14			
14		65	29		≤ 14			
15		65	30		≤ 14			

The results of the cycling summarized in Table XXIV indicated that the cells cycled longer at 50% DOD than at 75% DOD and also, that the sintered type of electrodes generally cycled longer than the pressed electrodes.

c. Post Cycling Capacity

After removal from cycling, the cells were subjected to a "C" rate charge and discharge cycle. This data is shown in Table XXV.

TABLE XXV. - POST CYCLING CAPACITY DETERMINATION

C/1 Charge for 70 Minutes
C/1 Discharge to 0.6 V

ELECTRODE TYPE	CELL NO.	AVG. FORMATION CAP. (Ah)	AVG. POST CYCLING CAP.	AVG. PERCENT CAP. RETAINED
Teflonated $Cd(OH)_2$	1-10	3.74 Ah	1.55 Ah	41.5%
$Cd(OH)_2$-Sintered Silver	11-20	1.85	0.72	39 %
$3Cd(OH)_2$:CdO	21-30	2.78	0.86	31 %
$Cd(OH)_2$:3CdO (Standard)	31-40	2.67	0.91	34 %

The post cycling capacity data indicated that both the teflonated $Cd(OH)_2$ and $Cd(OH)_2$ impregnated sintered silver electrodes were superior to either of the two varieties of pressed electrodes.

d. Physical Inspection of Electrodes

All cells (numbers 1-40) were disassembled and the negative electrodes examined.

The teflonated $Cd(OH)_2$ electrodes (Cells 1-10) showed no signs of physical damage and were quite flexible. The $Cd(OH)_2$ impregnated sintered silver electrodes (cells 11-20) showed no signs of physical damage. The $3Cd(OH)_2$/CdO electrodes (Cells 21-30) showed severe damage in that most of the active material (70-80%) had fallen away from the substrate. The standard Gulton electrodes (Cells 31-40) showed minor physical damage--a small amount of shedding.

The testing of electrodes for silver-cadmium cells was narrowed down to the following cadmium electrode types:

1) The teflonated $Cd(OH)_2$ electrode.
2) The $Cd(OH)_2$ impregnated silver sinter.
3) The standard Gulton cadmium electrode as a control.

C. CHARACTERIZATION OF CELL HARDWARE & ELECTRODE MATERIALS

1. Magnetic Testing of Cell Hardware

Since the ultimate silver-cadmium cells are to be used in an aerospace application where the absence of magnetism is a prime consideration, not only must the electrodes be non-magnetic, but the assembly hardware must also be non-magnetic. The magnetic testing was performed at Goddard Space Flight Center under the direction of Mr. T. Hennigan, and under the cognizance of the NASA Project Manager and Gulton Staff.

Table XXVI lists the cell hardware and the results of the testing. All the failed parts were replaced by parts made of beryllium-copper.

TABLE XXVI. - RESULTS OF MAGNETIC TESTING

PART TYPE	NO. REQ'D	MATERIAL	RESULTS	REMARKS (3)
Terminals	2	300 SS(1)	Pass	Needs demagnitization prior to use
Belville Washers	4	Be-Cu(2)	Pass	
Spacers	10	300 SS	Pass	
Lg. Flat Washers	2	SS	Fail	Replaced with Be-Cu
Champer Washers	2	SS	Fail	Replaced with Be-Cu
Snap Rings	2	Be-Cu	Pass	
Screws	2	300 SS	Pass	Needs demagnitization prior to use
Nuts	2	300 SS	Pass	Needs demagnitization prior to use
Lock Washers	2	SS	Pass	
Sm. Flat Washers	2	SS	Fail	Replaced with Be-Cu

(1) SS = Stainless Steel
(2) Be-Cu = Beryllium-Copper
(3) A 5 Ah silver-cadmium cell constructed with Be-Cu and demagnitized parts was delivered to Goddard Space Flight Center for magnetic testing. The cell satisfactorily passed the specified requirements.

2. Chemical Analysis of Gulton Prepared $Cd(OH)_2$

The $Cd(OH)_2$ used in the pressed $Cd(OH)_2$ electrodes is prepared in the following manner. Battery grade $Cd(NO_3)_2$ is reacted with KOH to form $Cd(OH)_2$. The precipitated product is washed with distilled water until neutral, dried at 70°C and ground. To determine the purity of the $Cd(OH)_2$, an analysis was carried out. The procedure is as follows:

A weighed amount of $Cd(OH)_2$ is dissolved in dilute HNO_3. The $Cd(OH)_2$ is reprecipitated with 5% KOH. Solid KCN is added until the precipitate redissolves. The cadmium is then determined by electroplating onto a platinum cathode. Table XXVII shows the results.

TABLE XXVII. - RESULTS OF $Cd(OH)_2$ ANALYSIS

Molecular Weight, $Cd(OH)_2$ = 146.40
Molecular Weight, Cd = 112.40
% Cd in $Cd(OH)_2$ = 76.78

Wt. sample taken = 0.5412 g
Wt. Cd in sample as $Cd(OH)_2$ taken = 0.4155 g
Wt. Cd Plated out = 0.4045 g
0.4045 g Cd = 0.5268 g $Cd(OH)_2$
Actual % $Cd(OH)_2$ = 97.34%

Moisture Determination:

Dried 1.0360 g $Cd(OH)_2$ @ 70°C for 48 hours

Dry Weight = 1.0132 g
Weight Loss = 2.2% water
Total $Cd(OH)_2$ corrected for moisture = 99.54%

3. Differential Thermal Analysis (DTA) of Negative Electrode Materials

Three electrode materials were run on the DTA. These were:

(a) $3CdO/Cd(OH)_2$ (Gulton Standard Mix)
(b) $CdO/3Cd(OH)_2$
(c) teflonated $Cd(OH)_2$

The results are shown in Figures 2-4. The initial peak between 80 and 150°C represents a loss of adsorbed moisture. The peak at 270-275°C represents the conversion of $Cd(OH)_2$ to CdO. The intensity of the peak at 275°C may be used as a qualitative measure of the ratio of CdO to $Cd(OH)_2$. Since in Figure 2 we know that the intensity of the peak represents 25% $Cd(OH)_2$, we should be able, from the intensity of peak in the teflonated $Cd(OH)_2$, to determine qualitatively the amount of $Cd(OH)_2$ left after curing of the Teflon (Figure 3). However, the presence of reacting Teflon at temperatures only slightly higher than $Cd(OH)_2$ prevents an accurate determination, as the DTA curve does not return to base line. We can estimate, nevertheless, that the teflonated $Cd(OH)_2$ is in actuality mostly CdO.

4. X-ray Analysis of Negative Electrode Materials

X-ray diffraction diagrams were taken of $Cd(OH)_2$ precipitated from $Cd(NO_3)_2$ and KOH, CdO obtained from Asarco, the 3CdO (Asarco): $1Cd(OH)_2$ (Gulton) standard electrode mixture, and the teflonated $Cd(OH)_2$. These are shown in Figures 5-8 respectively. We can use Figures 7 and 8 to determine the approximate ratio of CdO to $Cd(OH)_2$ in the teflonated material. In both figures, we will choose the CdO line at 33° and the $Cd(OH)_2$ line at 19°. We will also ignore any contribution of the

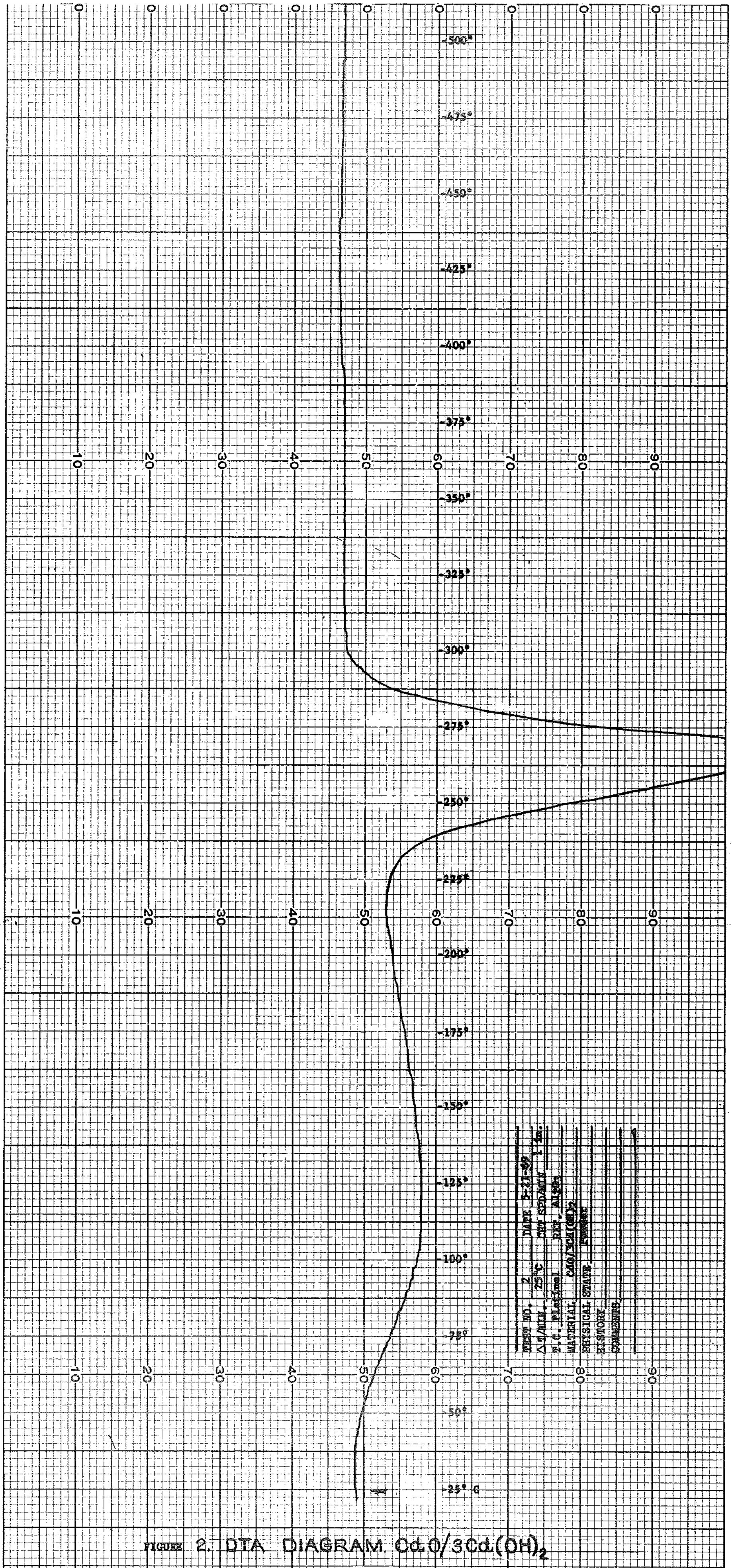

TEST NO. 2 DATE 5-21-69
ΔT/MIN. 25°C CHT SPD/MIN 1 in.
T.C. Platinel REF. Al_2O_3
MATERIAL $CdO/3Cd(OH)_2$
PHYSICAL STATE Powder
HISTORY
COMMENTS

FIGURE 2. DTA DIAGRAM $CdO/3Cd(OH)_2$

4-2831

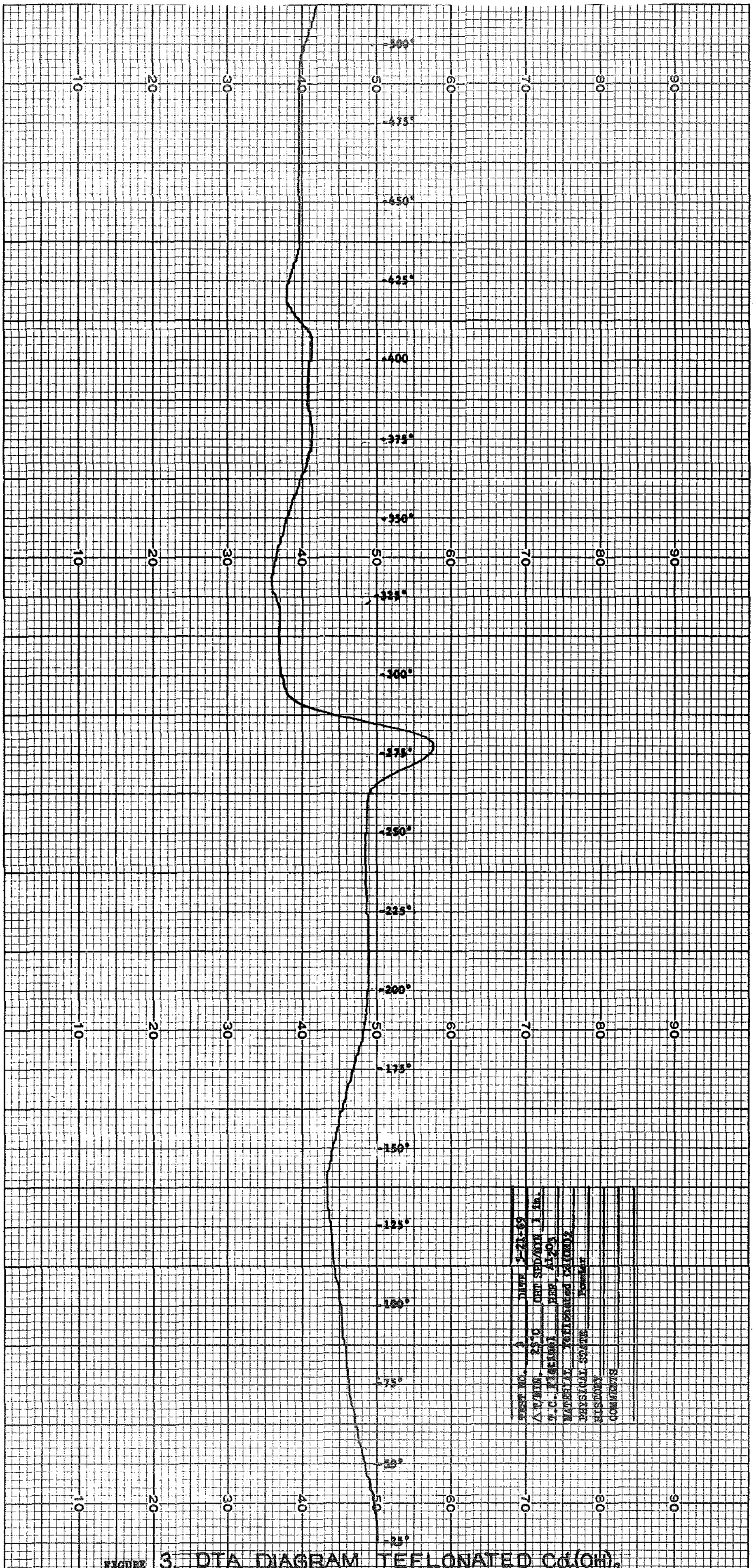

FIGURE 3. DTA DIAGRAM TEFLONATED $Cd(OH)_2$

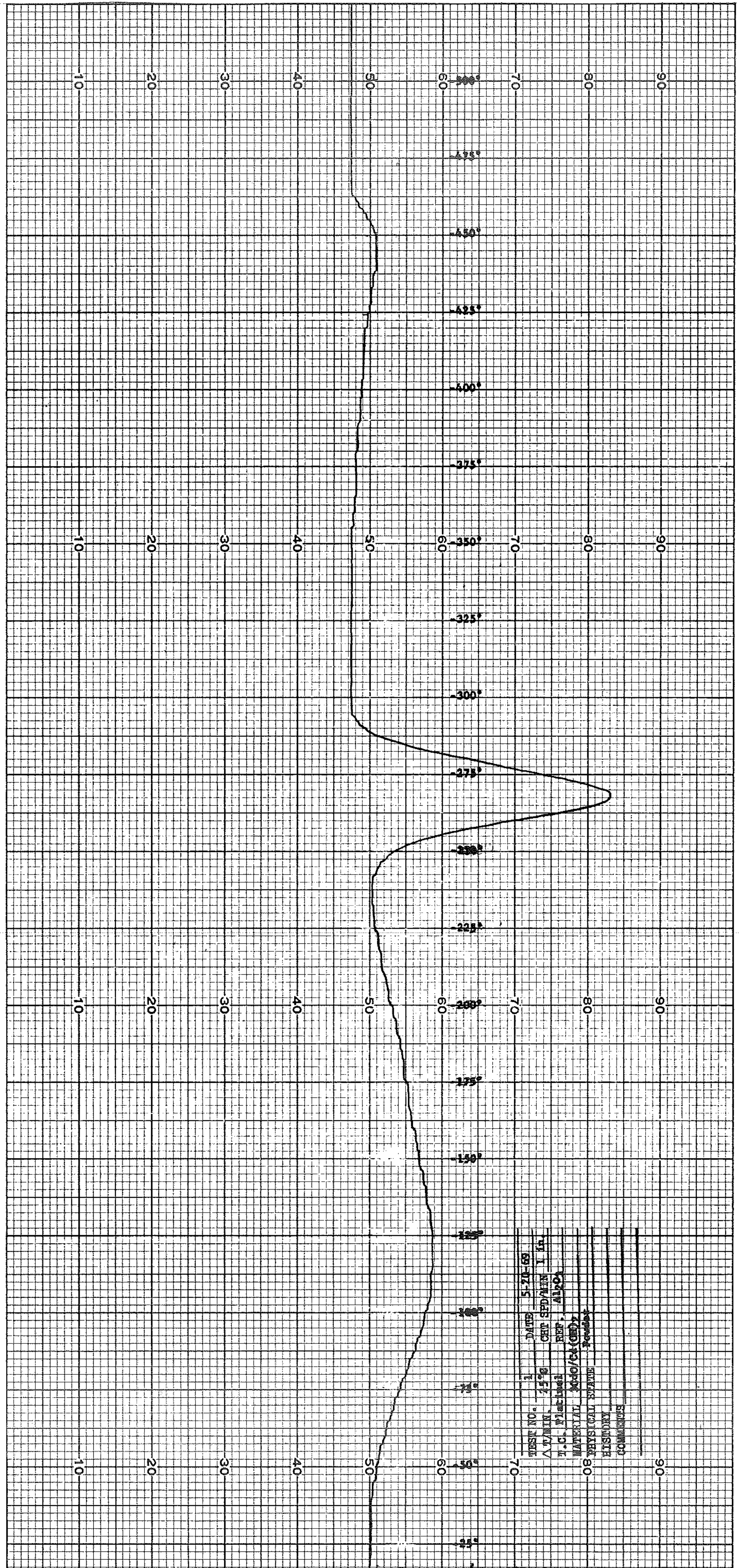

FIGURE 4. DTA DIAGRAM $3CdO/Cd(OH)_2$

4-2833

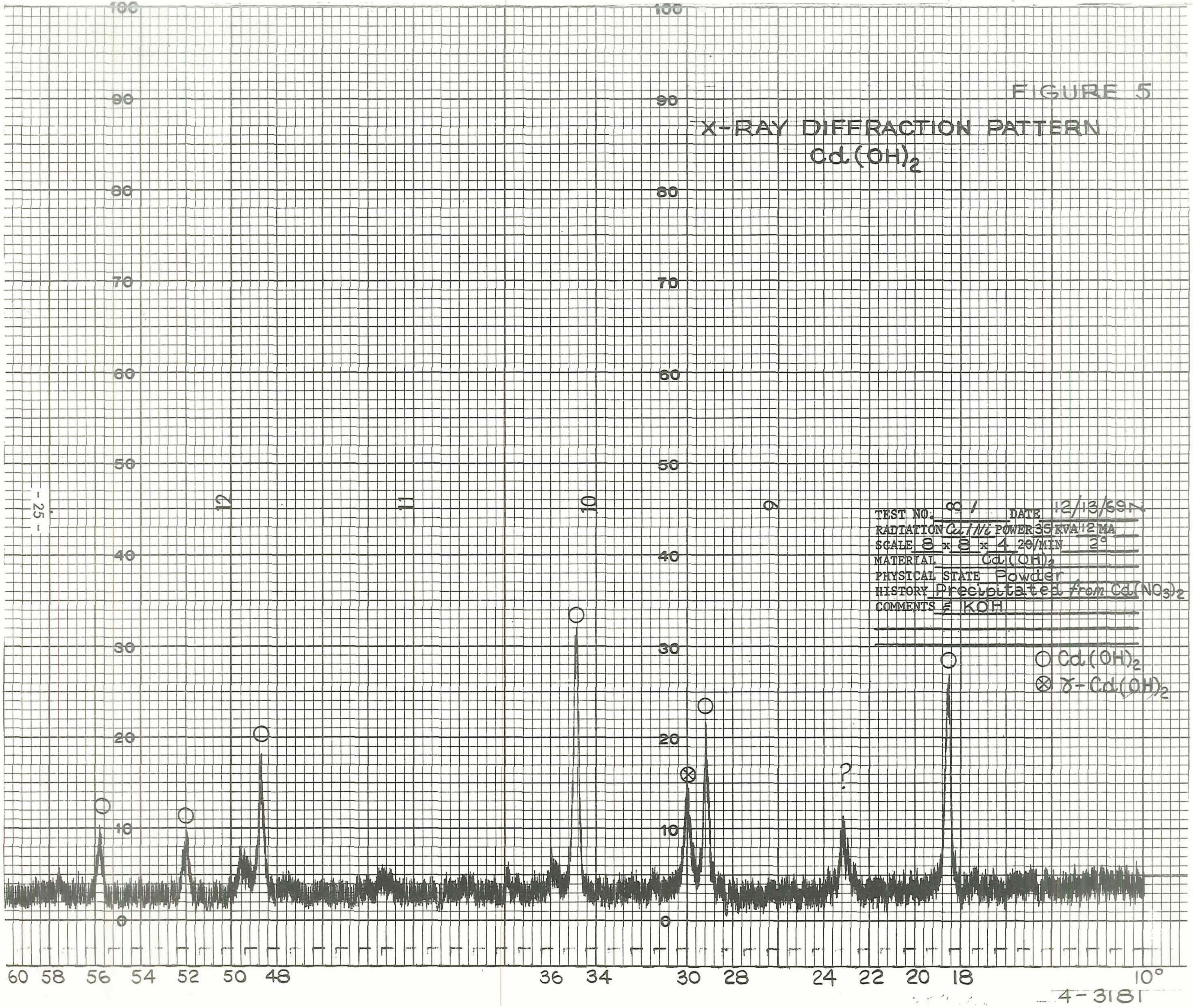

FIGURE 5

X-RAY DIFFRACTION PATTERN
$Cd(OH)_2$

TEST NO. 8 / DATE 12/13/69
RADIATION Cu/Ni POWER 35 KVA 12 MA
SCALE 8 x 8 x 4 2θ/MIN 2°
MATERIAL $Cd(OH)_2$
PHYSICAL STATE Powder
HISTORY Precipitated from $Cd(NO_3)_2$
COMMENTS $\bar{c}$ KOH

○ $Cd(OH)_2$
⊗ γ-$Cd(OH)_2$

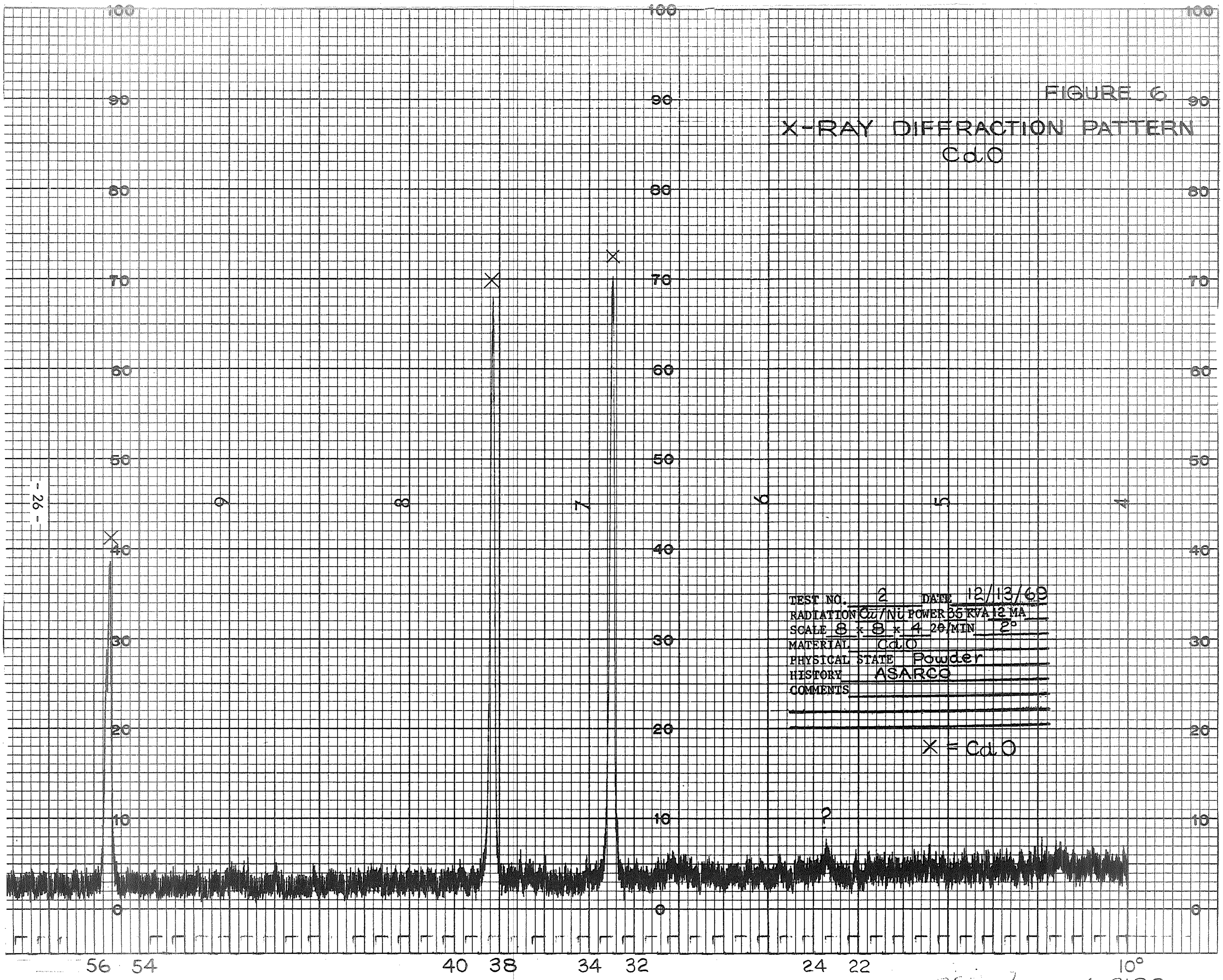
FIGURE 6

X-RAY DIFFRACTION PATTERN

CdO

TEST NO. 2 DATE 12/13/69
RADIATION Cu/Ni POWER 35 KVA 12 MA
SCALE 8 x 8 x 4 2θ/MIN 2°
MATERIAL CdO
PHYSICAL STATE Powder
HISTORY ASARCO
COMMENTS

X = CdO

4-3182

FIGURE 7

X-RAY DIFFRACTION PATTERN

$3CdO/Cd(OH)_2$

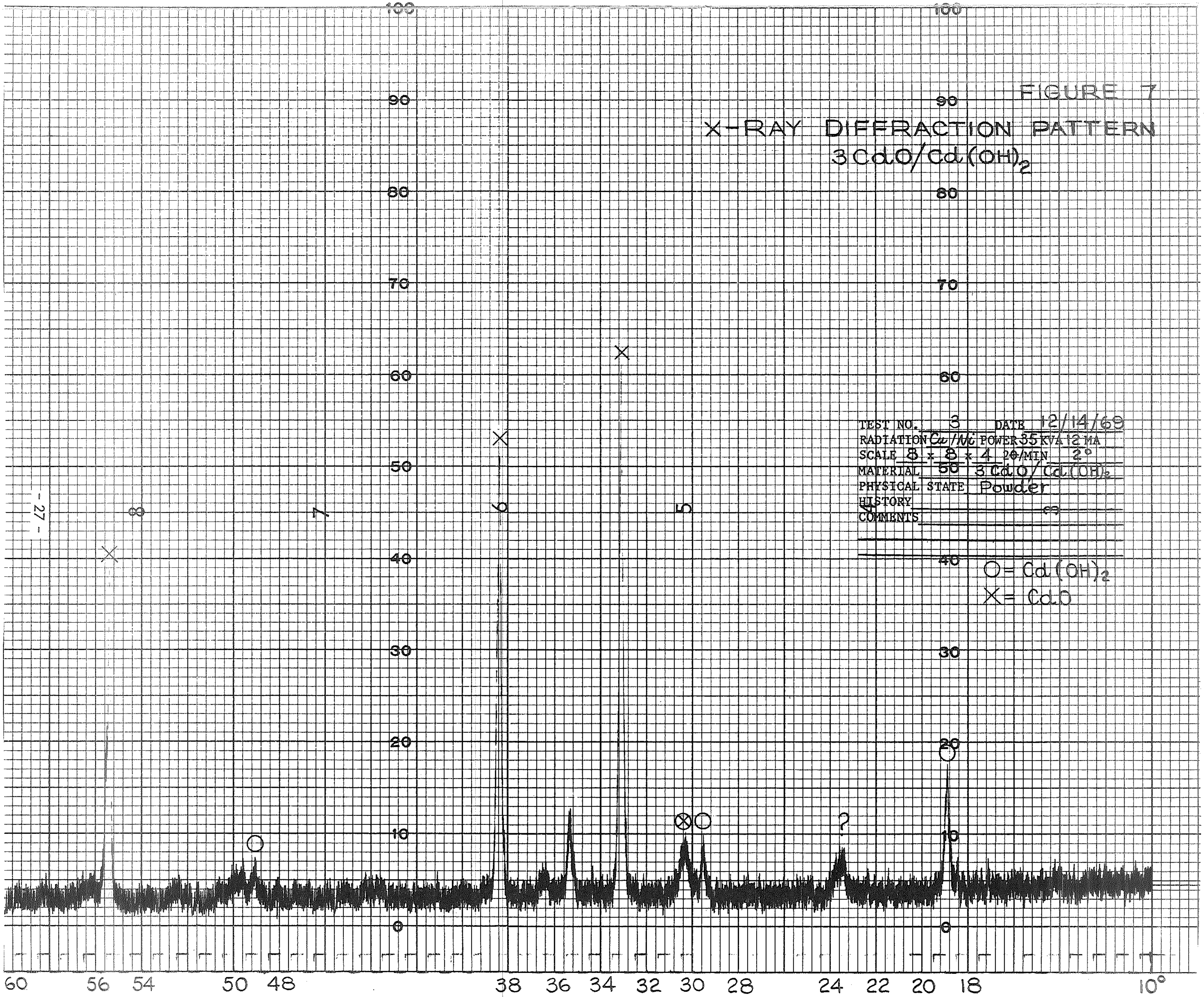

TEST NO. 3 DATE 12/14/69
RADIATION Cu/Ni POWER 35 KV 12 MA
SCALE 8 x 8 x 4 2θ/MIN 2°
MATERIAL 50 $3CdO/Cd(OH)_2$
PHYSICAL STATE Powder
HISTORY
COMMENTS

○ = $Cd(OH)_2$
X = CdO

FIGURE 8

X-RAY DIFFRACTION PATTERN
TEFLONATED $Cd(OH)_2$

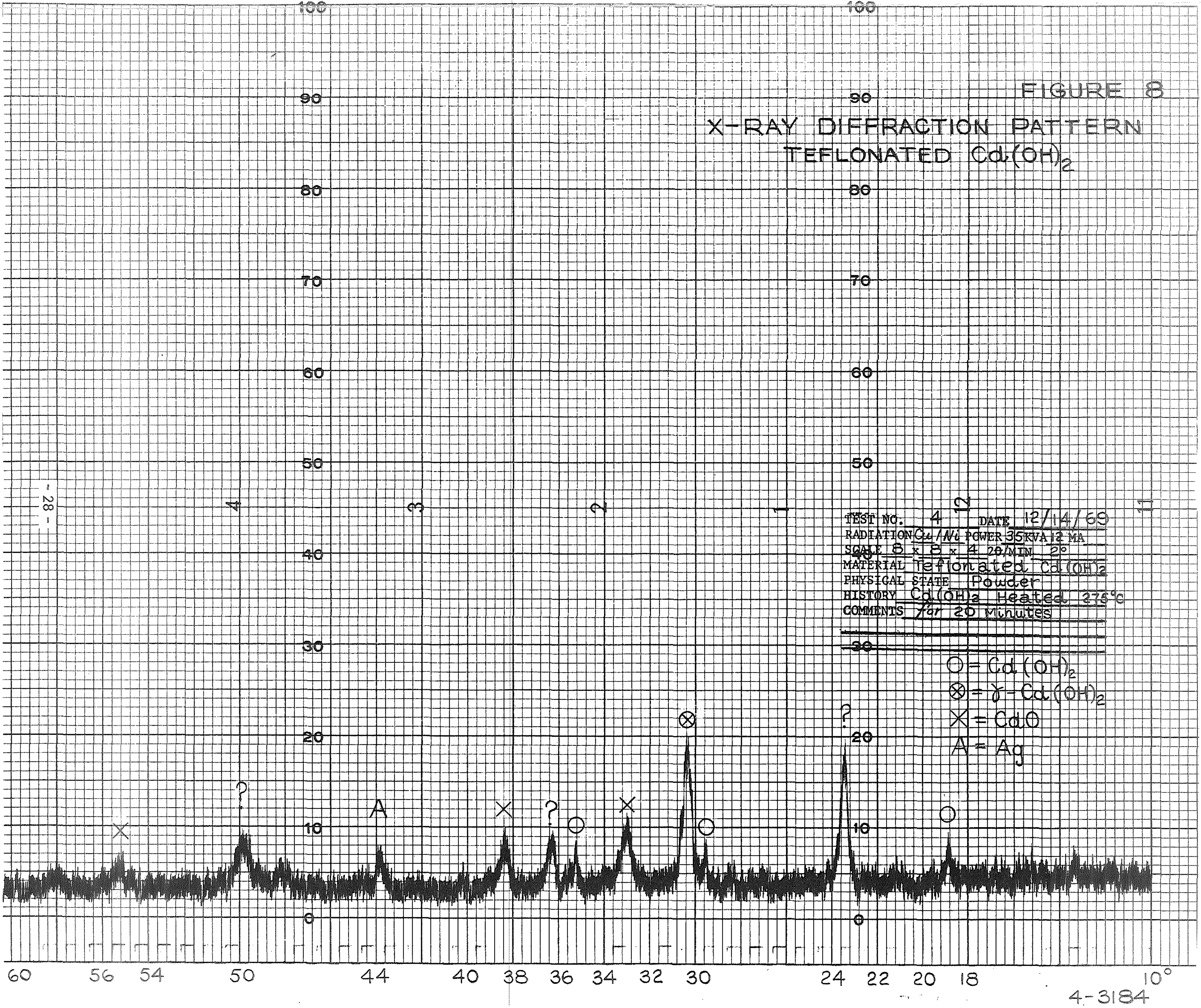

TEST NO. 4 12 DATE 12/14/69
RADIATION Cu/Ni POWER 35 KVA 12 MA
SCALE 8 x 8 x 4 2θ/MIN 2°
MATERIAL Teflonated $Cd(OH)_2$
PHYSICAL STATE Powder
HISTORY $Cd(OH)_2$ Heated 275°C
COMMENTS for 20 Minutes

○ = $Cd(OH)_2$
⊗ = γ-$Cd(OH)_2$
X = CdO
A = Ag

γ-$Cd(OH)_2$ line at 30.3°. In Figure 7, if we normalize the CdO line to 100%, then the height of the $Cd(OH)_2$ line becomes 27. We thus know that an intensity ratio of 4:1 is equivalent to 75% CdO-25% $Cd(OH)_2$.

In figure 8, after normalization, the intensity ratio is 1.7:1. We can now say that the teflonated $Cd(OH)_2$ actually contains more CdO than $Cd(OH)_2$. However, a quantitative estimate of the CdO content cannot be made since the relationship between diffracted intensity and concentration is not linear in all cases.

D. EVALUATION OF NEGATIVE ELECTRODE MATERIALS IN SILVER-CADMIUM CELLS (I)

1. Electrode Construction

a. Silver Electrodes

Silver electrodes, each with 4.0 grams of silver (2.0 Ah theoretical capacity) were fabricated. These electrodes were 0.030 inches thick.

b. Teflonated $Cd(OH)_2$ Electrodes

Teflonated $Cd(OH)_2$ containing 5 weight percent silver powder and 5 weight percent Teflon P-30 emulsion were fabricated. Each electrode contained 5.6 g (2.0 Ah theoretical capacity) of $Cd(OH)_2$. The electrodes pressed at 7 tons/in^2 were 0.040 inches thick.

c. Standard Gulton Pressed Electrode

The electrode composition is $3CdO{:}1Cd(OH)_2$--5 wt. percent silver. Each electrode contained 7 g (2.5 Ah theoretical capacity) of active material. The electrodes pressed at 7 tons/in^2 were 0.033 inch thick.

d. $Cd(OH)_2$ Impregnated Sintered Silver Electrodes

The fabrication of these electrodes is a two-step process. In the first step, silver powder is mixed with 30% paraffin wax (by weight) and heated at 100°C to allow the wax to coat the silver particles. The silver-wax misture is then spread on a substrate, pressed and fired at 1300°C. The firing sinters the silver powder and burns out the wax leaving a 72% (approx.) porous sinter, into which the $Cd(OH)_2$ is impregnated in the second step.

Step two consists of vacuum impregnating $Cd(NO_3)_2$ into the electrode sinter. After impregnation, the electrodes are dried at 70°C for four hours and then the $Cd(NO_3)_2$ is converted into $Cd(OH)_2$ in cold 25% KOH. After conversion, the electrodes are neutralized in water, dried, and reimpregnated. The procedure is repeated until there is no further pickup of $Cd(OH)_2$ on two consecutive cycles. Electrodes of this type pick up between 2.8 and 3.1 grams of $Cd(NO_3)_2$ (1.0-1.1 Ah theoretical capacity). These electrodes are 0.050 inch thick.

e. Separator Systems

The separator system used was as follows:

Positive Electrode - One turn of dynel and one layer of silver impregnated regenerated sausage casing (cellulose).

Negative Electrode - One turn of dynel and one turn of non-woven nylon.

2. Cell Fabrication

Five cells with each type of cadmium electrode were fabricated. Each cell contained 8 silver electrodes and 9 cadmium electrodes. The cell cases, made of nylon, were epoxy sealed and were fitted with pressure gauges and current limiting diodes when they were cycled as sealed cells. The diodes, two 1N645 silicon diodes in series, were used to limit the charging voltage to less than 1.65 V. Cell formation was carried out in the vented state.

Table XXVIII lists the theoretical, expected and formation capacities of the various types of cells. The theoretical capacity was determined from the weight of active material, the expected capacity from average utilization data taken earlier in the program, and the formation capacity from a 1 A, 24 hour charge and a 2 A discharge to 0.8 V.

TABLE XXVIII. - FORMATION CAPACITY DATA

ELECTRODE TYPE		THEORETICAL CAP. (Ah)	EXPECTED CAP. (Ah)	AVG. FORMATION CAP. (Ah)
Teflonated $Cd(OH)_2$	(9)	18.0	12.6	8.0
Gulton Standard Pressed $Cd(OH)_2:3CdO$	(9)	22.5	9.0	8.0
$Cd(OH)_2$ Impregnated Ag Sinter	(9)	9.7	5.4	6.0
Silver Electrode	(9)	16.0	9.0	

From a comparison of the expected negative capacities with the actual cell capacities, it is shown that those cells with teflonated $Cd(OH)_2$ electrodes and the Gulton standard pressed electrodes are positive limiting, while the cells with the $Cd(OH)_2$ impregnated silver sinters are negative limiting. However, there is considerably more expected negative capacity in the cells with the teflonated $Cd(OH)_2$ electrodes. This indicated that those cells with teflonated $Cd(OH)_2$ electrodes should cycle for a longer time as positive limiting cells than cells with the Gulton standard electrode.

In addition, the greater expected capacity for a lower theoretical capacity means that cells using teflonated $Cd(OH)_2$ weigh less than cells using other types of electrodes, making these electrodes even more advantageous. Figure 9 shows typical discharge curves for each type of cell.

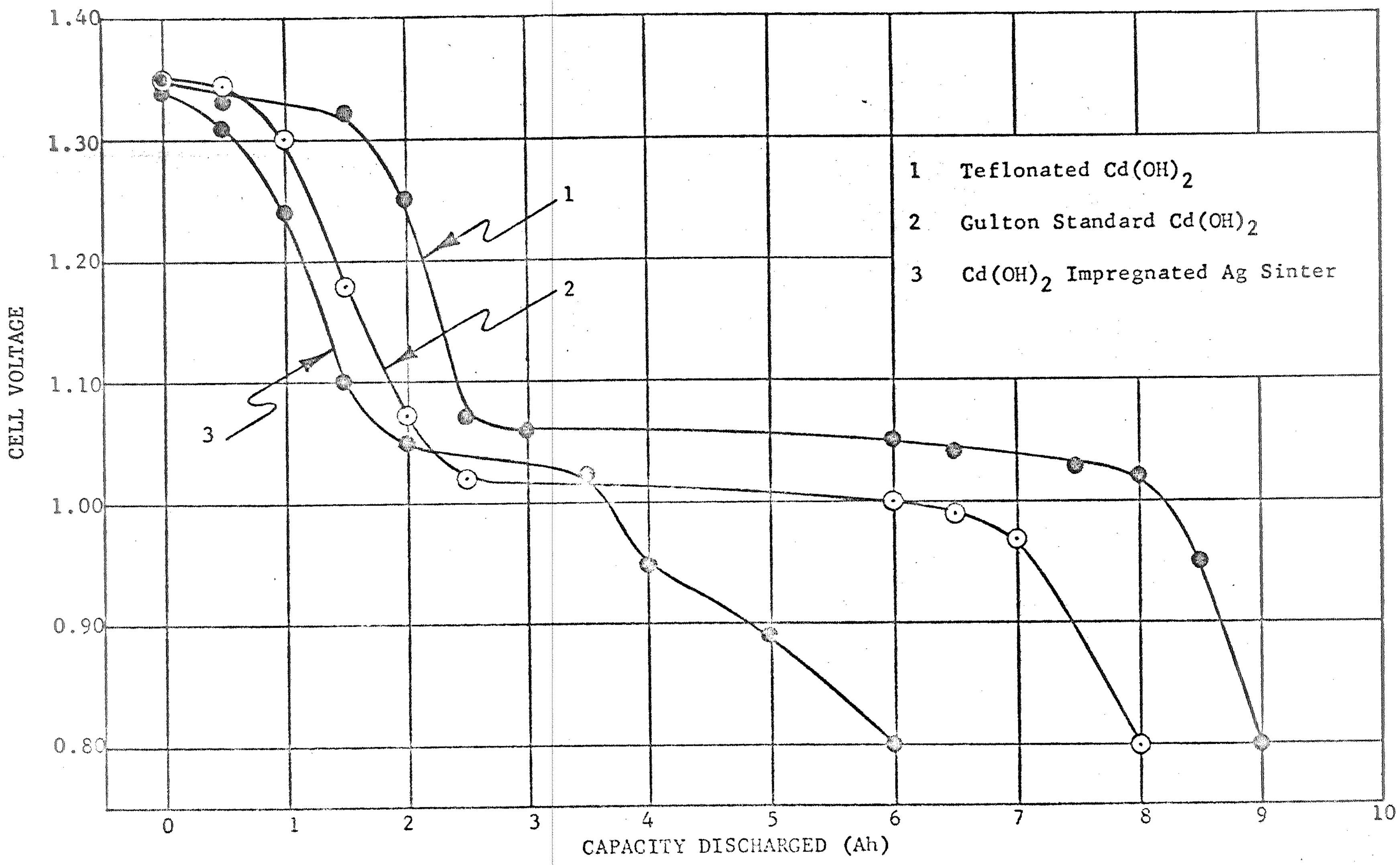

FIGURE 9 TYPICAL FORMATION DISCHARGE CURVES, 2.0 A DISCHARGE

3. Cell Cycling

The fifteen silver-cadmium cells were placed on cycle on June 1, 1969. The 15 cells consisted of 5 cells each of three different types of cadmium electrodes. Table XXIX delineates the cell types. All cells were rated at 5.0 Ah.

TABLE XXIX. - CADMIUM ELECTRODE CELL TYPES

CELLS	TYPE OF Cd ELECTRODE
1-5	Teflonated $Cd(OH)_2$
6-10	Gulton Standard Pressed Electrode
11-15	$Cd(OH)_2$ Impregnated Silver Sinters

The cycling regime consisted of a one-hour 2.5 A discharge (50% DOD) and an eleven hour 300 mA charge, with a requirement of 200 cycles. Each cell is paralleled with 2, 1N645 silicon diodes in series. This limits the charge voltage to less than 1.65 V.

A typical charge-discharge cycle (cycle 107) for the cells with teflonated $Cd(OH)_2$ negatives is shown in Figures 10 and 11 respectively.

The results of the cycling are shown in Table XXX.

TABLE XXX. - CYCLING RESULTS

CELL	FAILURE AT CYCLE	REMARKS	AVG. NO. CYCLES
1	289	Apparent short	226
2	277	Apparent short	
3	175	Apparent short	
4	134	Apparent short	
5	255	Apparent short	
6	80	Apparent short	104
7	134	Apparent short	
8	52	Low end of discharge voltage	
9	107	Apparent short	
10	148	Low End of discharge voltage	
11	134	Apparent short	35
12	10	Apparent short	
13	12	Apparent short	
14	11	Low end of discharge voltage	
15	8	Low end of discharge voltage	

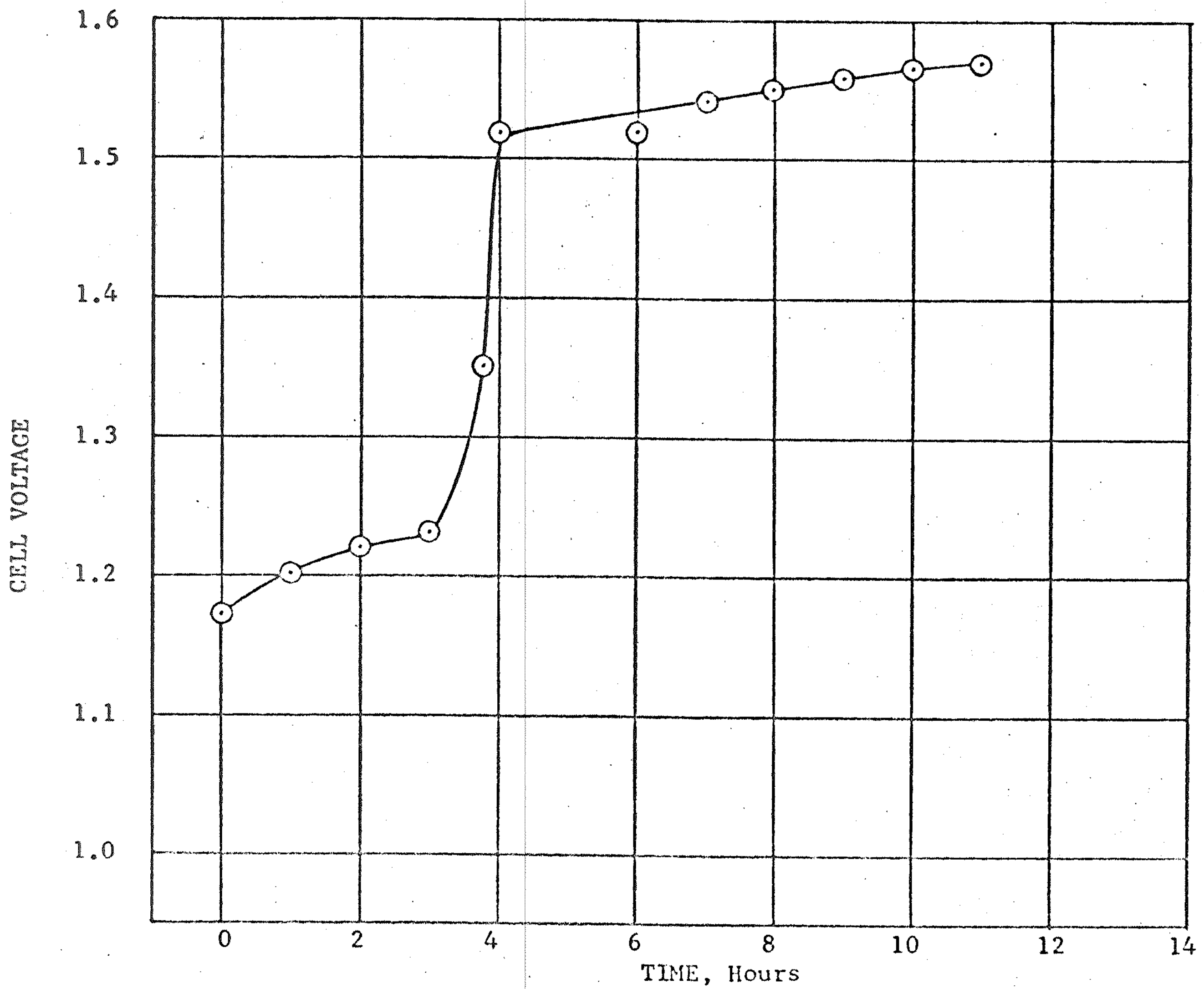

FIGURE 10 CHARGE CURVE - CELL WITH TEFLONATED Cd ELECTRODES

CYCLE NO. 107 - CHARGE RATE 0.3 A

4-2888

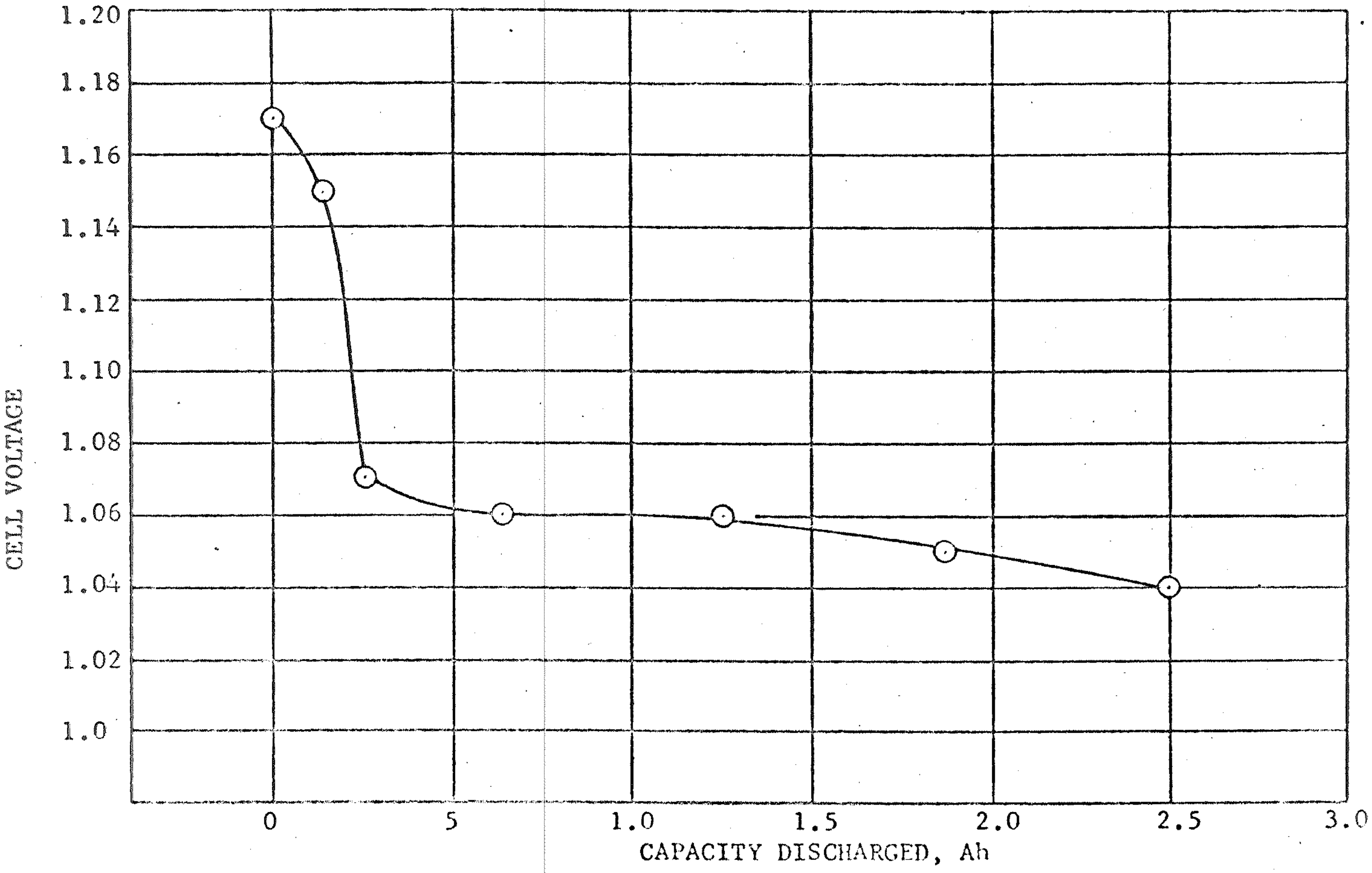

FIGURE 11 DISCHARGE CURVE - CELL WITH TEFLONATED Cd ELECTRODES

CYCLE NO. 107 - DISCHARGE RATE 2.5 A

In the case of cells 1-7, 9, 11-13 "apparent short" indicates that the cell failed rapidly within 1-2 cycles from its normal operating condition. Low end of discharge voltage indicates that the end of discharge voltage decreased from cycle to cycle until the end of discharge voltage was less than 0.6 V.

Table XXX indicates that on the average only those cells with teflonated $Cd(OH)_2$ electrodes met the 200 cycle requirement. These cells lasted more than twice as long as those cells fabricated with standard pressed electrodes and almost seven times longer than cells with the sintered silver impregnated negatives.

4. Post Mortem of Failed Cells

All the failed cells were removed from their cases and examined to determine the cause of failure.

Each cell was connected to a voltmeter and the electrodes separated one by one. An increase in voltage when a plate was separated from the pack indicated an area of shorting. For identification, the cells were placed with the positive terminal on the left and the electrodes numbered in serial order with the top negative electrode as plate one and the bottom negative electrode as plate 17, as shown below:

N	P	N	P	N	P	N	P	N	P	N	P	N	P	N	P	N
1	2	3	4	5	6	7	8	9	10	11	12	13	14	15	16	17

1) Cell No. 1 - Teflonated Negatives - 289 Cycles

Heavy silver migration through both separators on the negative electrodes. Shorts between electrodes 3 and 4, 4 and 5, and 13 and 14.

2) Cell No. 2 - Teflonated Negatives - 277 Cycles

Heavy silver migration through both separators on the negative electrodes. Shorts between electrodes 5 & 6 and 9 & 10.

3) Cell No. 3 - Teflonated Negatives - 175 cycles

Light silver migration through both separators on the negative electrodes. Shorts between electrodes 2 & 3 and 11 & 12, and 16 & 17.

4) Cell No. 4 - Teflonated Negatives - 134 Cycles

Light silver migration through both separators on the negative electrodes. Shorts between electrodes 5 & 6 and 9 & 10.

5) Cell No. 5 - Teflonated Negatives - 255 Cycles

Heavy silver migration through both separators on the negative electrodes. Shorts between electrodes 4 & 5, 8 & 9, and 16 & 17.

6) Cell No. 6 - Standard Negatives - 80 Cycles

Minimal silver migration through both separators on the negative electrodes. Shorts between electrodes 6 & 7, 7 & 8, and 14 & 15.

7) Cell No. 7 - Standard Negatives - 134 Cycles

Minimal silver migration through both separators on the negative electrodes. Shorts between electrodes 5 & 6, 6 & 7, 8 & 9, 9 & 10, and 10 & 11.

8) Cell No. 8 - Standard Negatives - 107 Cycles

Heavy silver migration through both separators on the negative electrodes and heavy silver deposits near the negative electrode tabs. No shorts detected.

9) Cell No. 9 - Standard Negatives - 152 Cycles

Heavy silver migration through both separators on the negative electrodes, especially in the area of shorting. Shorts between electrodes 1 & 2 and 6 & 7.

10) Cell No. 10 - Standard Negatives - 148 Cycles

Minimal silver migration through both separators on the negative electrodes. No shorts detected.

11) Cell No. 11 - Sintered Negatives - 134 Cycles

Heavy silver migration through both separators on the negative electrodes.

Shorts detected between all electrodes.

12) Cells No. 12 - 15 - Sintered Negatives, 8-12 Cycles

All cells showed a large amount of silver migration and no voltage when the plates were separated.

The results of the cell post mortems indicated that one of the major reasons for failure was migration of silver to the negative electrodes and shorting through the separator in the vicinity of the tab area.

A second set of silver-cadmium cells was fabricated with an improved construction so that the electrode collector tabs stand upright and do not contact the separator of an adjacent electrode.

5. Post Cycling Capacity

Subsequent to the post mortem examination, the electrodes in each pack were separated to remove any shorts and were given a charge and discharge capacity cycle.

All cells except numbers 1, 2, and 5 (which were charged and discharged at 5 A, the C/1 rate) were charged at C/10 for 24 hours (in open beakers) and then discharged at 2.0 A (C/2.5) to positive failure.

Typical discharge curves for one cell of each negative electrode type are shown in Figure 12.

Table XXXI lists the results and compares them to the precycling capacity. Except for cells 13-15, where the capacity loss is about 70%, the loss in capacity varies between 32 and 53%. The average loss is 41%.

Failure analysis on cells 1, 2, 3, and 5 have been carried out in accordance with NASA Document 51221, and are presented in Appendix I to this report. A photograph of a typical failed cell is also shown in Appendix I.

TABLE XXXI. - POST CYCLING CAPACITY

CELL	CAPACITY ON FORMATION (Ah)	POST CYCLING CAPACITY (Ah)	% CAPACITY LOSS
1	7.0	2.1 (C/1 Rate)	70%
2	8.0	3.3 (C/1 Rate)	58%
3	8.5	5.7	33%
4	9.0	5.4	41%
5	7.5	4.4 (C/1 Rate)	41%
6	8.0	4.8	40%
7	7.8	3.7	53%
8	7.8	4.8	38%
9	10.0	6.2	38%
10	7.0	5.3	32%
11	5.5	3.2	42%
12	6.0	3.2	47%
13	6.0	1.8	70%
14	5.5	1.8	67%
15	6.0	1.8	70%

Figure 13 presents a post cycling discharge curve for both electrodes of a typical cell with teflonated negatives, showing both positive and negative discharge curves.

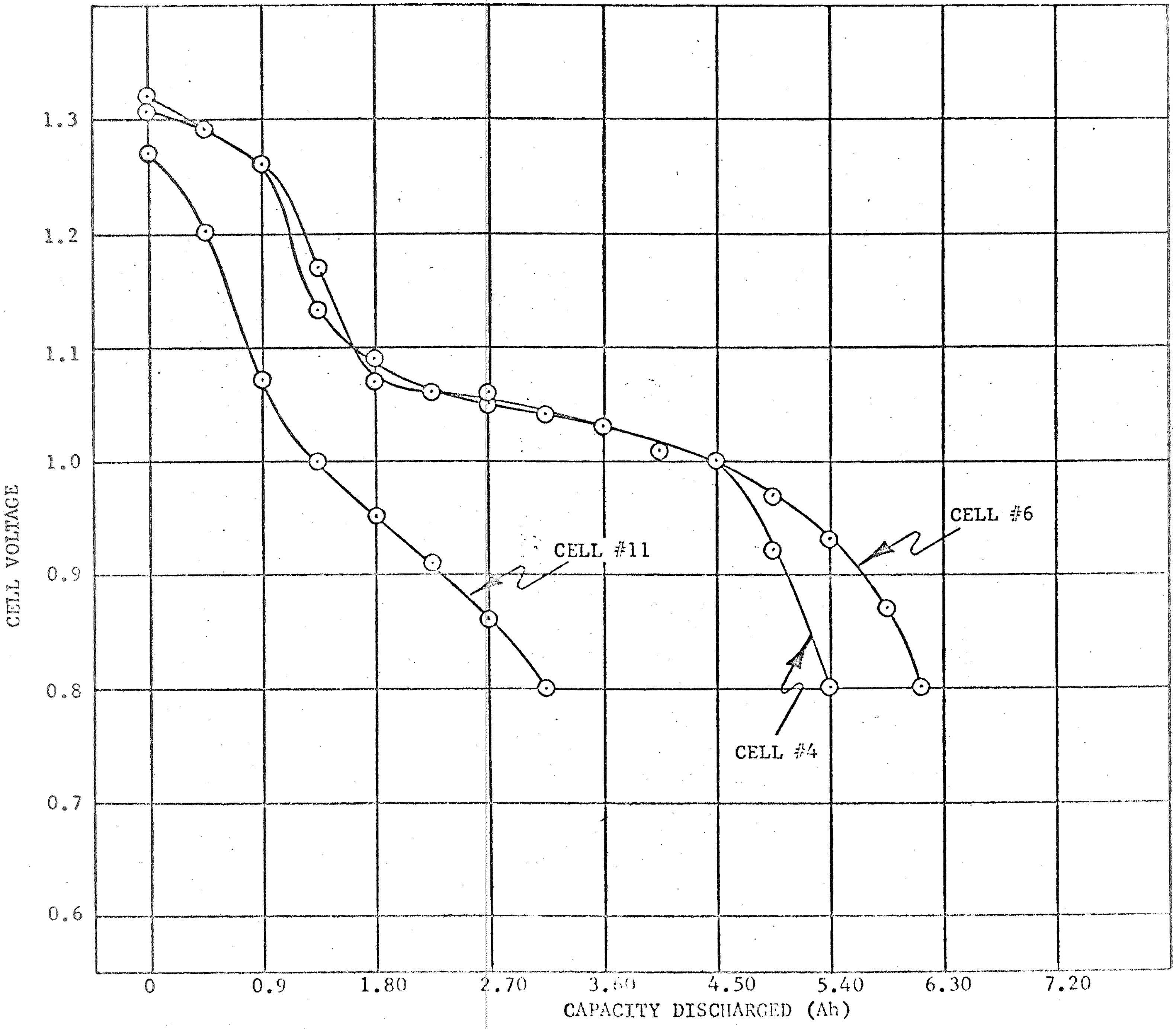

FIGURE 12 POST CYCLING DISCHARGE -- 2.0 A DISCHARGE (C/2.5)

4-2919

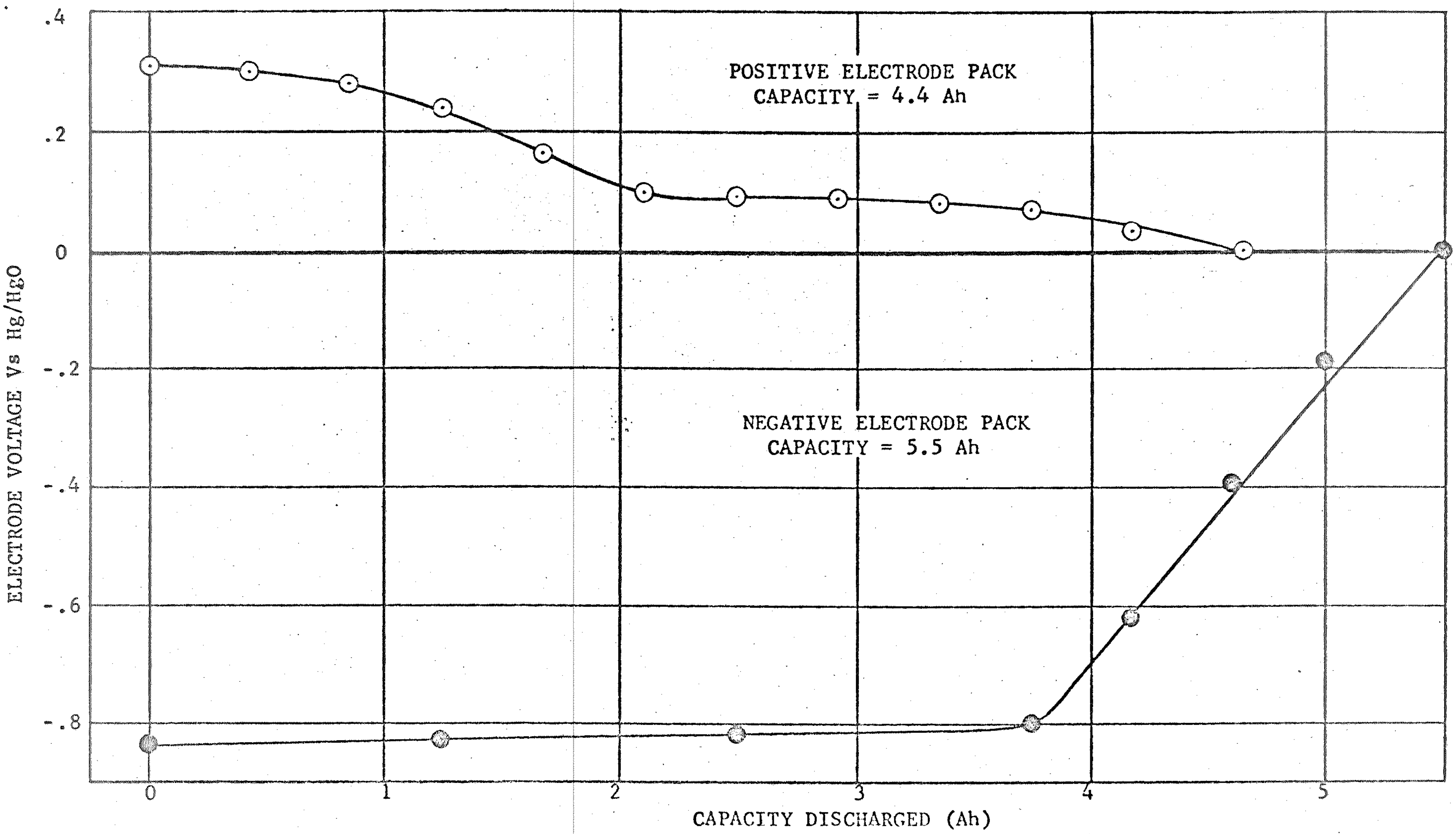

FIGURE 13

CELL WITH TEFLONATED $Cd(OH)_2$ NEGATIVE
C/10 x 24 HOUR CHARGE
C/5 (1 A) DISCHARGE Vs Hg/HgO

4-2959

E. EVALUATION OF NEGATIVE ELECTRODE MATERIALS IN SILVER-CADMIUM CELLS (II)

A second set of silver-cadmium cells were fabricated. Ten cells in all were constructed; five with teflonated $Cd(OH)_2$ negative electrodes, and five with the standard pressed electrodes.

1. Electrode Fabrication

The electrodes for these cells were prepared by the same methods described earlier in Sections D.1.a,b, c.

2. Cell Fabrication

The cell construction in this second set of cells varied considerably from the first group.

In the first group, 9 negative and 8 positive electrodes were used; while in the second group, 8 negative and 7 positive electrodes were used. In addition, in the second set of cells, each electrode tab was separated from the adjacent tab by the use of a 0.057" stainless steel spacer, as shown in Figure 14. The first set of cells used only five 0.092 spacers. The use of the smaller spacers helps prevent shorting by preventing a tab from contacting migrated silver particles on the separator of an anti-polar electrode.

3. Cell Testing

a. Formation

The formation procedure consisted of filling the cells with 38% KOH, soaking for 72 hours, and charging the cells at C/10 for 7 hours and at C/5 for 16 hours (based on negative capacity)in the vented condition. This allows, essentially, all of the $Cd(OH)_2$ to be converted to Cd metal, thus assuring a physically strong electrode with all of the active material adhering to the substrate.

The cells were then discharged at 2.0 A until negative exhaustion (-1.0 V). Table XXXII lists the results of the formation discharge and Table XXXIII gives the utilization data.

Figure 15 is a typical discharge curve.

The average weight for Cells 1-5 was 239.52 grams (0.525 lbs), while that for Cells 6-10 was 246.869 (0.545 lbs). Therefore, the average weight for all 10 cells was calculated as 243.19 grams (0.535 lbs.)

The average positive capacity for all cells was 9.3 Ah and the discharge voltage was 1.12 V, for an average value of 10.4 Wh or 19.5 Wh/lb. This compares more than favorably with a standard 6.0 Ah space cell which yields about 14 Wh/lb.

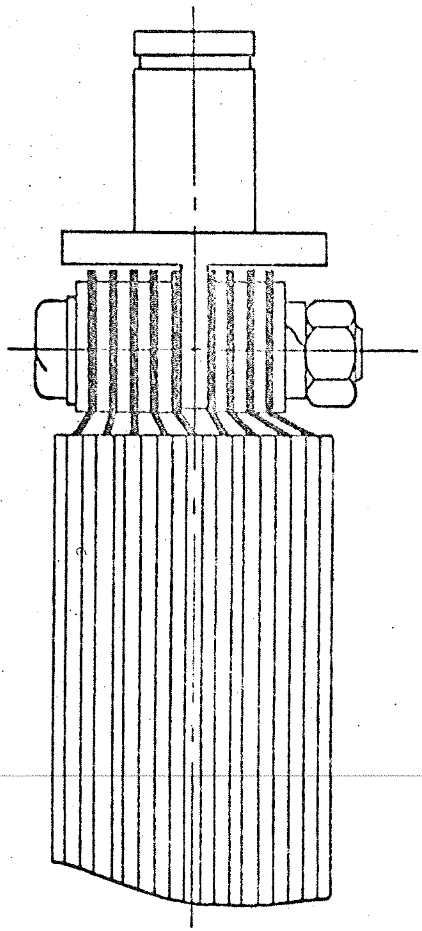

FIGURE 14 ELECTRODE STACK CONFIGURATION

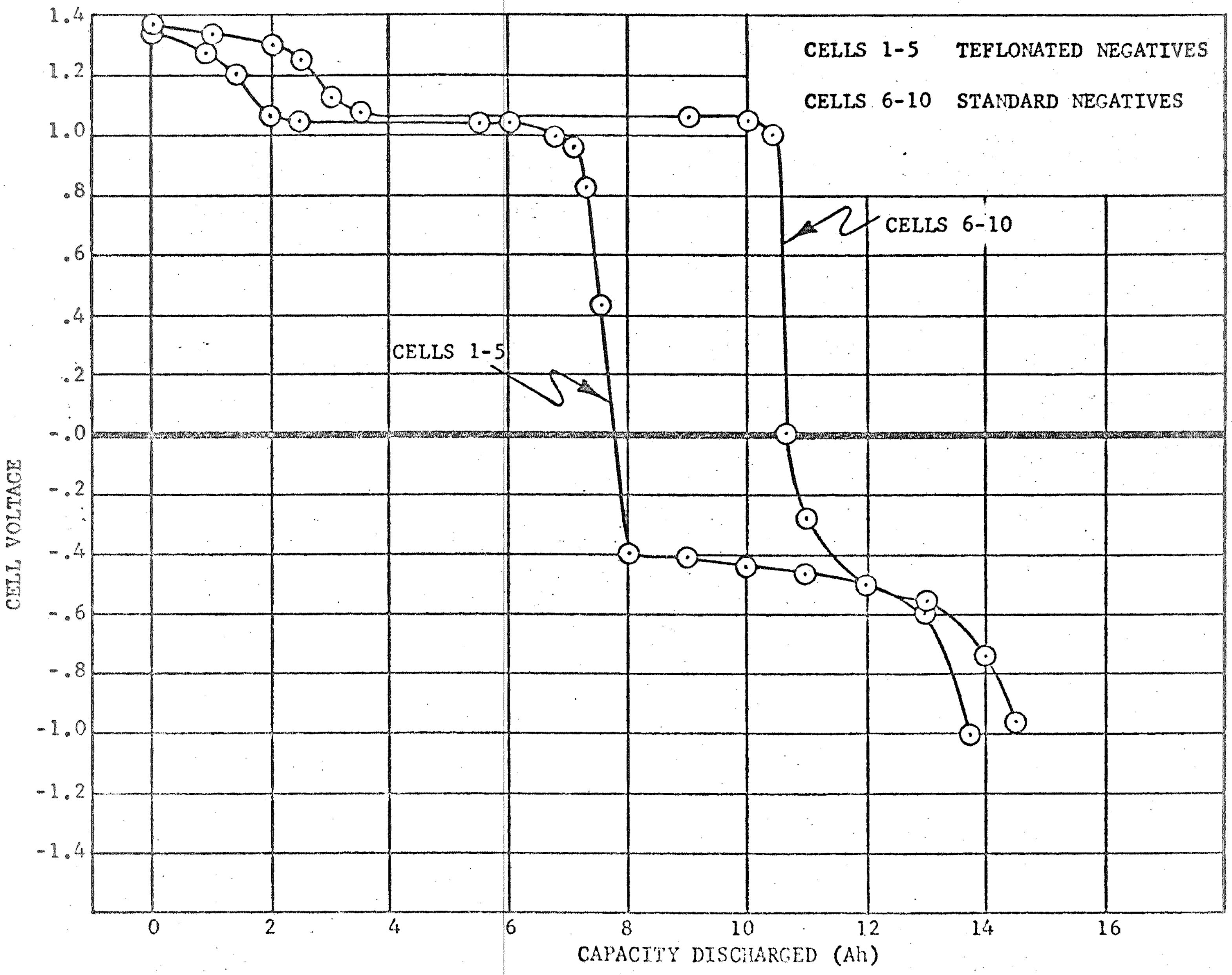

FIGURE 15. TYPICAL FORMATION DISCHARGE, SEALED Ag/Cd CELLS
Discharge Rate = 2A

TABLE XXXII. - FORMATION CAPACITIES (2 A Discharge Rate)

ELECTRODE TYPE	CELL	POSITIVE CAPACITY (To 0.5 V)	NEGATIVE CAPACITY (To -1.0 V)
Teflonated $Cd(OH)_2$	1	7.5 Ah	13.7 Ah
	2	7.7	13.9
	3	7.2	13.7
	4	7.4	13.7
	5	7.8	13.6
	Avg.	7.5	13.7
Standard Pressed	6	11.1 Ah	14.7 Ah
	7	10.6	14.7
	8	10.3	14.8
	9	10.7	14.6
	10	11.1	15.1
	Avg.	10.8	14.8

TABLE XXXIII. - UTILIZATION DATA

ELECTRODE	THEORETICAL CAPACITY	EXPERIMENTAL CAPACITY		% UTILIZATION
		Teflonated Cd Electrode	Standard Cd Electrode	
Silver	18 Ah	7.5 Ah	10.8 Ah	42-60
Teflonated Cadmium	18.3	13.7		75
Standard Cadmium	25		14.8	59

b. Cycling

After formation, two 1N645 diodes, in series with each other, were placed in parallel with each cell. These diodes limit the cell voltage to 1.60-1.65 volts. The cells, rated as nominally 5.0 Ah, were charged at C/10 (0.5 A) for 24 hours. At the end of charge, the electrolyte level was adjusted to just below the tops of the electrode stack. The cells were then sealed with pressure gauges and started on cycle.

The cycle consisted of a 1.2 hour discharge to 50% depth of discharge, which corresponds to a removal of 2.5 Ah, and a 22.8 hour charge.

This cycle required rates of 2.1 A for discharge and 0.13 mA for charge.

Due to the cell construction schedule, cells 6-10 were placed on cycle after cells 1-5 had completed 40 cycles.

As of the end of the program, cells 1-5 (teflonated electrodes) had completed 382 successful cycles, and cells 6-10 (standard electrodes) had completed 342 successful cycles.

Figure 16 shows a charge curve for cells 1-5 on cycle 382. Figure 17 is the charge curve for cells 6-10 on cycle 342. Figure 18 is the discharge curve for all cells on the same cycle as the charge curves.

At the end of charge for cycles 342 and 382, the cell pressures were as shown in Table XXXIV.

TABLE XXXIV. - CELL PRESSURES

ELECTRODE TYPE	CELL NO.	CYCLE NO.	PRESSURE
Teflonated $Cd(OH)_2$	1	382	4 psig
	2	382	6
	3	382	5
	4	382	5
	5	382	9
Standard Pressed	6	342	0 psig
	7	342	3
	8	342	0
	9	342	0
	10	342	0

During the entire course of cycling, only one problem was encountered. At the end of the 12th cycle, cells 3 and 5 had positive pressures of 15 and 19 psig, and the pressure had steadily risen to that value while the other cells had either 0 or 5 psig. The two pressure cells were vented and the gas analyzed to be oxygen. An additional 1 cc of electrolyte was removed from cells 1 thru 5. This solved the pressure buildup problem.

At the end of the program, after one year of successful cycling, the cells were removed from cycling and forwarded to the NASA/Lewis Research Center for further testing and disposition.

F. MATERIALS AND UNIFORMITY OF TEFLONATED CADMIUM ELECTRODES

This investigation, undertaken as Amendment No. 3 to Contract NAS 3-11829, was designed in order that the best type of teflonated cadmium electrode be determined.

The experimental work was divided into three phases. The first phase investigated the cadmium form; the second phase investigated the effect of particle size; and the final phase consisted of a more detailed evaluation of the best material obtained from the first two phases.

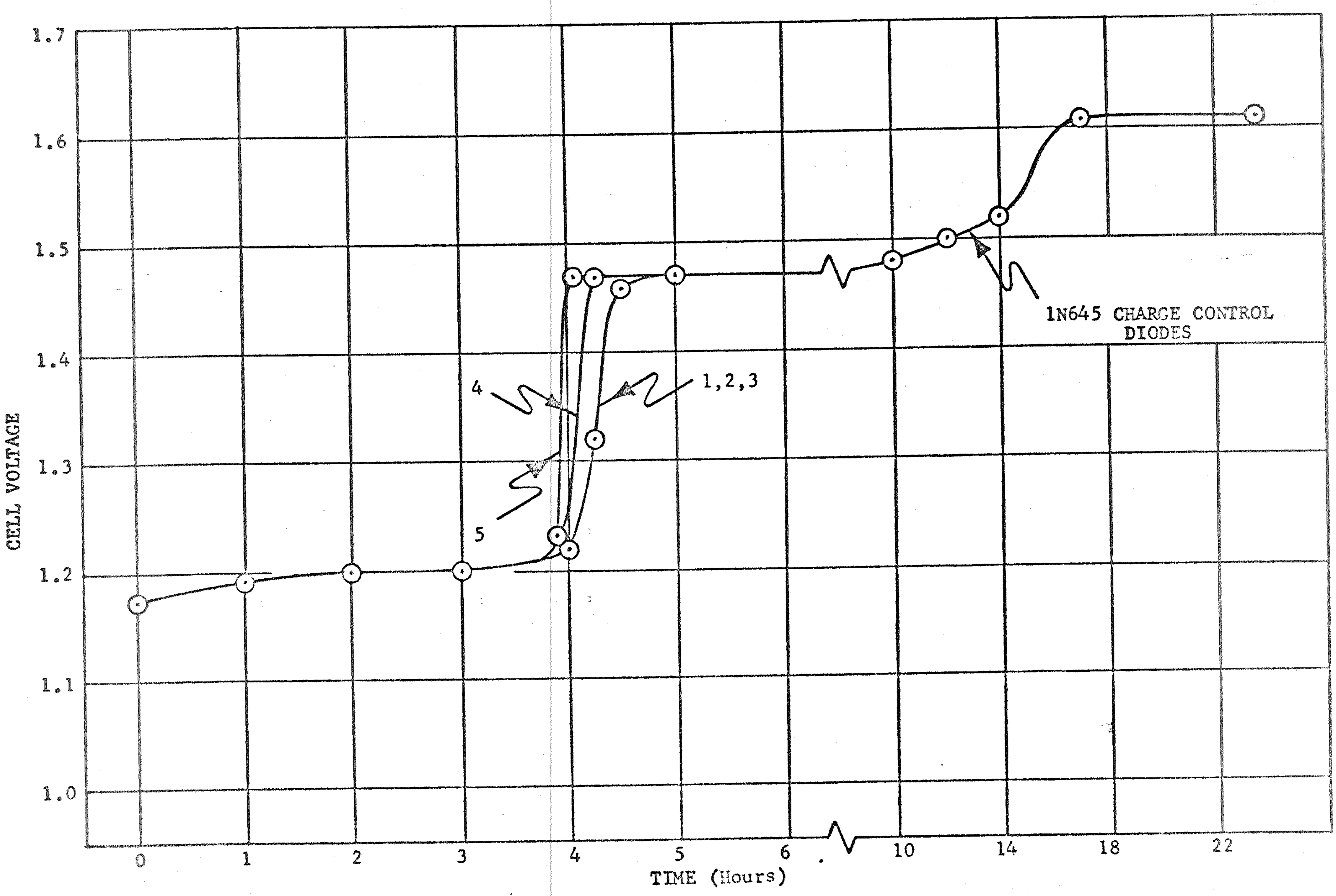

FIGURE 16. CHARGE CURVE - AG-5 SEALED CELLS (1-5) - CYCLE 382
TEFLONATED $Cd(OH)_2$

4-3177

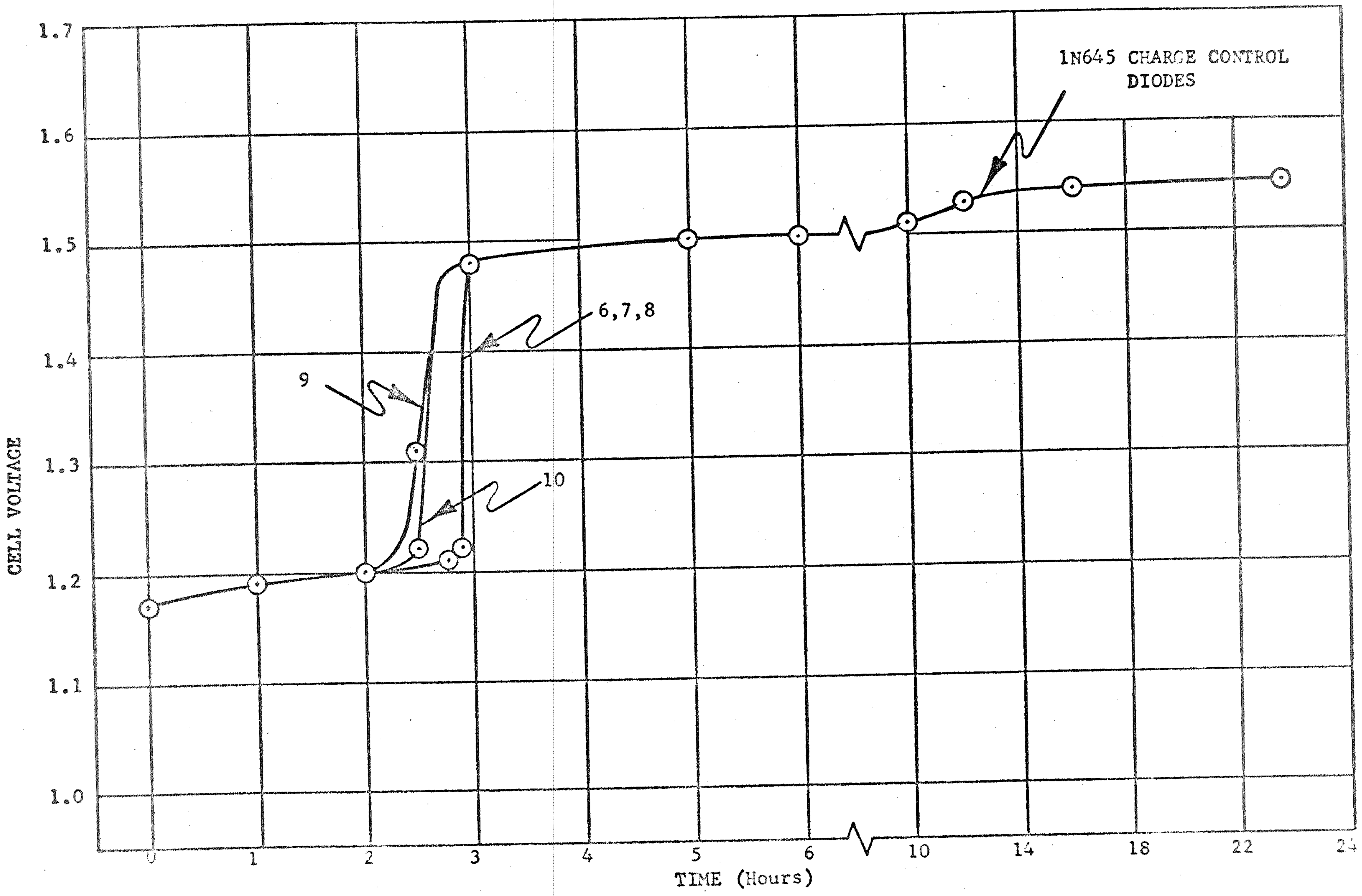

FIGURE 17. CHARGE CURVE - AG-5 SEALED CELLS (6-10) - CYCLE 342
STANDARD PRESSED ELECTRODES

4-3178

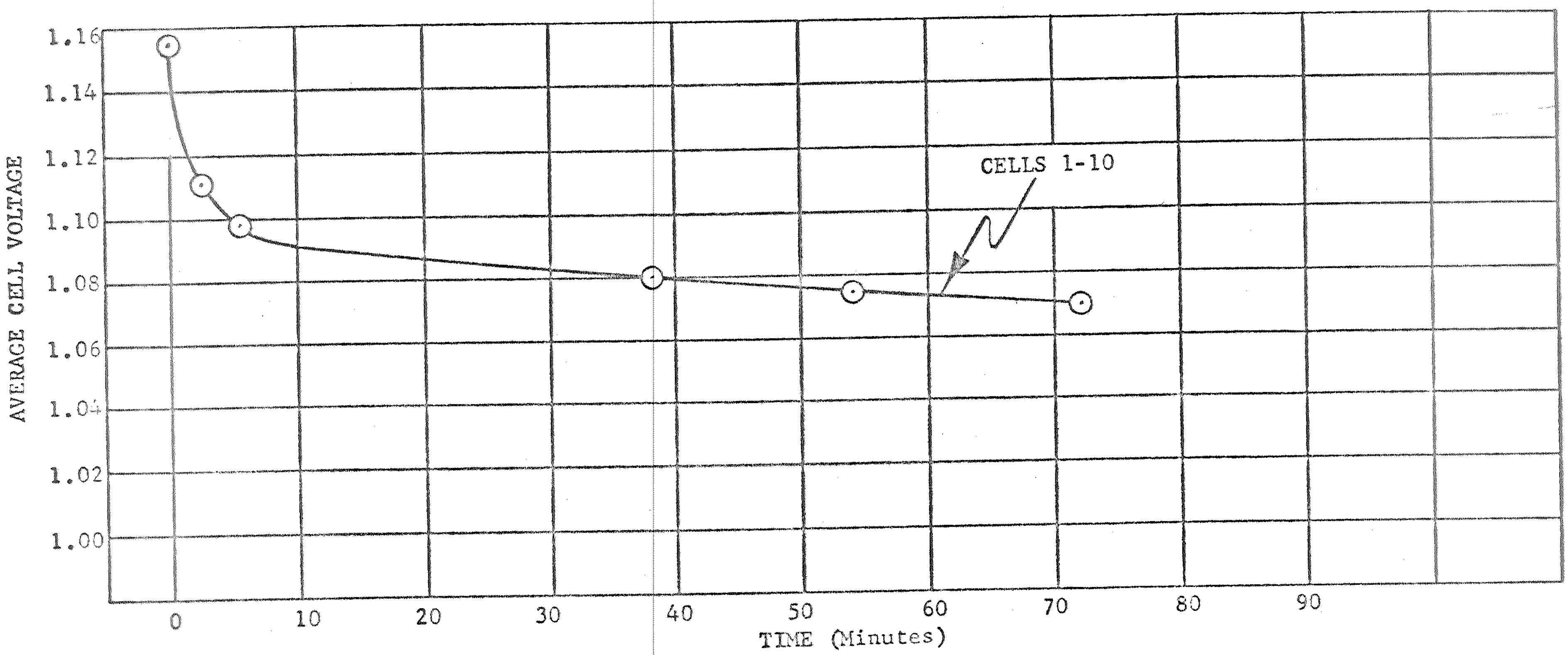

FIGURE 18. AVERAGE DISCHARGE - AG-5 SEALED CELLS ON CYCLE -
CELLS 1-5, CYCLE 382
CELLS 6-10, CYCLE 342

4-3179

1. Cadmium Form

a. Electrode Fabrication

Twelve negative electrodes, using the standard particle size $Cd(OH)_2$ as a starting material, were fabricated. Four electrodes of each of three groups, shown in Table XXXV, were prepared.

TABLE XXXV. - NEGATIVE ELECTRODE TYPES

GROUP	NAME	FORMULATION
1	Uncured $Cd(OH)_2$	$Cd(OH)_2$ mixed with Teflon but not cured at 275°C
2	Cured $Cd(OH)_2$	Cd(OH)2 mixed with Teflon and cured at 275°C
3	Cured CdO	$Cd(OH)_2$ converted to CdO at 275°C - CdO mixed with Teflon and cured at 275°C

The theoretical capacity for each type of electrode was calculated as 1.5 Ah.

b. Electrode Characterization

One electrode of each group was set aside for measurements of porosity.

(1) Porosity

Electrode porosity was measured by methanol absorption. The porosity was obtained by determining the electrode volume, weighing the electrode dry and weighing the electrode after impregnation with methanol.

The percent porosity is defined as:

$$P = \frac{\left[\frac{\text{Wet Weight - Dry Weight}}{\text{Density Methanol}}\right]}{\text{Electrode Volume}} \times 100$$

Table XXXVI lists the results of the porosity determinations.

TABLE XXXVI. - POROSITY DETERMINATION

GROUP	NAME	THICKNESS (Mils)	% POROSITY
1	Uncured $Cd(OH)_2$	35	34.5
2	Cured $Cd(OH)_2$	30	44.9
3	Cured CdO	33	48.1

The uncured $Cd(OH)_2$ electrodes registered lower porosity values than the cured electrodes.

c. Cell Testing

(1) Fabrication

Three electrodes of each group were fabricated into three-plate negative limiting nickel-cadmium cells (total 9 cells) and activated with 34% KOH and allowed to soak 24 hours.

(2) Pre-Cycling Tests

After activation, the cells were formed by charging at C/10 for 24 hours and discharging at C/5 to 0.9 V.

Figure 19 is an average discharge curve for each type of electrode and shows that the average capacity for the uncured $Cd(OH)_2$ is 0.84 Ah while for the other two groups (i.e., cured $Cd(OH)_2$ and cured CdO), the average capacity is 0.97 Ah.

The cells were then given two C/10 discharges as shown in Figures 20 and 21. A second C/5 discharge is shown in Figure 22. Two C/1 discharges are shown in Figure 23. The capacity results are summarized in Table XXXVII.

TABLE XXXVII. - AVERAGE PRE-CYCLING CAPACITIES

RATE	GROUP 1	GROUP 2	GROUP 3
	Uncured $Cd(OH)_2$	Cured $Cd(OH)_2$	Cured CdO
C/5	0.84 Ah	0.97 Ah	0.97 Ah
C/10	0.94	1.08	1.08
C/10	0.90	1.00	1.00
C/5	0.82	0.92	0.92
C/1	0.63	0.63	0.63
C/1	0.65	0.63	0.63

(3) Cycling

After completion of the precycling tests, the cells were placed on a one-week cycle at 50% depth of discharge. The cycle consisted of a 30 minute discharge at the C/1 (0.6 A) rate and a 60 minute charge at 0.33 A. The rates were chosen based on the C/1 capacity data obtained in the precycling tests.

Table XXXVIII shows the end of discharge voltage versus cycle number for each group of cells.

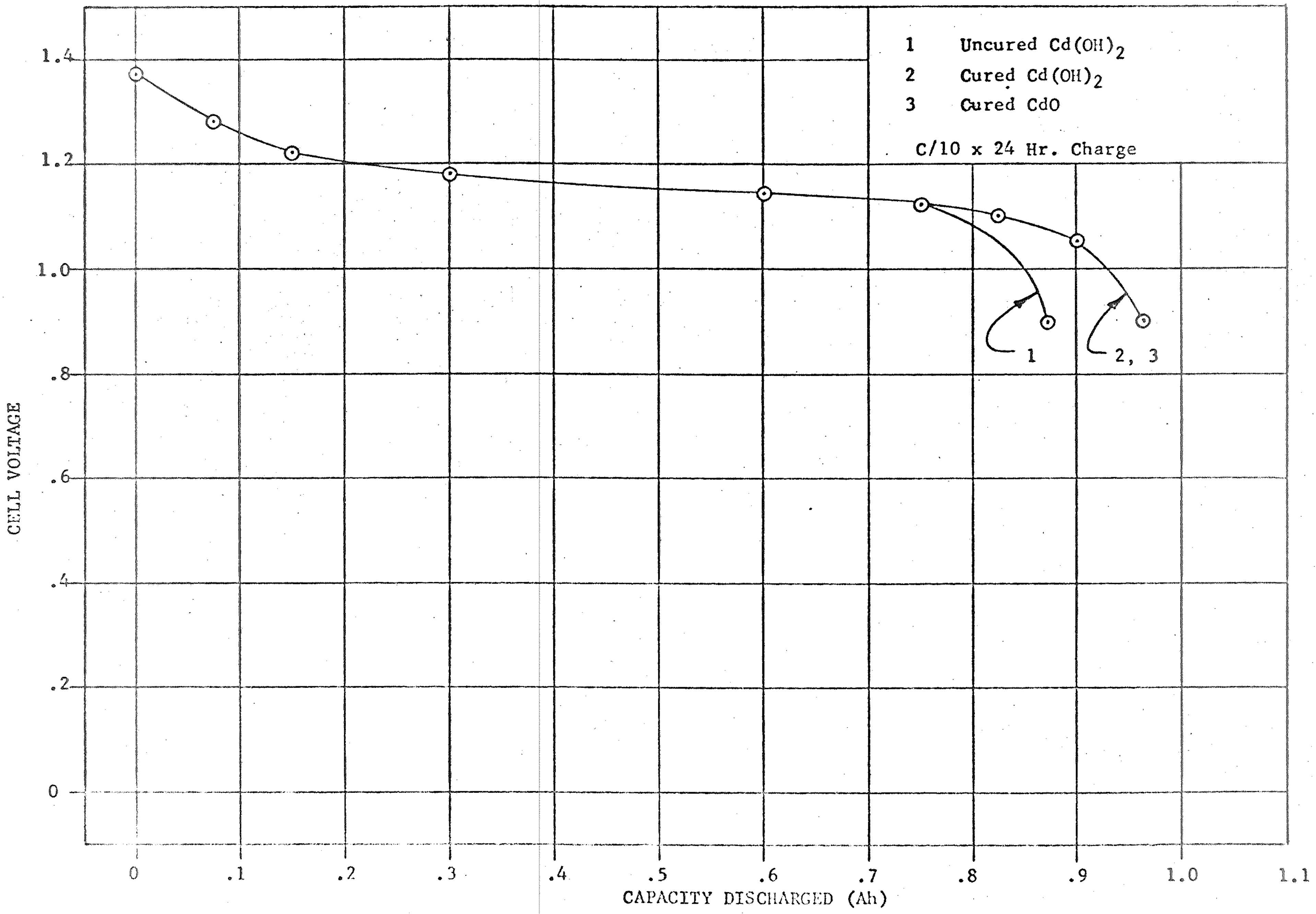

FIGURE 19 AVERAGE FORMATION DISCHARGE C/5

4-3042

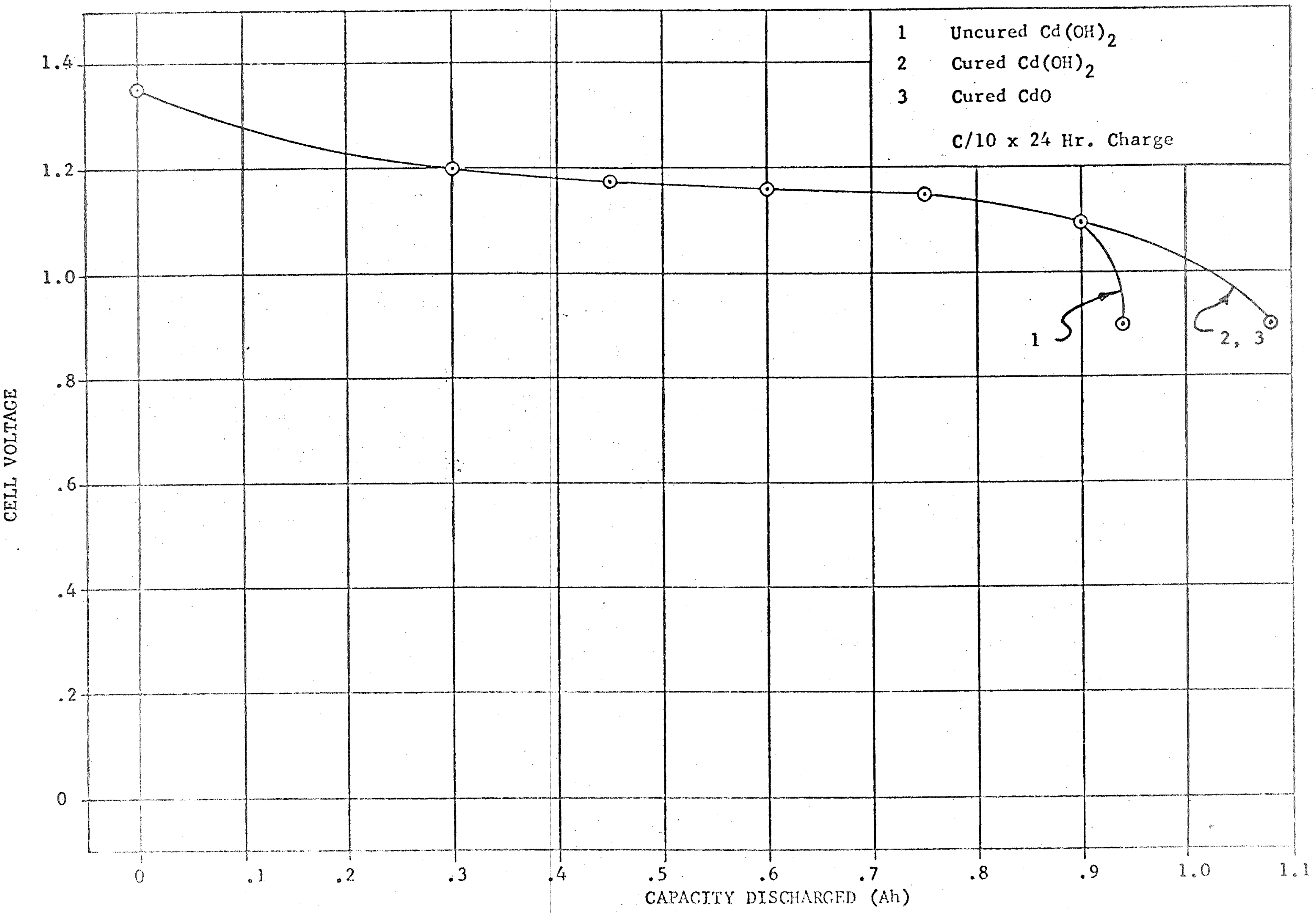

FIGURE 20 AVERAGE C/10 DISCHARGE, CYCLE #1
PRE-CYCLING

4 -3043

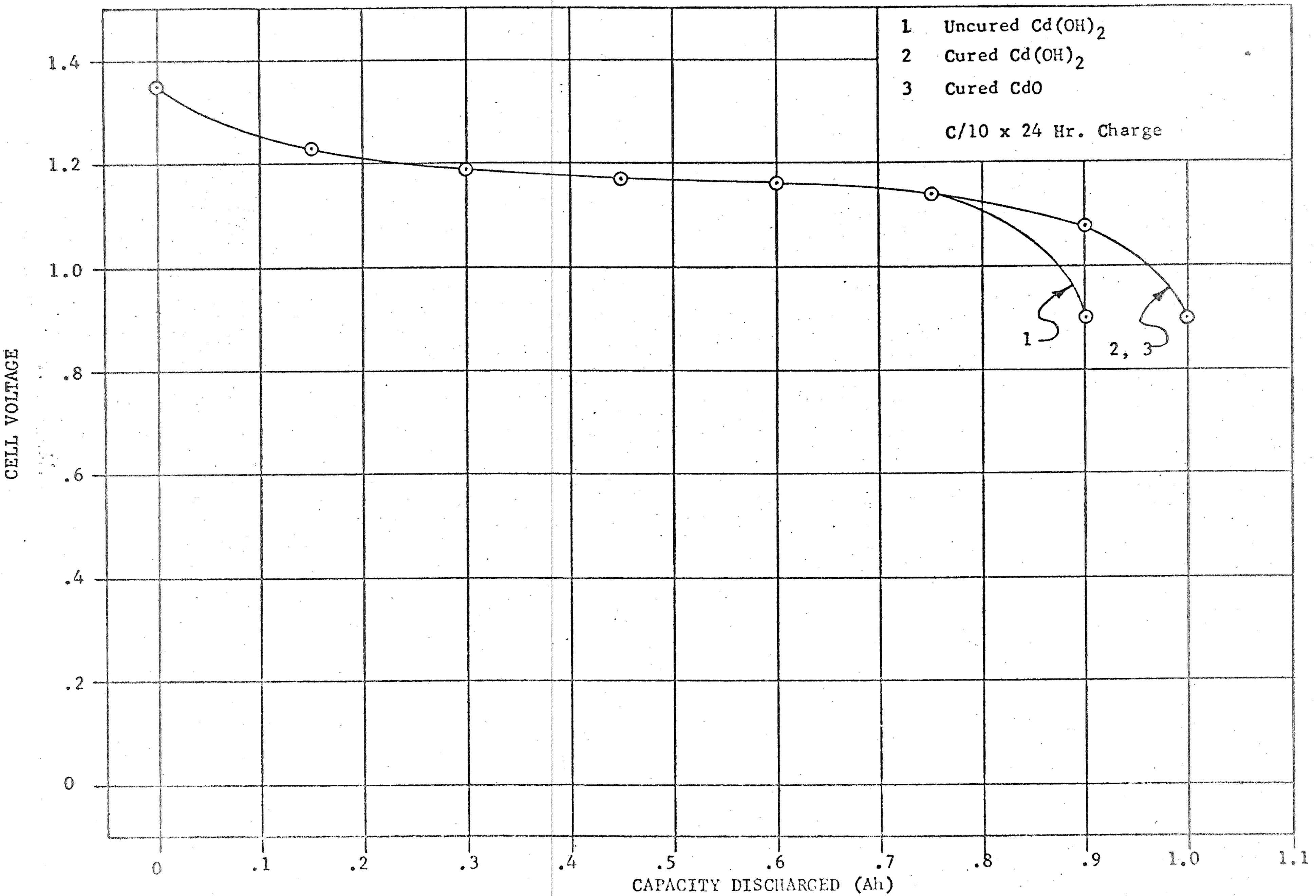

FIGURE 21 AVERAGE C/10 DISCHARGE, CYCLE #2 - PRE-CYCLING

4-3044

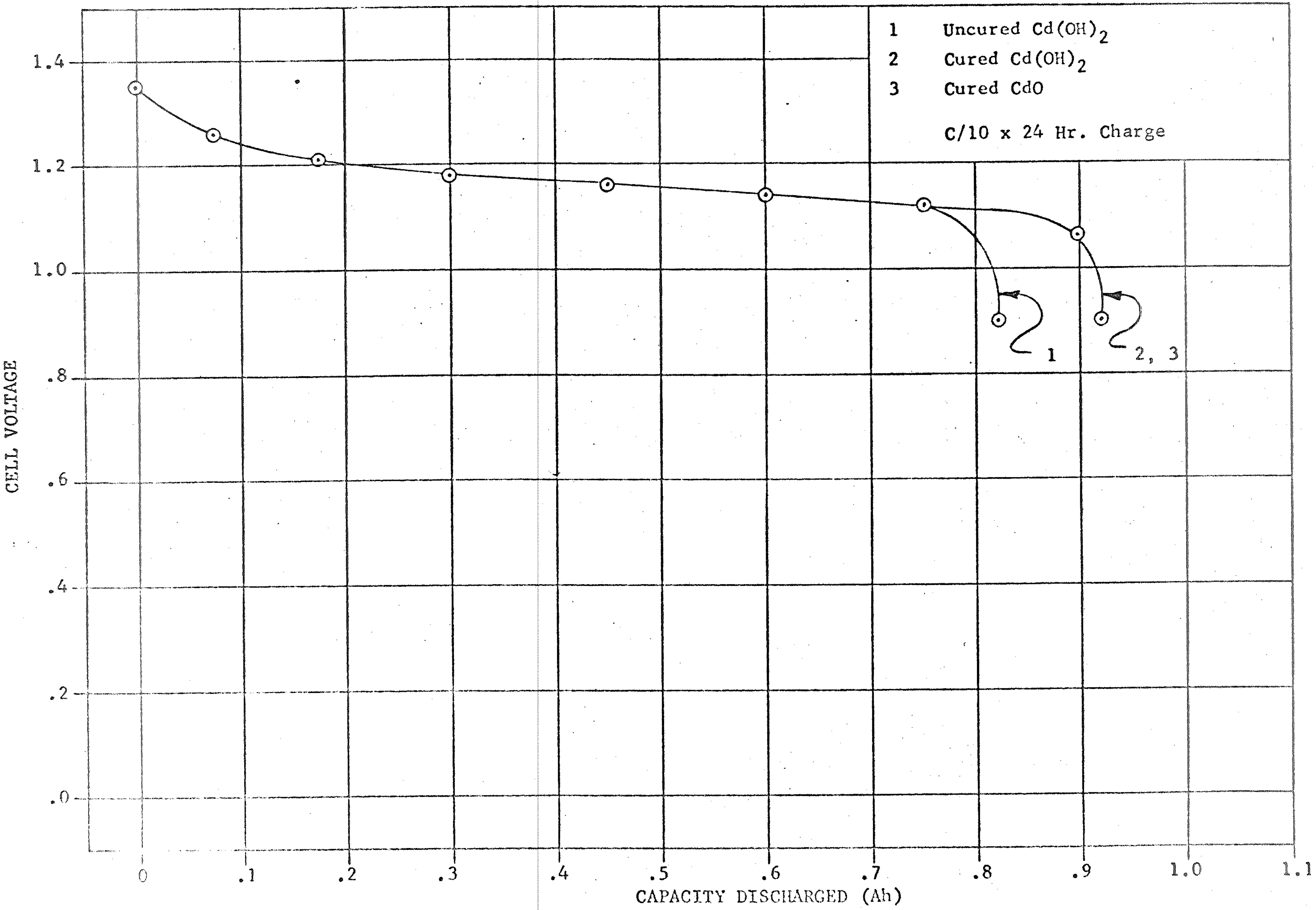

FIGURE 22 AVERAGE C/5 DISCHARGE, CYCLE #2 - PRE-CYCLING

4-3045

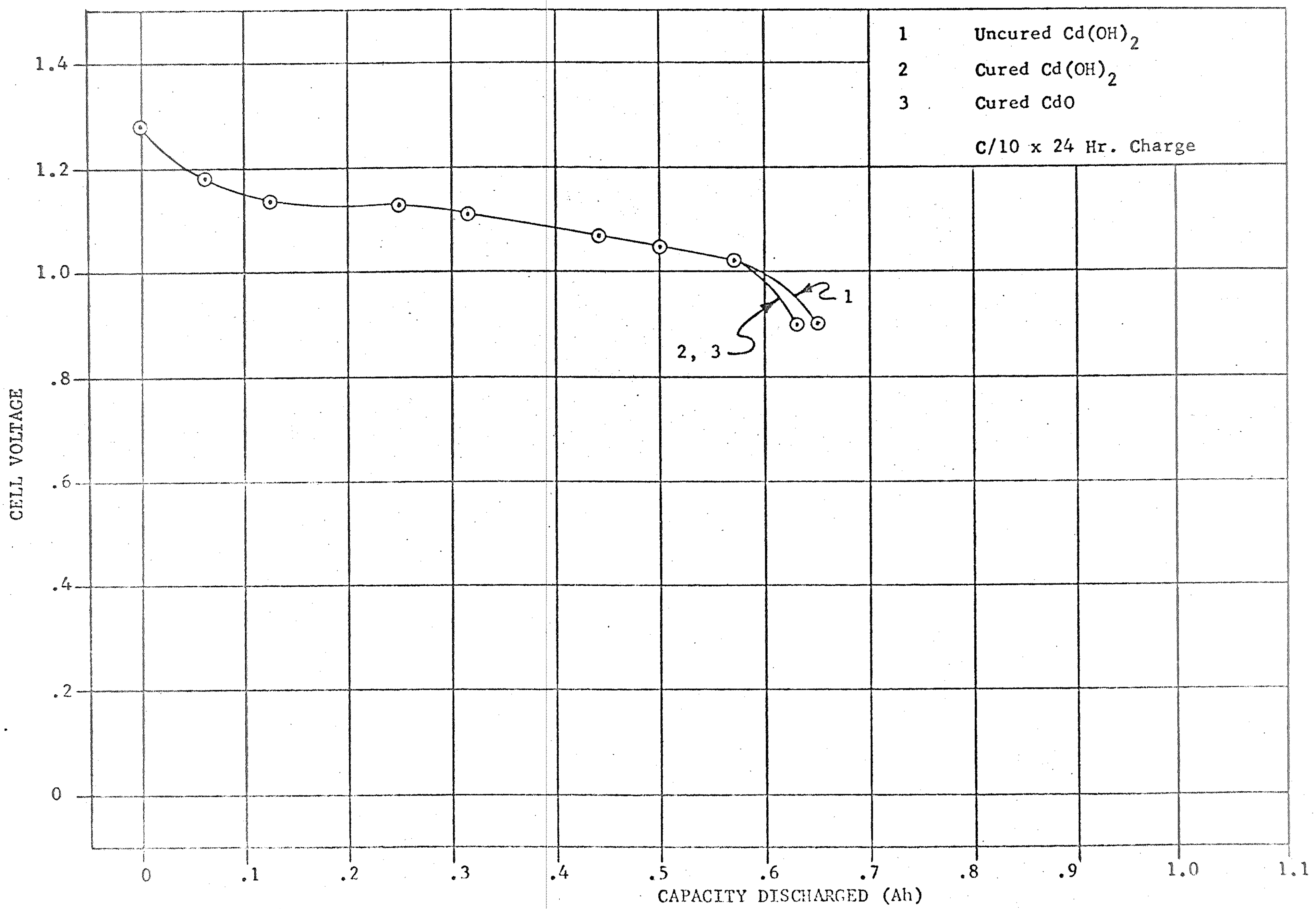

FIGURE 23 AVERAGE C/1 DISCHARGE CYCLES 1 & 2 - PRE-CYCLING

4-3046

TABLE XXXVIII. - END OF DISCHARGE VOLTAGE Vs CYCLE NUMBER

CYCLE NO.	GROUP 1	GROUP 2	GROUP 3
	EODV *	EODV	EODV
1	1.18	1.20	1.21
16	1.15	1.18	1.18
32	1.13	1.16	1.17
48	1.13	1.16	1.17
64	1.13	1.16	1.17
80	1.13	1.16	1.17
96	1.13	1.16	1.17
112	1.13	1.16	1.17

* EODV - End of Discharge Voltage

The Table shows that the Group 1 (uncured $Cd(OH)_2$) cells cycle 30 millivolts below Group 2 (cured $Cd(OH)_2$) cells and 40 millivolts below Group 3 (cured CdO) cells.

On Cycle 113, the discharge was allowed to continue until the cells reached 0.9 V in order that the total capacity be determined. The results of this test are shown in Figure 24 and are summarized and compared to the pre-cycling C/1 capacity in Table XXXIX.

TABLE XXXIX. - TOTAL CAPACITY AFTER CYCLING (Cycle 113)
Discharged at C/1 (0.6A)

GROUP	CAPACITY TO 0.9V (Cycle 113)	PRECYCLING CAPACITY	% CAPACITY RETENTION
1	0.47 Ah	0.65 Ah	73%
2	0.51 Ah	0.63 Ah	81%
3	0.57 Ah	0.63 Ah	91%

(4) Post Cycle Tests

After the completion of cycling, the cells were subjected to two cycles at each of the following rates: C/10, C/5, and C/1. The discharge curves of this cycling are shown in Figures 25-30, and the capacity data is summarized in Table XL.

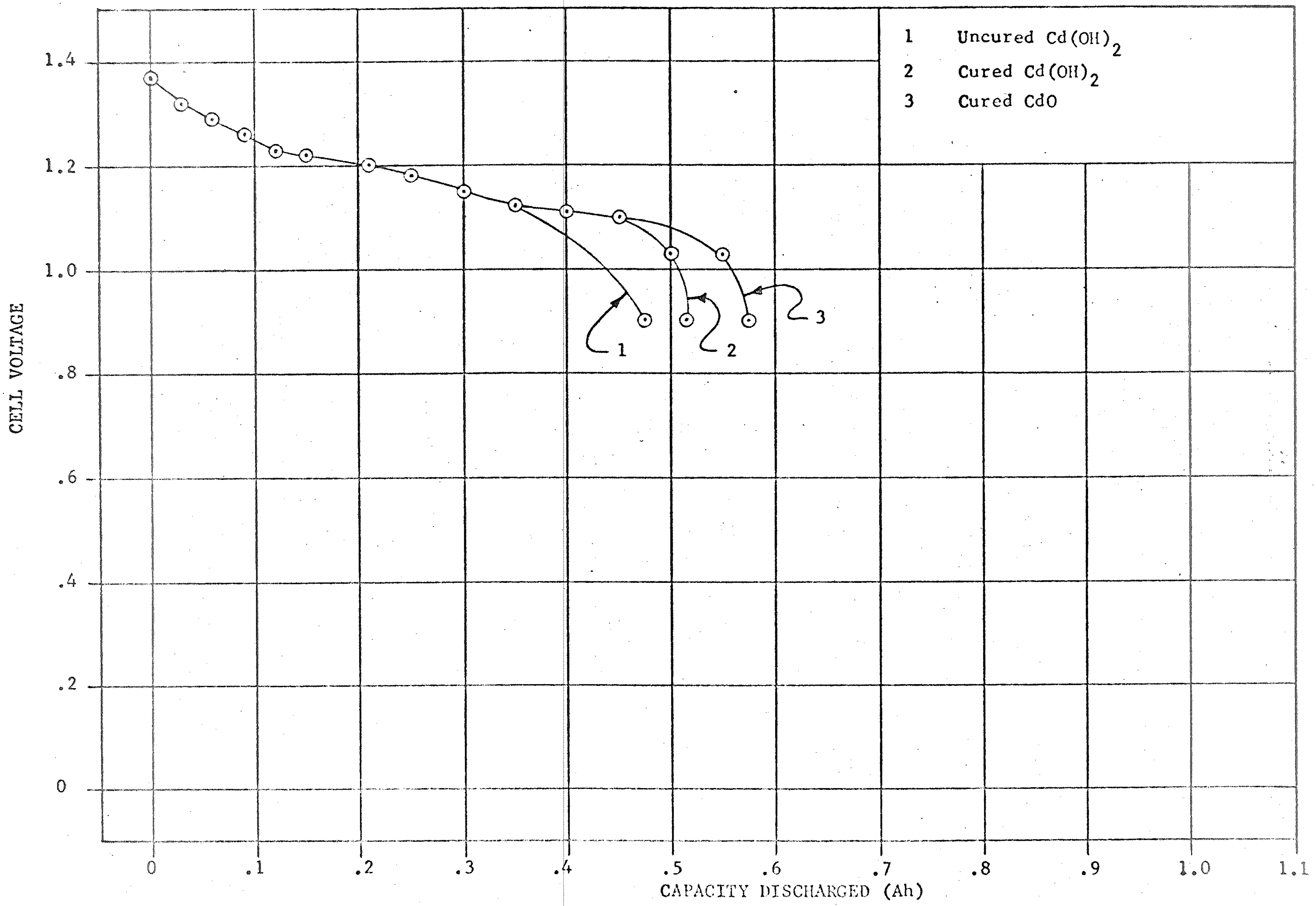

FIGURE 24 AVERAGE RESIDUAL CAPACITY - DISCHARGE CYCLE 113

4-3047

TABLE XL. - AVERAGE POST CYCLING CAPACITIES

RATE	FIGURE NO.	GROUP 1	GROUP 2	GROUP 3
		UNCURED $Cd(OH)_2$	CURED $Cd(OH)_2$	CURED CdO
C/10	25	0.60	0.73	0.76
C/5	26	0.59	0.68	0.68
C/1	27	0.53	0.45	0.45
C/10	28	0.68	0.74	0.74
C/5	29	0.60	0.62	0.60
C/1	30	0.45	0.36	0.36

The post cycling capacity data indicate about a 70% retention in capacity at all rates as compared to the precycling data.

In general, the cured CdO performed on a par with the cured $Cd(OH)_2$ and both fared better than the uncured $Cd(OH)_2$. However, at the C/1 rate, the uncured $Cd(OH)_2$ averaged about 15% greater capacity over the short life.

(5) Physical Condition of Electrodes

Physical examination of the electrodes indicated that those negative plates fabricated from the cured $Cd(OH)_2$ and cured CdO had good structural integrity. However, those electrodes fabricated from the uncured $Cd(OH)_2$ showed blisters and flaking. Their physical integrity appears to diminish with cycle life.

From the above results, it was concluded that the cured electrodes were superior to the uncured electrodes and that the teflonated CdO, which was produced by heat treating $Cd(OH)_2$, performs on a par with the basic teflonated $Cd(OH)_2$.

All subsequent work was performed with the teflonated CdO. The use of this material eliminated the need for determining the exact ratio of $Cd(OH)_2$ to CdO in the teflonated $Cd(OH)_2$, and thus, improved the quality control of keeping the ratio constant from one lot to another.

2. Preparation & Characterization of Various Particle Size Negative Electrode Materials

In this phase of the program, experiments were conducted to determine the effect of particle size on electrode performance.

a. Preparation of Various Particle Size $Cd(OH)_2$

The standard size $Cd(OH)_2$ prepared by adding a 2% excess of 8.07N KOH directly to 8.26N $Cd(NO_3)_2$, adding water and washing immediately. The larger size $Cd(OH)_2$ was prepared in the same manner as the standard material, except that the $Cd(OH)_2$ was allowed to digest in the mother liquor for one week at 70°C.

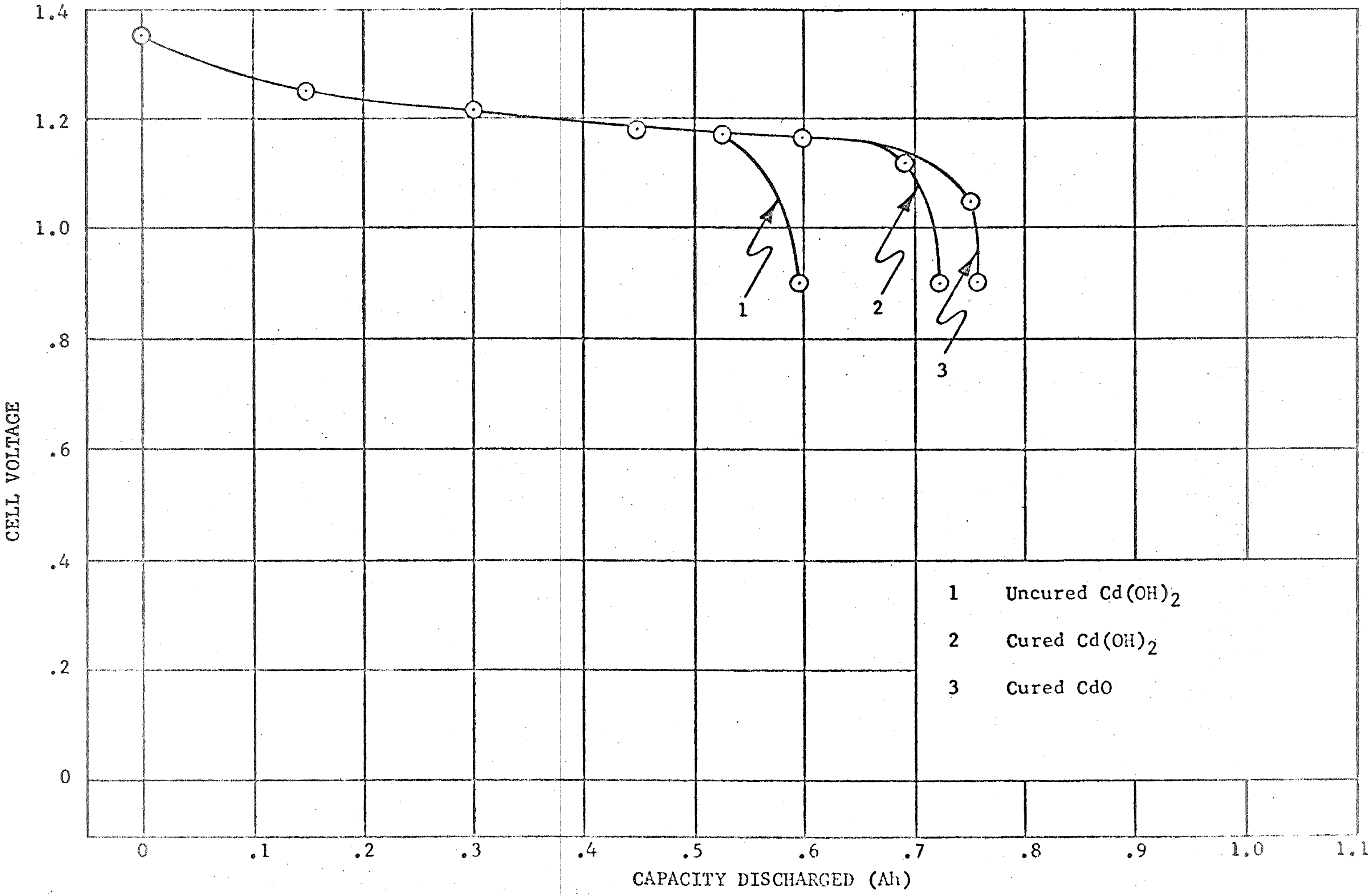

FIGURE 25

AVERAGE DISCHARGE
C/10 x 24 Hr. Charge
C/10 Discharge #1
Post Cycling

4-3065

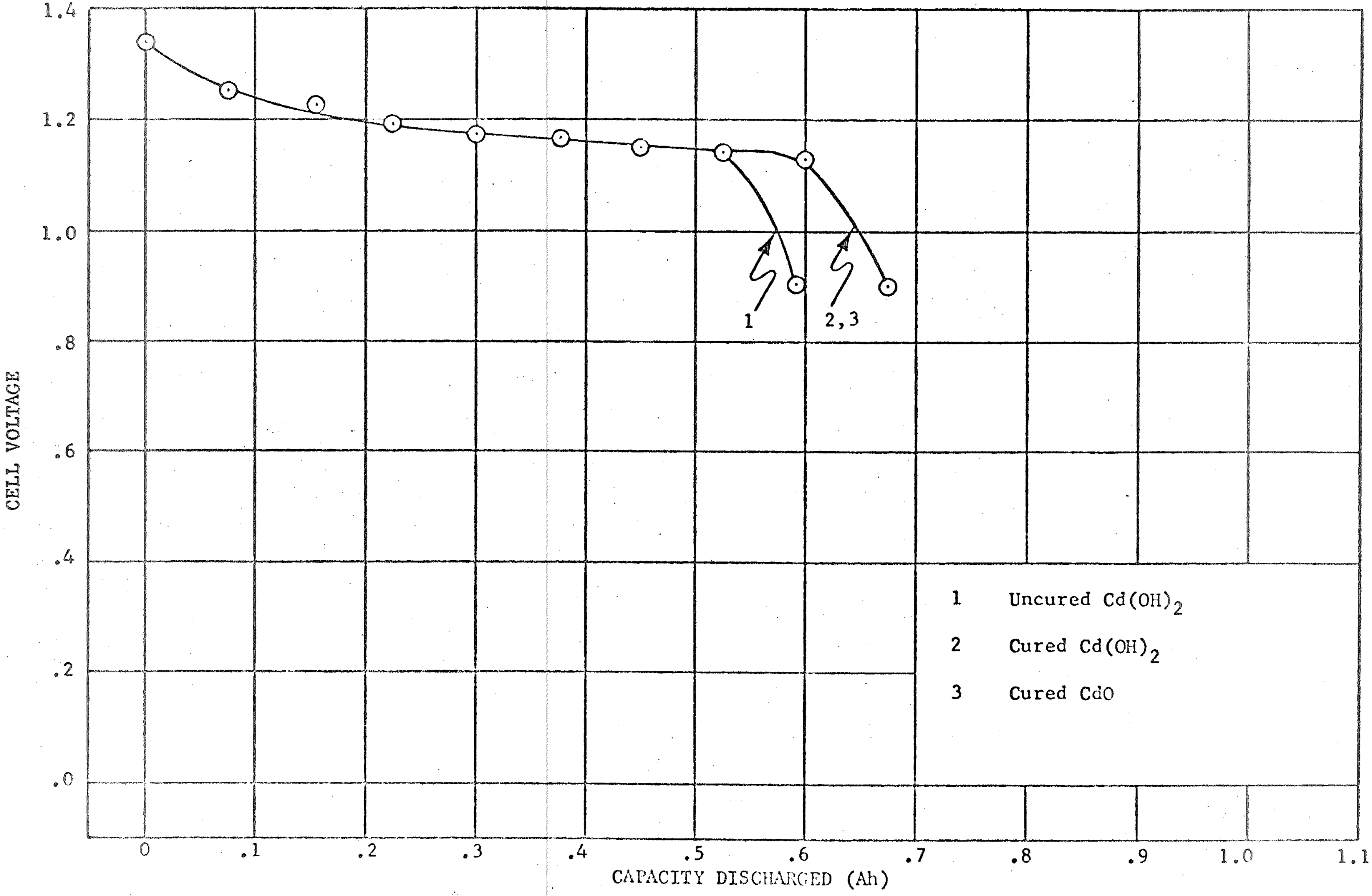

FIGURE 26

AVERAGE DISCHARGE
C/10 x 24 Hr. Charge
C/5 Discharge #1
Post Cycling

4-3066

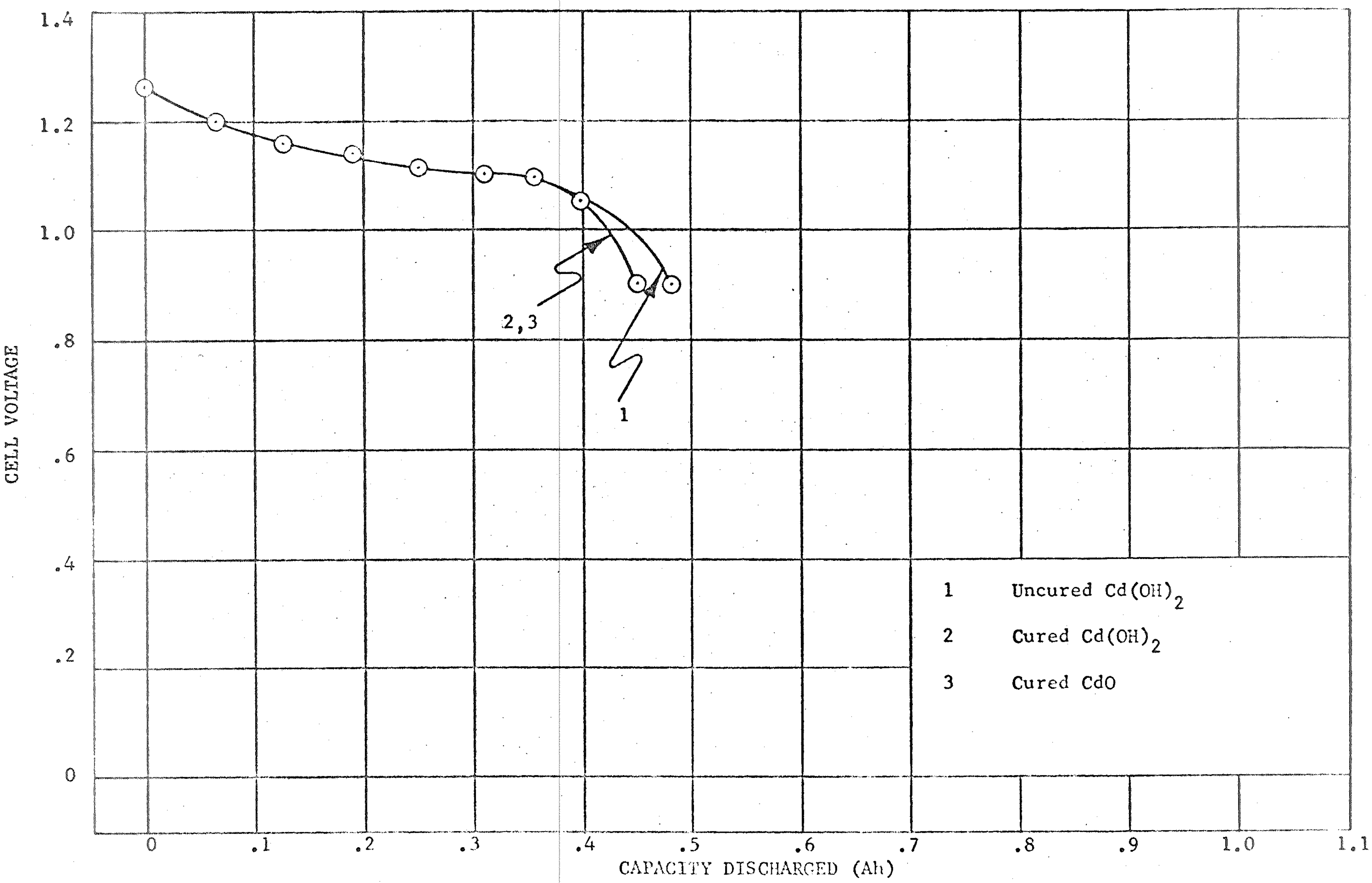

FIGURE 27

AVERAGE DISCHARGE

C/10 x 24 Hour Charge
C/1 Discharge #1
Post Cycling

4-3067

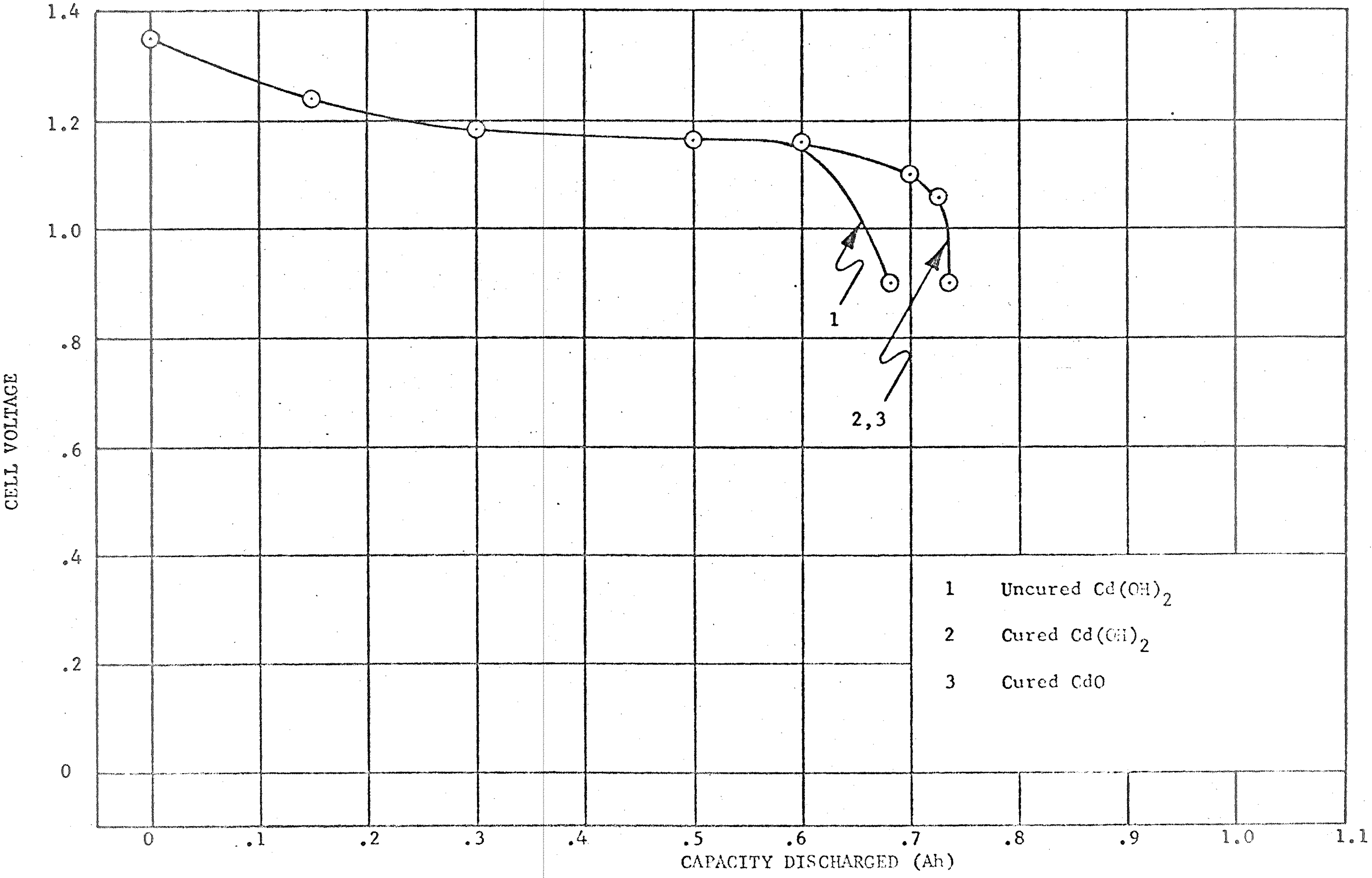

FIGURE 28

AVERAGE DISCHARGE

C/10 x 24 Hour Charge
C/10 Discharge #2
Post Cycling

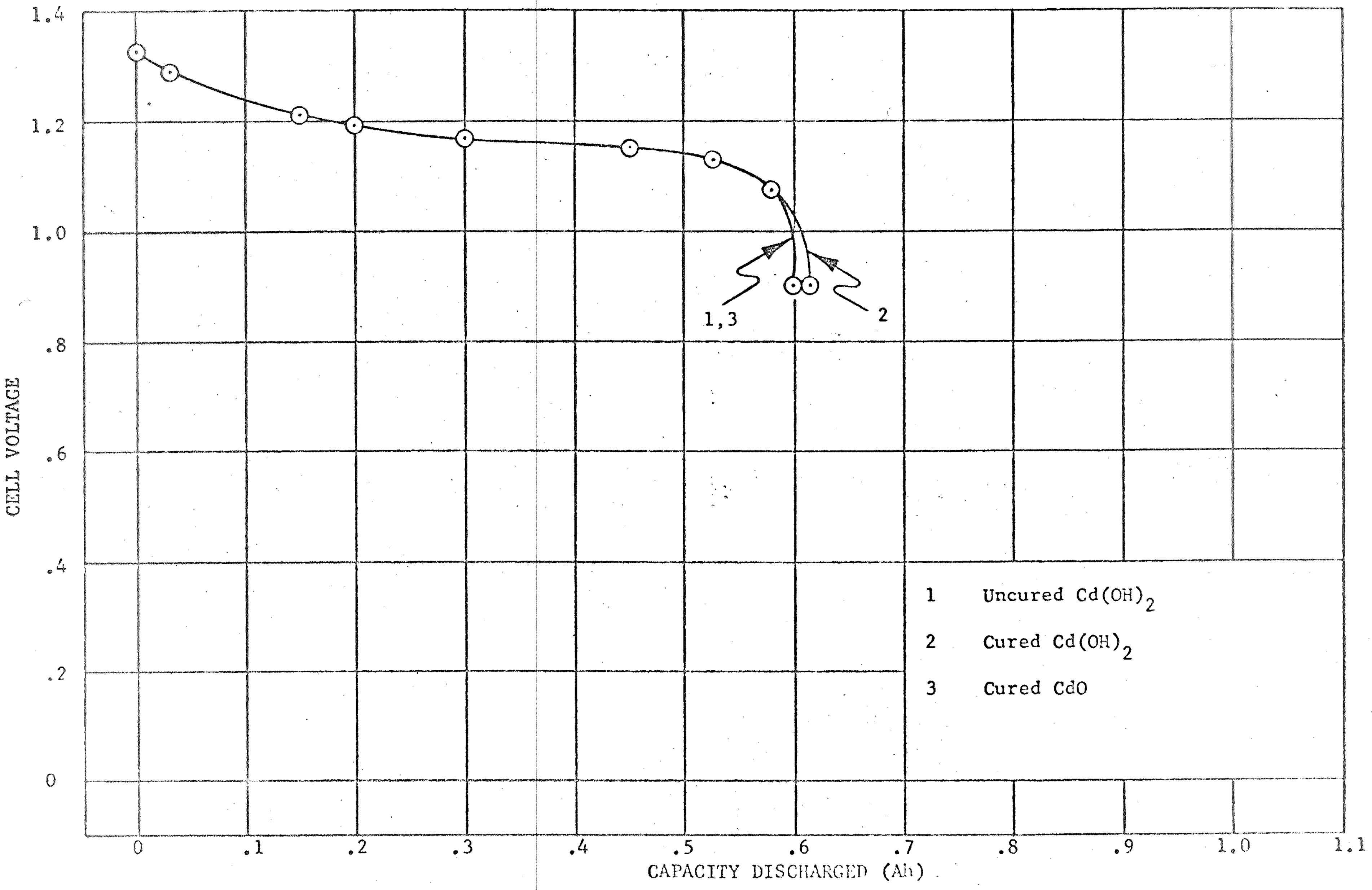

FIGURE 29

AVERAGE DISCHARGE

C/10 x 24 Hour Charge
C/5 Discharge #2
Post Cycling

4-3069

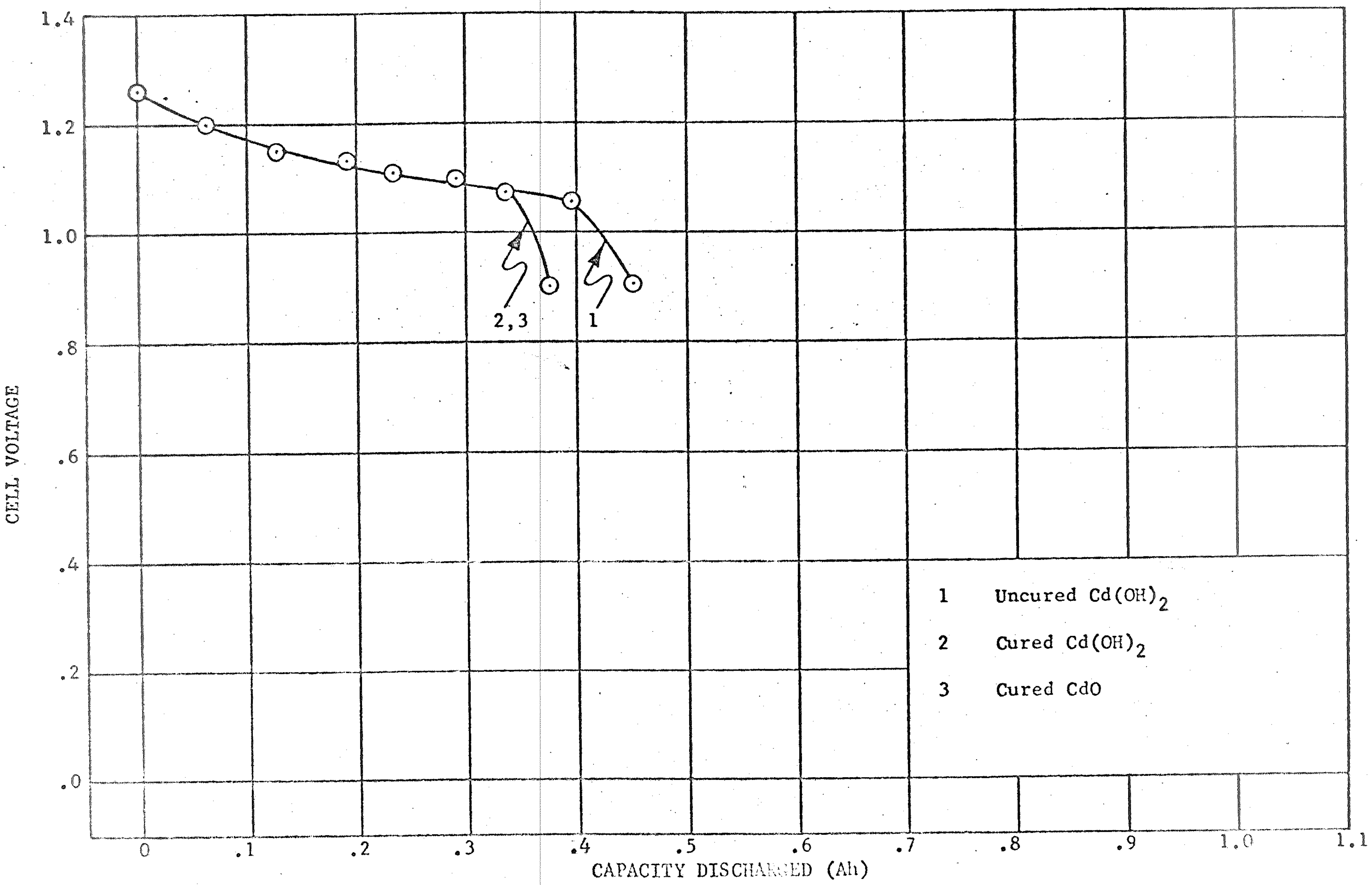

FIGURE 30

AVERAGE DISCHARGE

C/10 x 24 Hour Charge
C/1 Discharge #2
Post Cycling

4-3070

The smaller particle size $Cd(OH)_2$ was prepared by first diluting the $Cd(OH)_2$ with a ten-fold volume of distilled water prior to precipitating with KOH.

b. Measurement of $Cd(OH)_2$ Particle Size

(1) Method

The particle size distribution was measured by applying Stokes Law to particles falling through a viscous medium. A photograph of the apparatus is shown in Figure 31.

The equations used for determining the particle diameters are given below:*

Stokes Law for the velocity of a particle falling through a viscous (air) medium is:

$$V = \frac{2\ gr^2\ (\rho_p - \rho_1)}{9\eta} \qquad (1)$$

where: V = velocity in cm/sec
g = acceleration due to gravity (980 cm/sec^2)
r = radius of particle in cm
ρ_p = density of particle [$Cd(OH)_2$ = 4.8 g/cc CdO = 8.2 g/cc]
ρ_1 = density of settling medium (H_2O = 1 g/cc)
η = viscosity of settling medium (H_2O = 8.74×10^{-3} poises)

To obtain the particle diameter, in microns, as a function of the time (t) it takes to fall through a given height (h) under any acceleration, we can rearrange the equation to the form:

$$\frac{h}{t} = \frac{2a \times 60\ (\rho_p - \rho_1)}{9\eta} \times \frac{d^2 \times 10^8}{4} \qquad (2)$$

where: h = distance particle falls through (in cm)
t = time for particle to fall through distance h (in minutes).
a = acceleration of particle (in cm/sec^2)
60 = converts seconds to minutes
d = particle diameter (in cm)
$\frac{d^2}{4}$ = r^2(cm^2)
10^8 = converts particle size from cm to microns

---

* Handbook of Chemistry and Physics, 36, 2833, Chemical Rubber Publishing Co., Cleveland (1955)

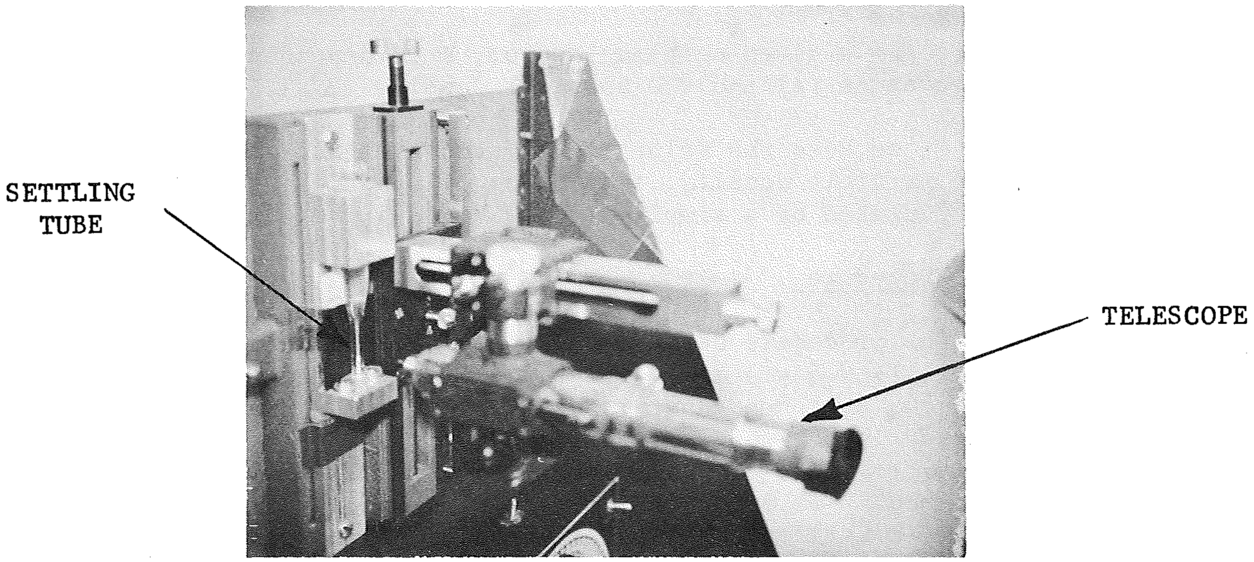

FIGURE 31. APPARATUS FOR DETERMINING PARTICLE SIZE DISTRIBUTION

Rearranging (2) to a useful form, we get:

$$d = \sqrt{\frac{18 \times 10^{8}}{(\ _{p} - 1)\ a \times 60}} \times \sqrt{h/t} \qquad (3)$$

For any particle, we can simplify (3) to:

$$d^{2} = \frac{K}{t} \qquad (4)$$

where, for a given settling medium, K is dependent upon the acceleration (a) and the particle density (ρ_p).

If we keep the value for "a" constant and calculate K for a one particle density, then K for all particle densities can be calculated by a simple ratio.

(2) Procedure

The procedure used for making the measurement was as follows: A small (~ 0.5 gm) amount of solid was added to 50 ml of a 70% water-30% acetone dispersing medium. The mixture was then agitated in a blender for 3 minutes.

About 1 ml of the dispersed solid was added to the settling medium (distilled water) contained in the measuring tube (shown in the foreground on the far left of Figure 31). The particles were allowed to settle and the height of the column of settled particles, as a function of time, was measured.

Since only large particles will settle under the acceleration due to gravity in a reasonable length of time, the smaller particles are made to settle out by accelerating them (at a known value) in a centrifuge.

(3) Results

The results of the particle size determinations are shown in Figures 32 through 36. The graphs show plots of the particle size distribution as percent of particles finer than a given particle size.

Figure 32 shows the particle size distribution for the standard particle size $Cd(OH)_2$. The size distribution is almost linear between 0.5 and 50 microns with 50% of the material finer than 5 microns and 50% coarser than 5 microns.

Figure 33 is the distribution of CdO prepared from the standard size $Cd(OH)_2$. This distribution is also roughly linear except that the particles are smaller, ranging from 0.25 to 35 microns with the median particle size 2 microns.

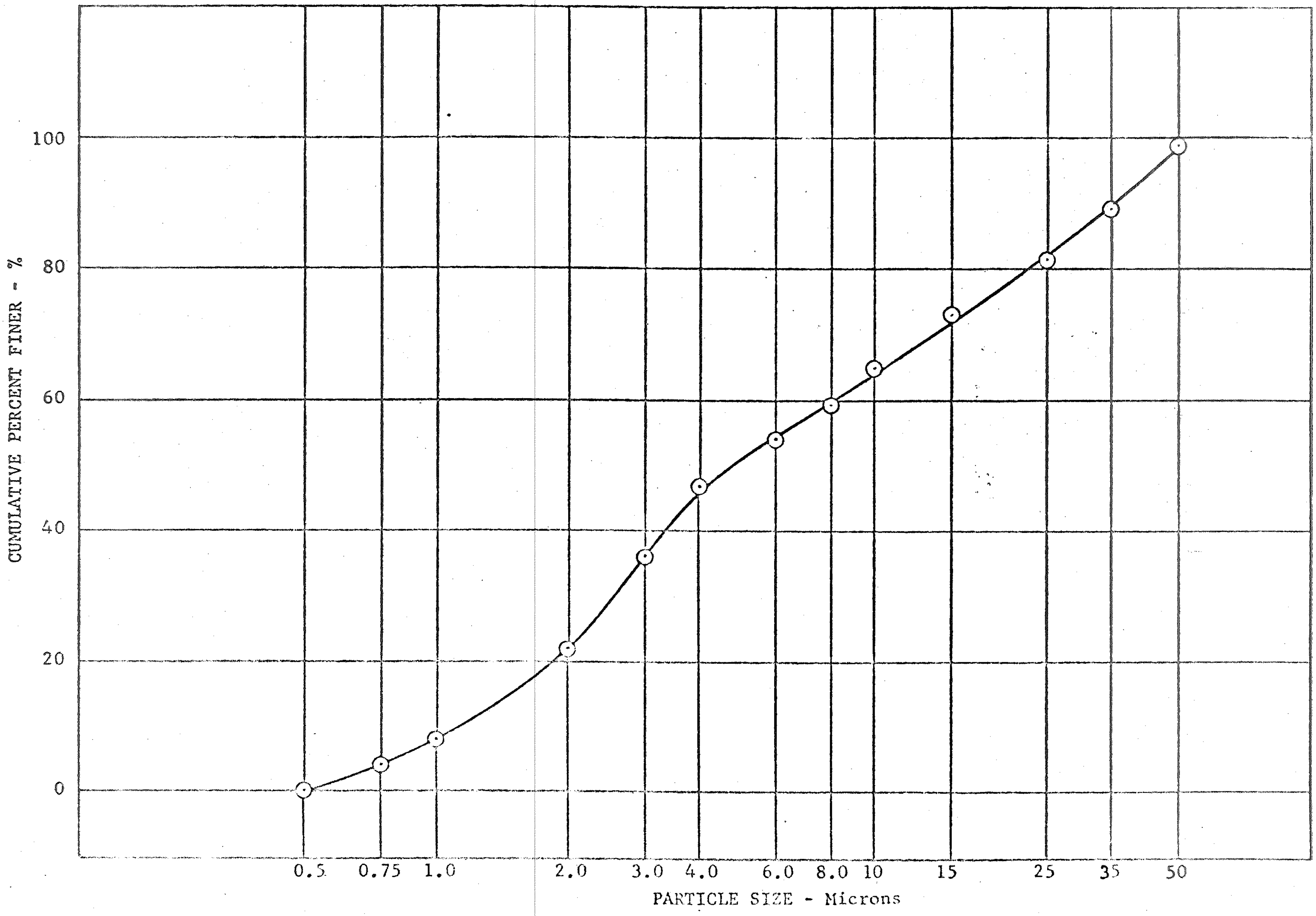

FIGURE 32 PARTICLE SIZE DISTRIBUTION, STANDARD SIZE $Cd(OH)_2$

4-3054

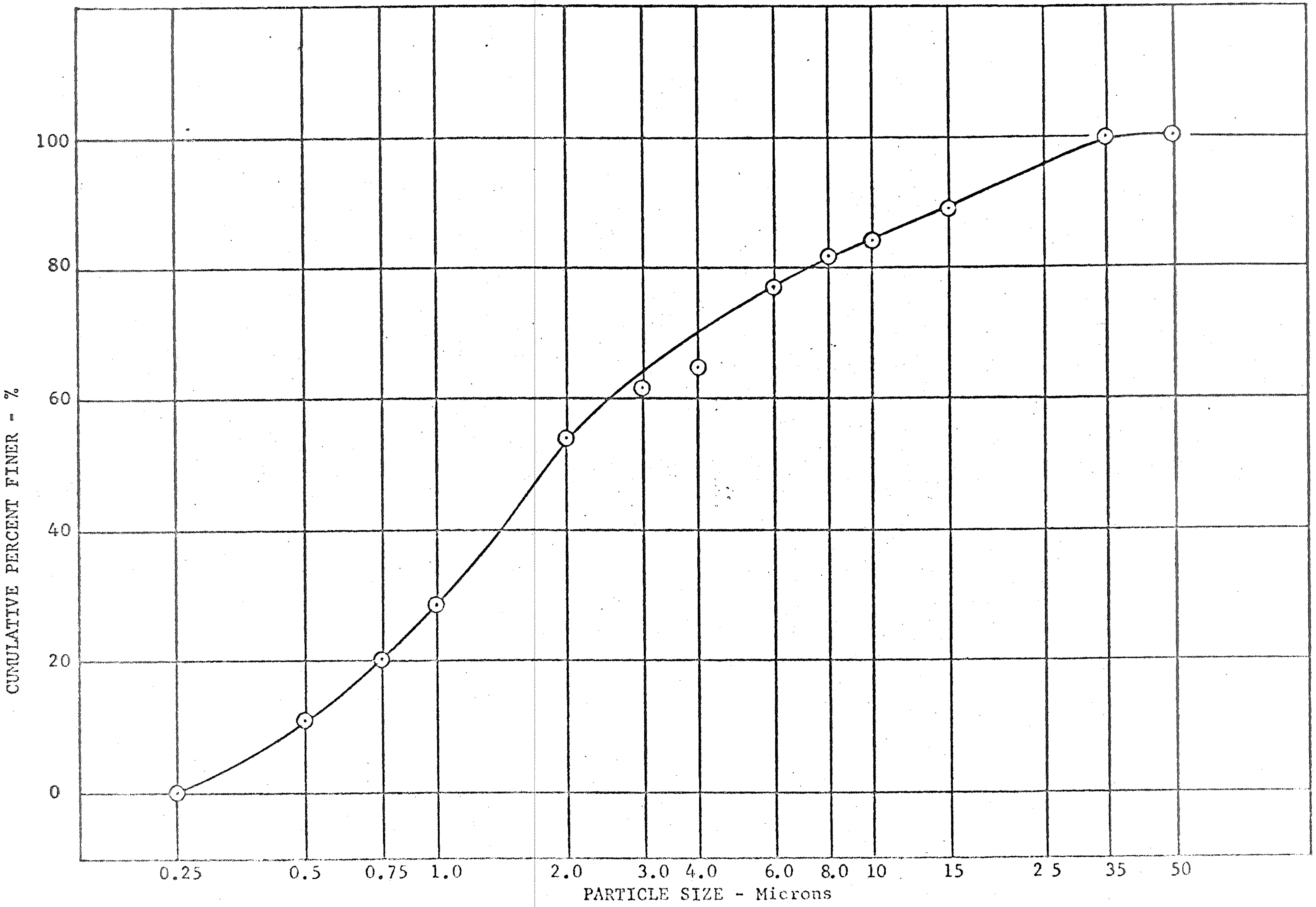

FIGURE 33 PARTICLE SIZE DISTRIBUTION, STANDARD SIZE CdO

4-3055

Figure 34 gives the particle size distribution of the large size $Cd(OH)_2$ and is similar to Figure 32. However, the median particle size is 6 microns.

Figure 35 gives the distribution of the small size $Cd(OH)_2$. This material has a considerably smaller particle size than the standard or large size material. The particle size range is 0.5 to 25 microns and the median size is 2 microns. However, the most outstanding feature of this material is that it is considerably more uniform than any of the other samples. Almost 90% of the material is smaller than 4 microns and more than 75% of the material is smaller than 3 microns.

The size distribution of the small CdO, shown in Figure 36 has the same general features as that of the small $Cd(OH)_2$, shown in Figure 35, except the material is generally made up of smaller and even more uniform particles, with the largest size particles ranging between 10 and 15 microns. Almost 80% of the material lies between 0.25 and 2 microns with a median particle size of .1 micron. One explanation for the CdO being smaller than the $Cd(OH)_2$ is that the abstraction of water from $Cd(OH)_2$ may cause the crystals to fracture. However, this may not be the only explanation.

c. Measurement Of BET Surface Area

The BET surface area measurements were performed by Micromeretics Instrument Corp., Norcross Georgia 30071, on a Model 2100A Orr Surface Area-Pore Volume Analyzer. The BET surface areas are shown in Table XLI.

TABLE XLI. - BET SURFACE AREA

MATERIAL	SPECIFIC SURFACE AREA (m^2/gm)
Small $Cd(OH)_2$ - Unteflonated	4.0
Standard $Cd(OH)_2$ - Unteflonated	4.8
Teflonated $Cd(OH)_2$ (Standard Size) - Uncured	8.4
Teflonated $Cd(OH)_2$ (Standard Size) - Cured	7.1
Teflonated CdO (Small Size) - Cured	14.2
Teflonated CdO (Standard Size) - Cured	19.7
Teflonated CdO (Large Size) - Cured	21.9

The reason for the standard and large size materials having a larger surface area than the small size may be due to the fact that the larger particles, being made up of many small grains, apparently exhibit a higher porosity than the smaller particles by exposing both internal and external surfaces.

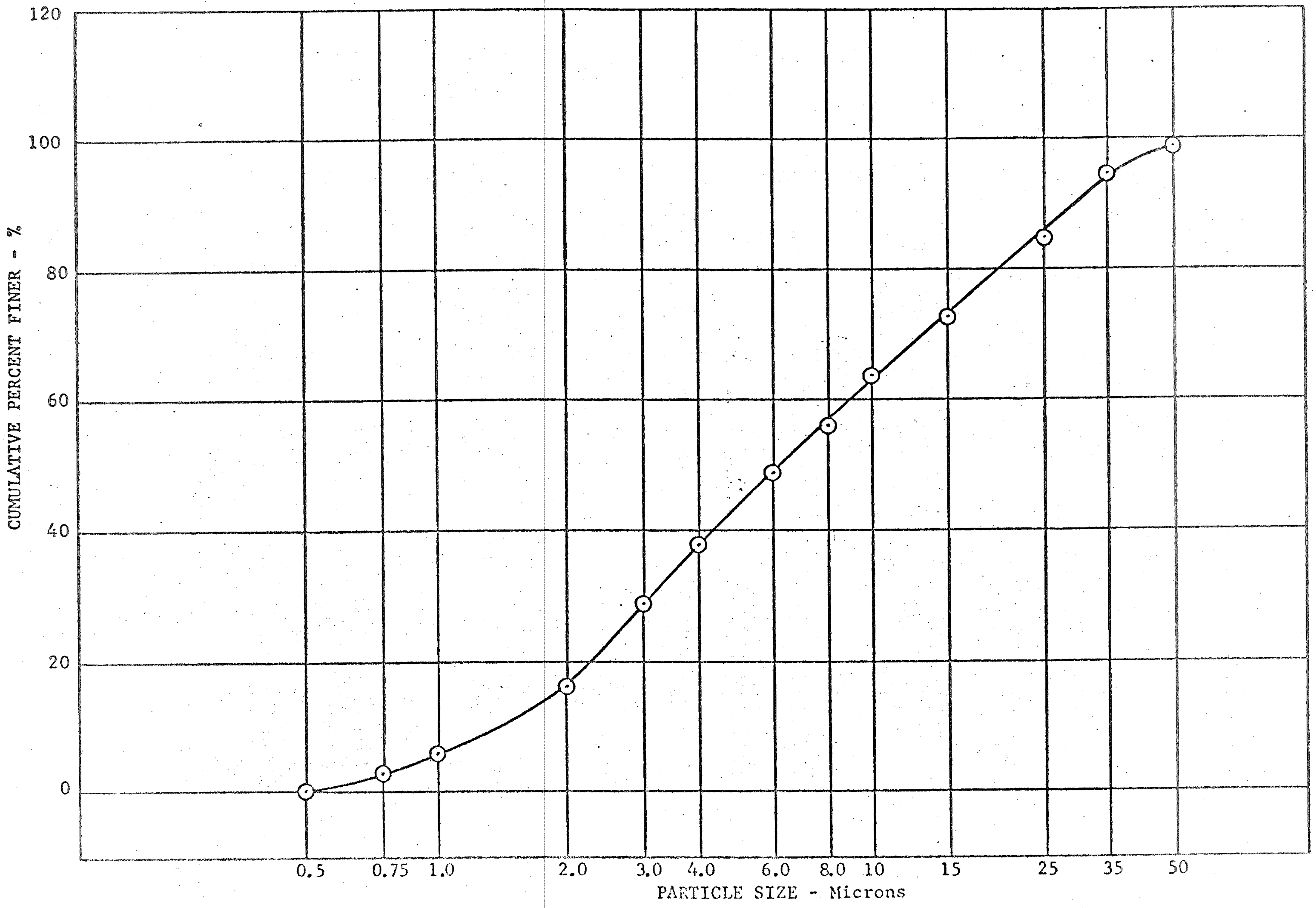

FIGURE 34 PARTICLE SIZE DISTRIBUTION, LARGE SIZE $Cd(OH)_2$

4-3056

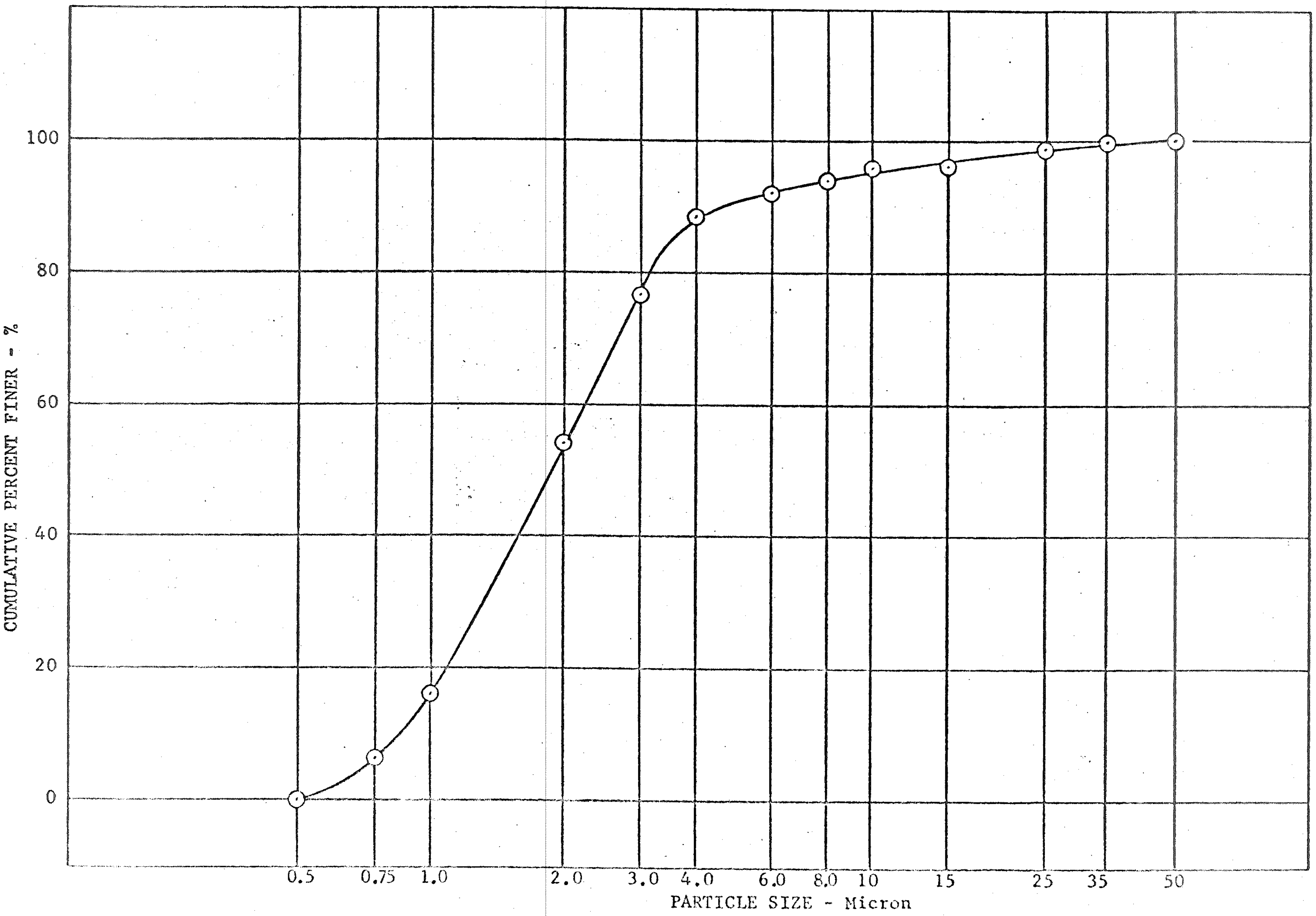

FIGURE 35 PARTICLE SIZE DISTRIBUTION, SMALL SIZE $Cd(OH)_2$

4-3057

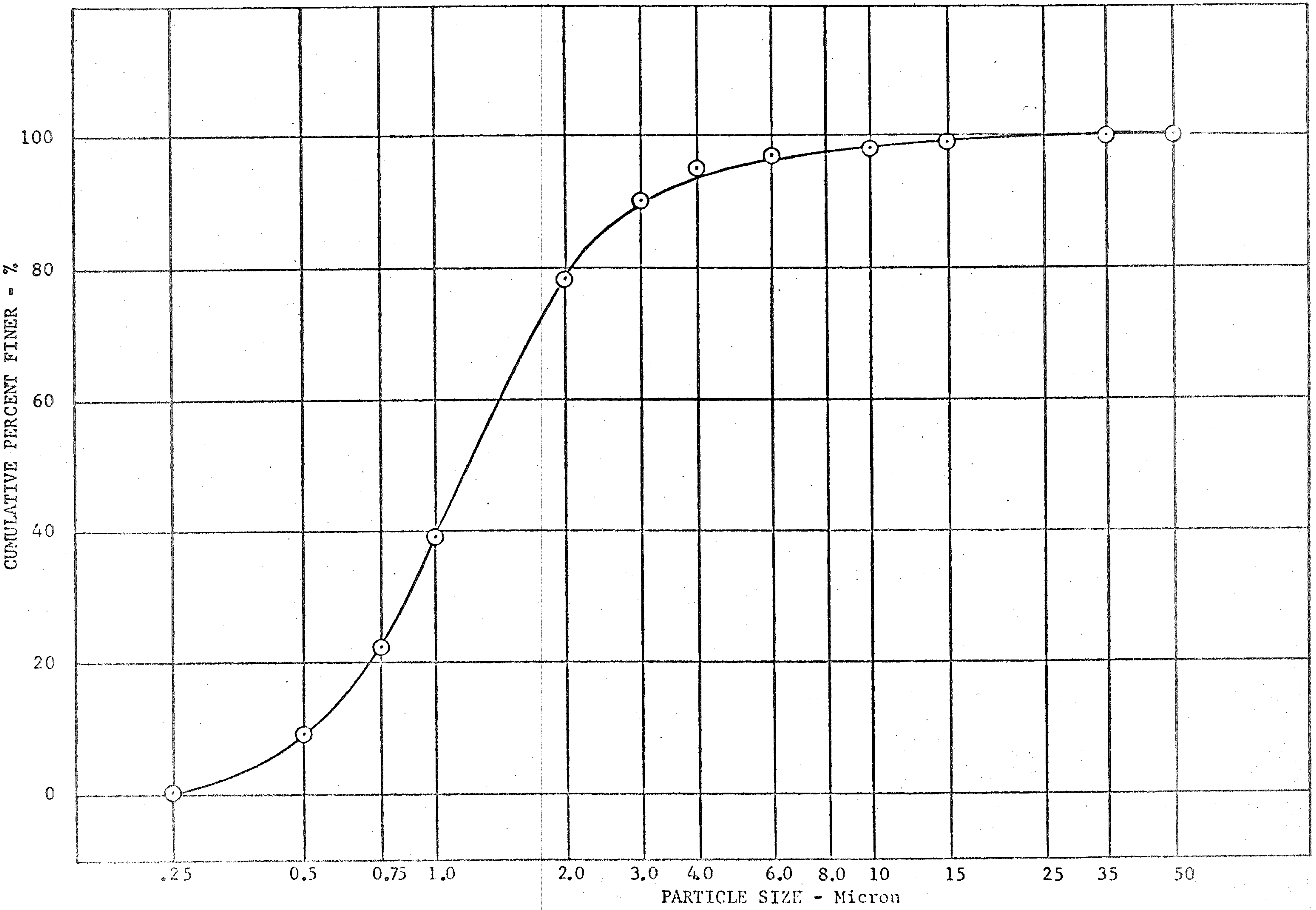

FIGURE 36 PARTICLE SIZE DISTRIBUTION, SMALL SIZE CdO

4-3058

The results of the specific surface area determination by the BET method provided additional justification for our choice of cured teflonated cadmium oxide (prepared from our own cadmium hydroxide) as the preferred starting material for our negative electrodes as the BET data indicated that the teflonated CdO has a BET specific surface area two to three times that of the teflonated $Cd(OH)_2$.

3. Testing of Various Particle Size Negative Electrodes

a. Electrode Fabrication

Twelve negative electrodes were fabricated. Four electrodes of each of three groups, as shown in Table XLII, were prepared.

TABLE XLII. - NEGATIVE ELECTRODE TYPES

GROUP	NAME	FORMULATION
4	Small CdO	Small particle size $Cd(OH)_2$ converted to CdO and teflonated
5	Standard CdO	Standard particle size $Cd(OH)_2$ converted to CdO and teflonated
6	Large CdO	Large particle size $Cd(OH)_2$ converted to CdO and teflonated

The theoretical capacity of the electrodes was calculated as 1.5 Ah.

b. Electrode Characterization

One electrode of each group was set aside for measurements of porosity.

(1) Porosity

Electrode porosity was measured by methanol abosrption as described earlier.

Table XLIII lists the results of the porosity determinations.

TABLE XLIII. - POROSITY DETERMINATION

GROUP	NAME	THICKNESS (Mils)	% POROSITY
4	Small CdO	30	49.7
5	Standard CdO	31	49.5
6	Large CdO	32	52.0

c. Cell Testing

(1) Fabrication

Three electrodes of each group were fabricated into three plate negative limiting nickel-cadmium cells (total 9 cells) and activated with 34% KOH and allowed to soak 24 hours.

(2) Pre-Cycling Tests

After activation, the cells were formed by charging at C/10 for 24 hours and discharging at C/5 to 0.9 V.

Figure 37 is an average discharge curve for each type of electrode and shows that the average capacity for the standard CdO is 1.09 Ah while for the other two groups (i.e., small CdO and large CdO), the average capacity is 1.04 Ah.

The cells were then given two C/10 discharges as shown in Figures 38 and 39. A second C/5 discharge is shown in Figure 40. The two C/1 discharges are shown in Figures 41 and 42. The capacity results are summarized in Table XLIV.

TABLE XLIV. - AVERAGE PRE-CYCLING CAPACITIES

RATE	GROUP 4	GROUP 5	GROUP 6
	Small CdO	Standard CdO	Large CdO
C/5	1.04 Ah	1.09 Ah	1.04 Ah
C/10	1.00	1.06	0.96
C/10	0.91	0.96	0.86
C/5	0.79	0.86	0.77
C/1	0.54	0.62	0.56
C/1	0.50	0.63	0.54

(3) Cycling

After completion of the precycling tests, the cells were placed on a one-week cycle at 50% depth of discharge. The cycle consisted of a 30 minute discharge at the C/1 (0.6 A) rate and a 60 minute charge at 0.33 A. The rates were chosen based on the C/1 capacity data obtained in the pre-cycling tests.

Table XLV shows the end of discharge voltage versus cycle number for each group of cells.

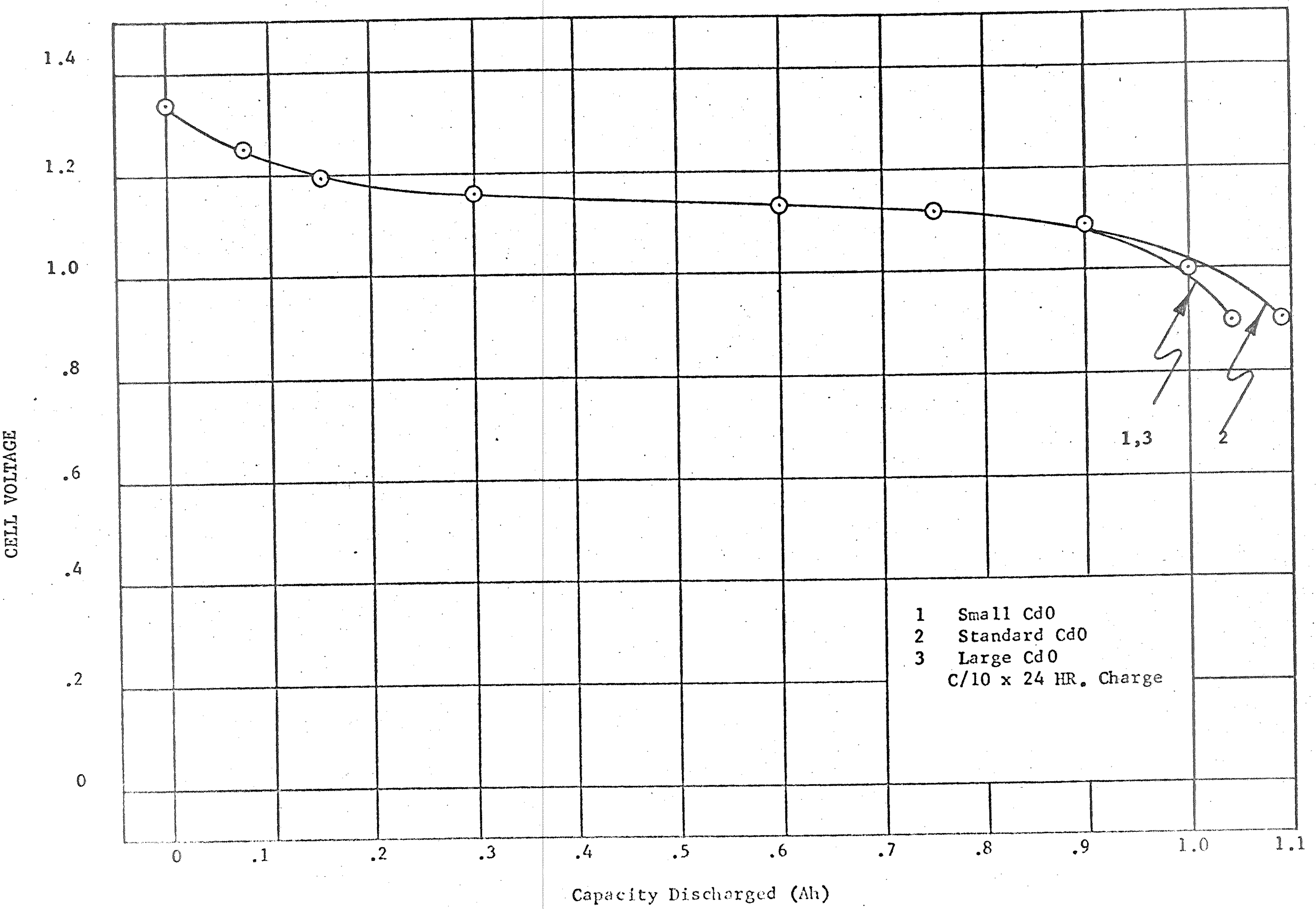

FIGURE 37 AVERAGE FORMATION DISCHARGE C/5 - PRE-CYCLING

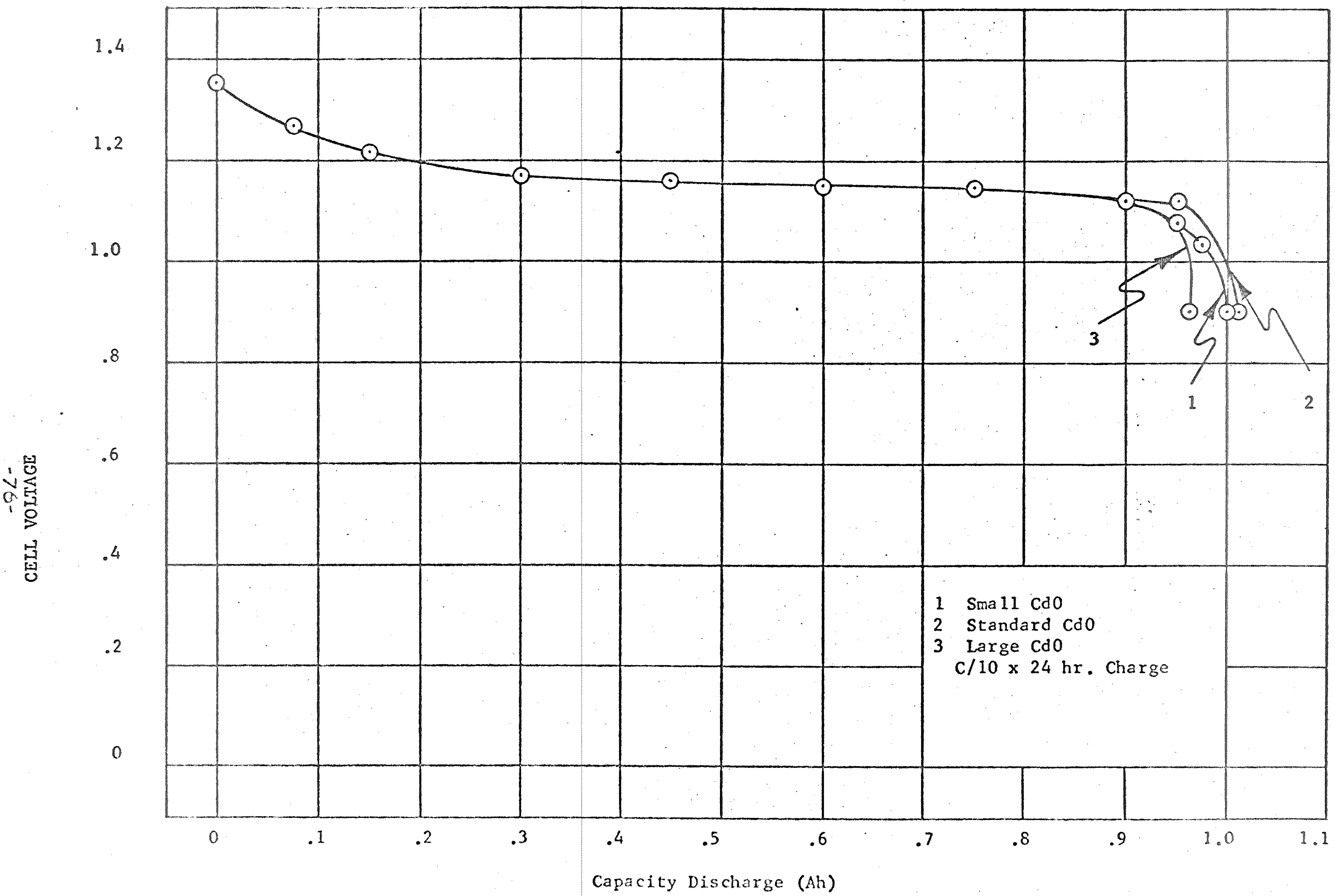

FIGURE 38 AVERAGE C/10 DISCHARGE CYCLE #1 PRE-CYCLING

4-3074

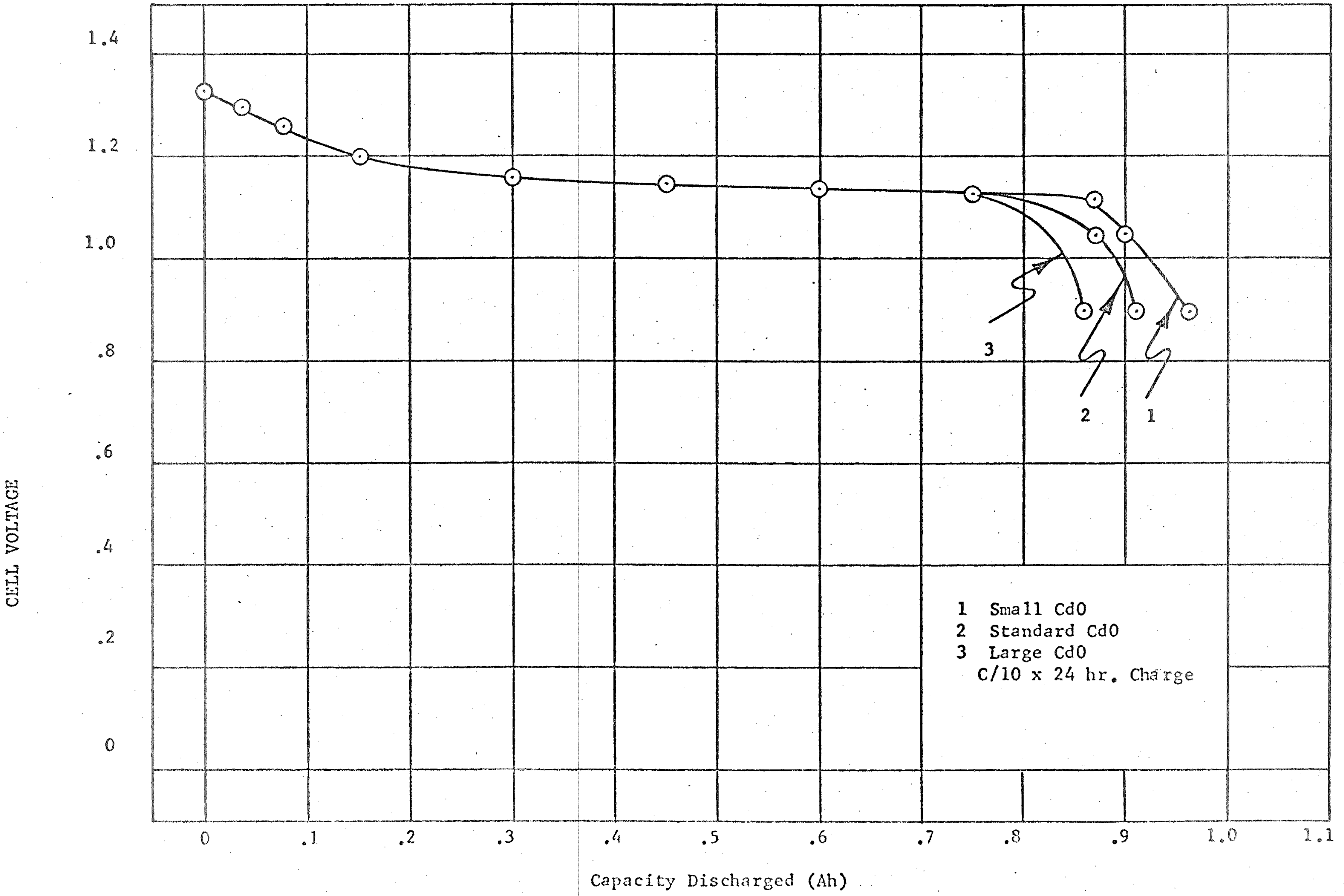

FIGURE 39 AVERAGE C/10 DISCHARGE CYCLE #2 PRE-CYCLING

4-3075

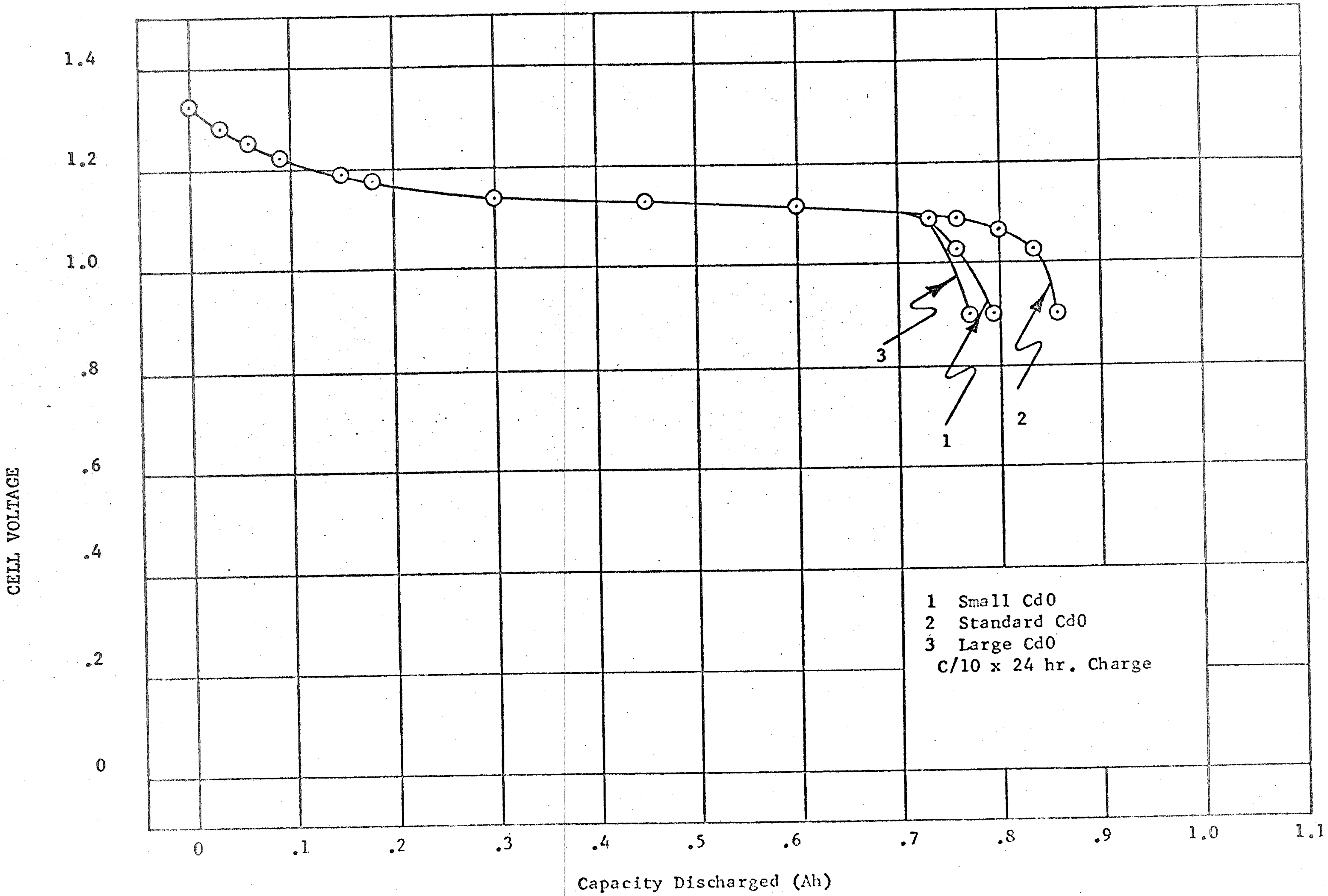

FIGURE 40 AVERAGE C/5 DISCHARGE CYCLE #2 PRE-CYCLING

4-3079

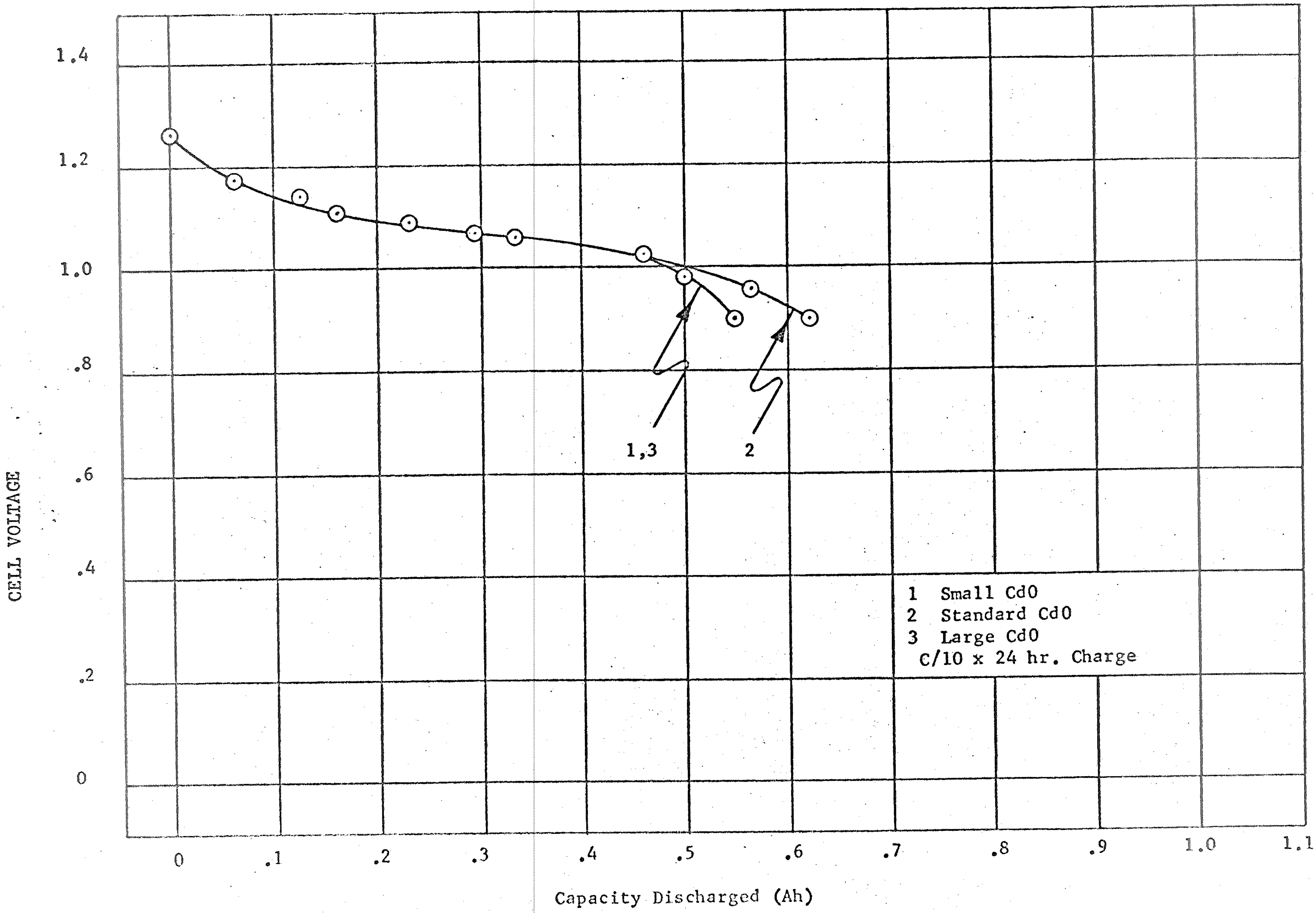

FIGURE 41 AVERAGE C/1 DISCHARGE CYCLE #1 PRE-CYCLING

4-3076

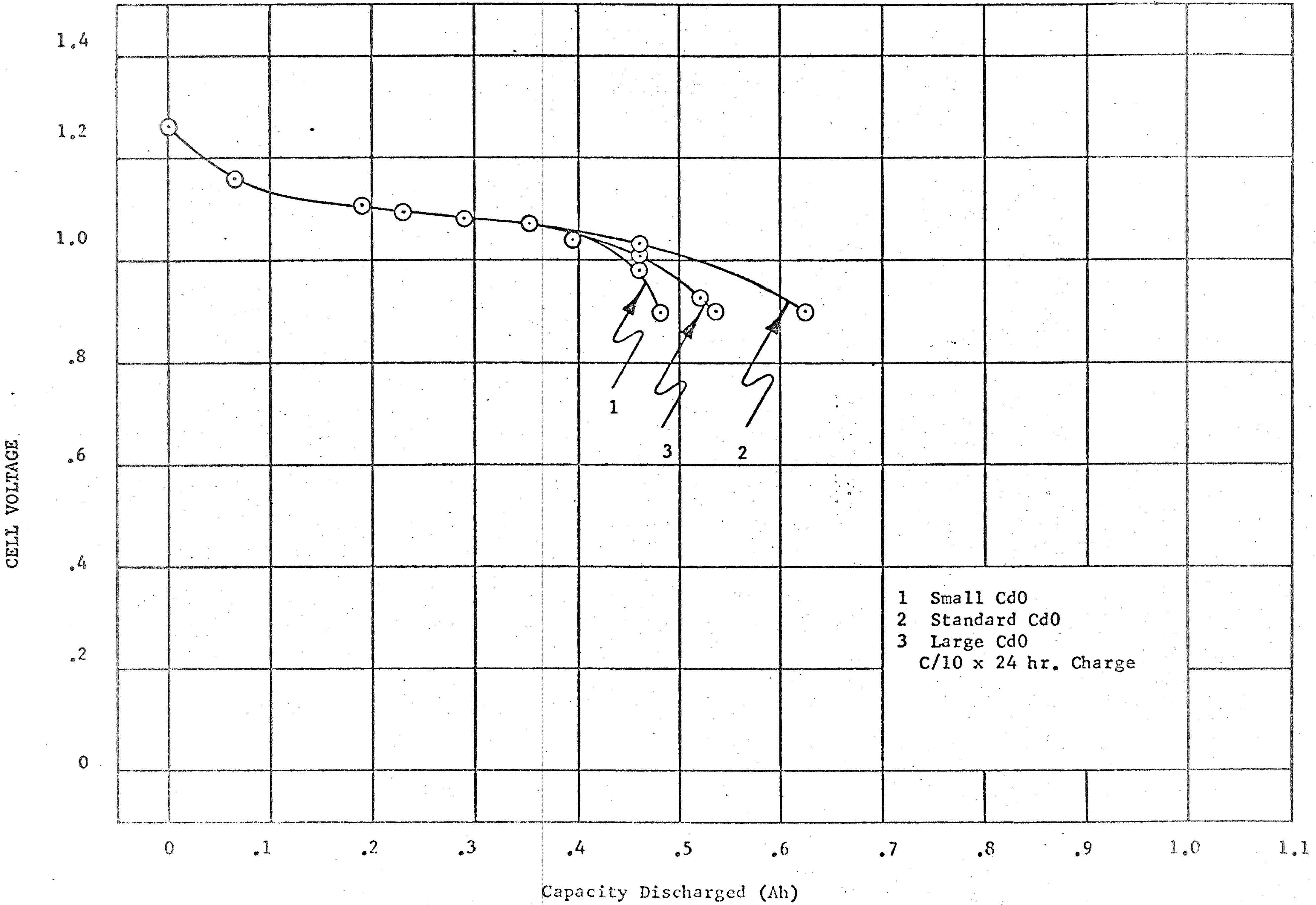

FIGURE 42 AVERAGE C/1 DISCHARGE CYCLE #2 PRE-CYCLING

TABLE XLV. - END OF DISCHARGE VOLTAGE Vs CYCLE NUMBER

CYCLE NO.	GROUP 4	GROUP 5	GROUP 6
	EODV*	EODV*	EODV*
1	1.13	1.19	1.12
16	1.10	1.17	1.12
32	1.09	1.17	1.12
48	1.08	1.16	1.12
64	1.08	1.16	1.11
80	1.08	1.15	1.10
96	1.08	1.15	1.10
112	1.08	1.15	1.08

* EODV = End of Discharge Voltage

The Table shows that the Group 4 (small CdO) and Group 6 (large CdO) cycle 70 millivolts below the Group 5 (standard CdO) cells.

On Cycle 113, the discharge was allowed to continue until the cells reached 0.9 V in order that the total capacity be determined. The results of this test are shown in Figure 43 and are summarized and compared to the pre-cycling C/1 capacity in Table XLVI.

TABLE XLVI. - TOTAL CAPACITY AFTER CYCLING (Cycle 113) DISCHARGED AT C/1 (0.6 A)

GROUP	CAPACITY TO 0.9 V (Cycle 113)	PRE-CYCLING CAPACITY	PERCENT CAPACITY RETAINED
4	0.41 Ah	0.50 Ah	82%
5	0.55	0.63	88%
6	0.44	0.54	81%

(4) Post Cycle Testing

After the completion of cycling, the cells were subjected to two cycles at each of the following rates: C/10, C/5, C/1. The results of these tests are shown in Figures 44-49 and summarized in Table XLVII.

TABLE XLVII. - AVERAGE POST CYCLING CAPACITIES

RATE	FIGURE	GROUP 4	GROUP 5	GROUP 6
		Small CdO	Standard CdO	Large CdO
C/10	44	0.51 Ah	0.65 Ah	0.53 Ah
C/5	45	0.50	0.57	0.50
C/1	46	0.30	0.40	0.33
C/10	47	0.58	0.62	0.54
C/5	48	0.51	0.52	0.47
C/1	49	0.37	0.41	0.33

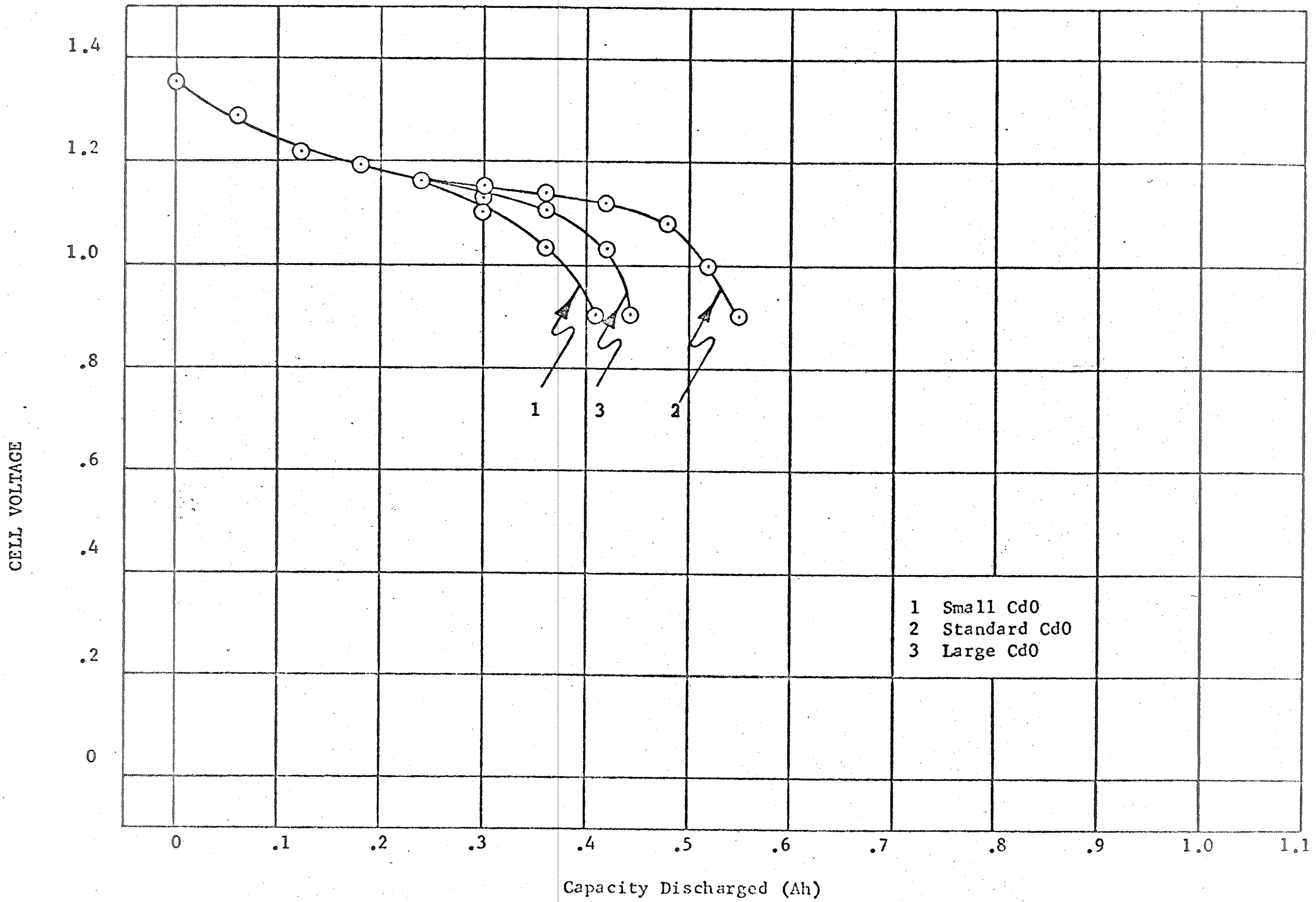

FIGURE 43 AVERAGE RESIDUAL CAPACITY DISCHARGE CYCLE 113

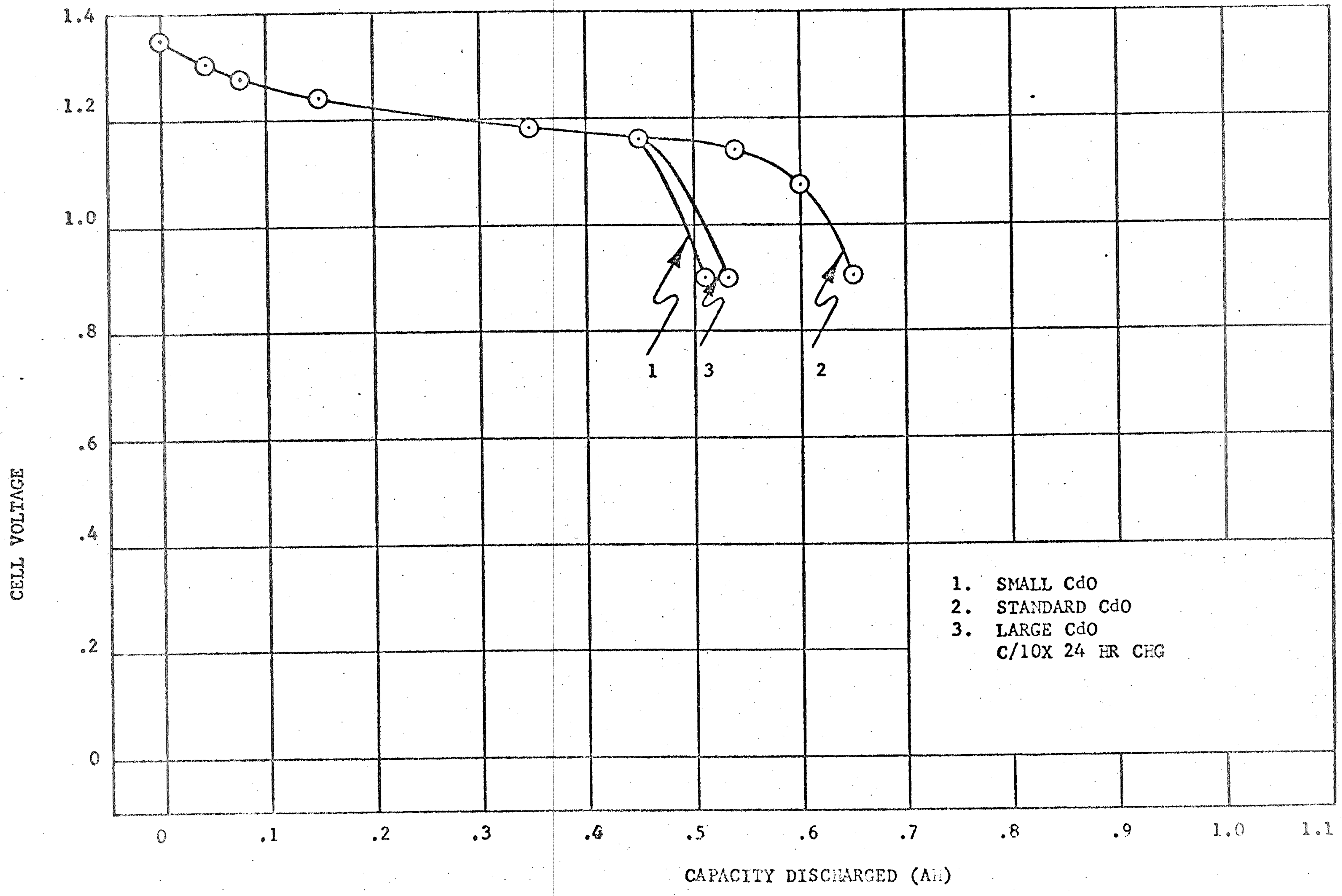

FIGURE 44 AVERAGE C/10 DISCHARGE CYCLE #1 POST CYCLING

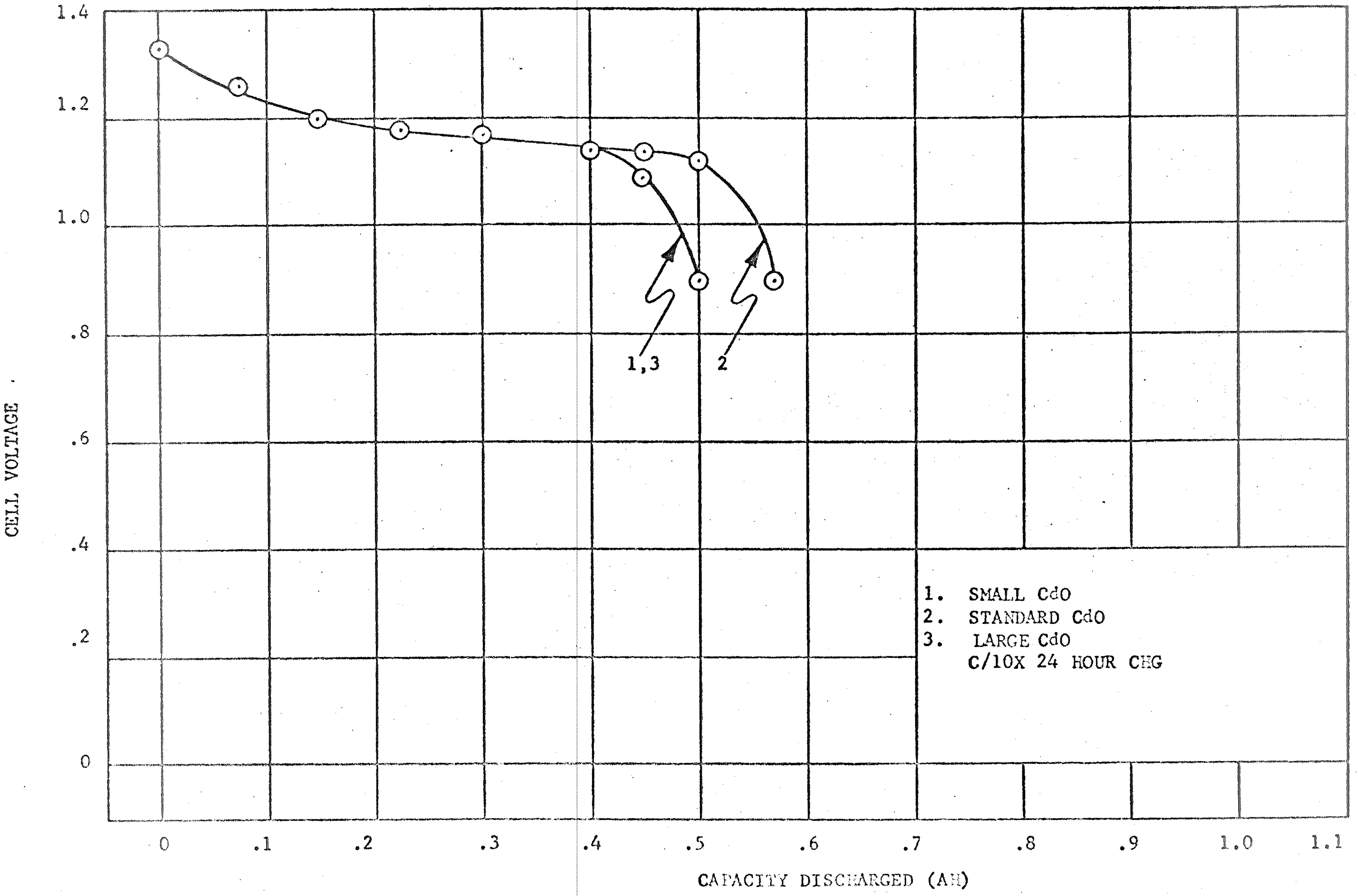

FIGURE 45 AVERAGE C/5 DISCHARGE, CYCLE #1 - POST CYCLING

4-3092

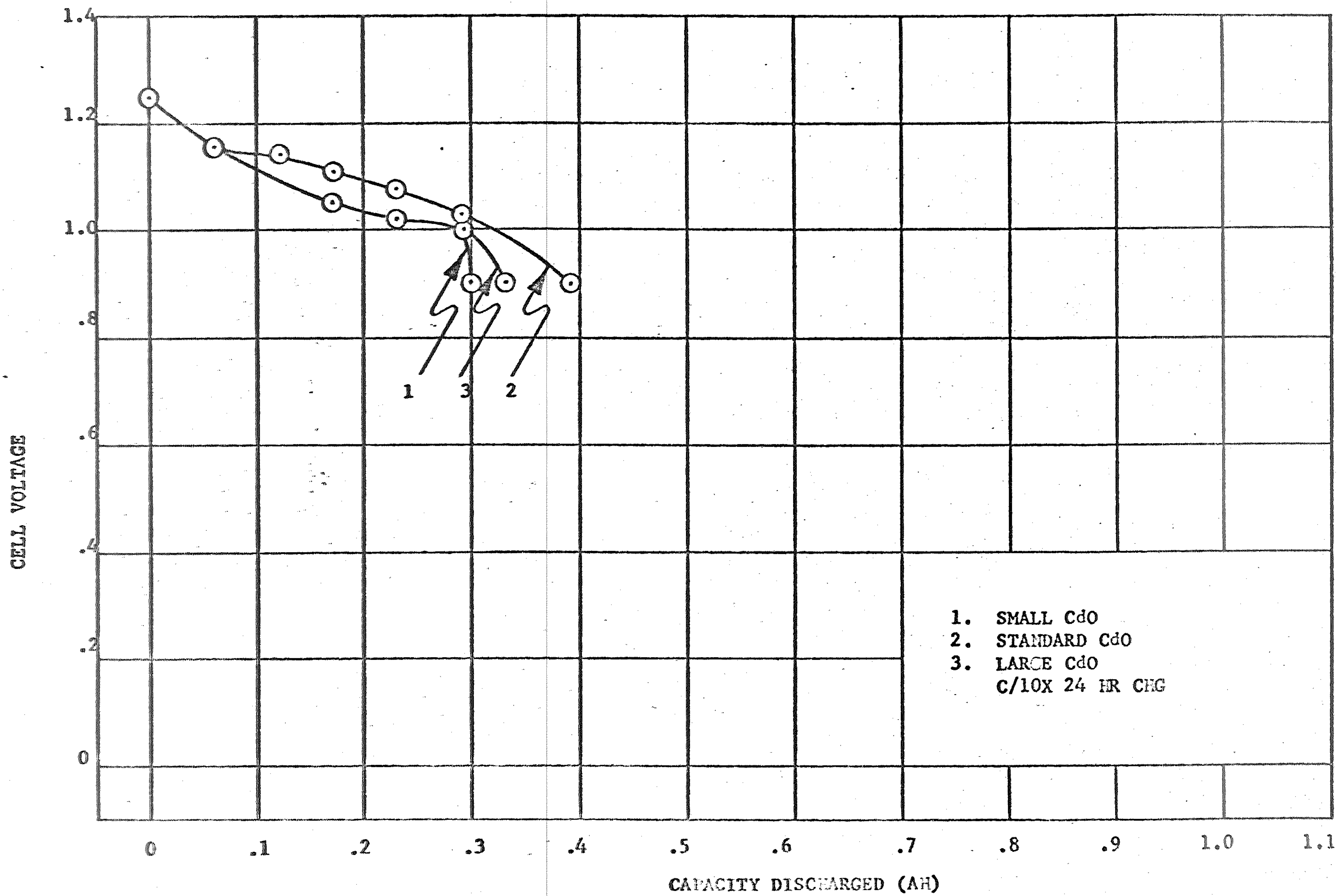

FIGURE 46 AVERAGE C/1 DISCHARGE CYCLE #1 POST CYCLING

4-3093

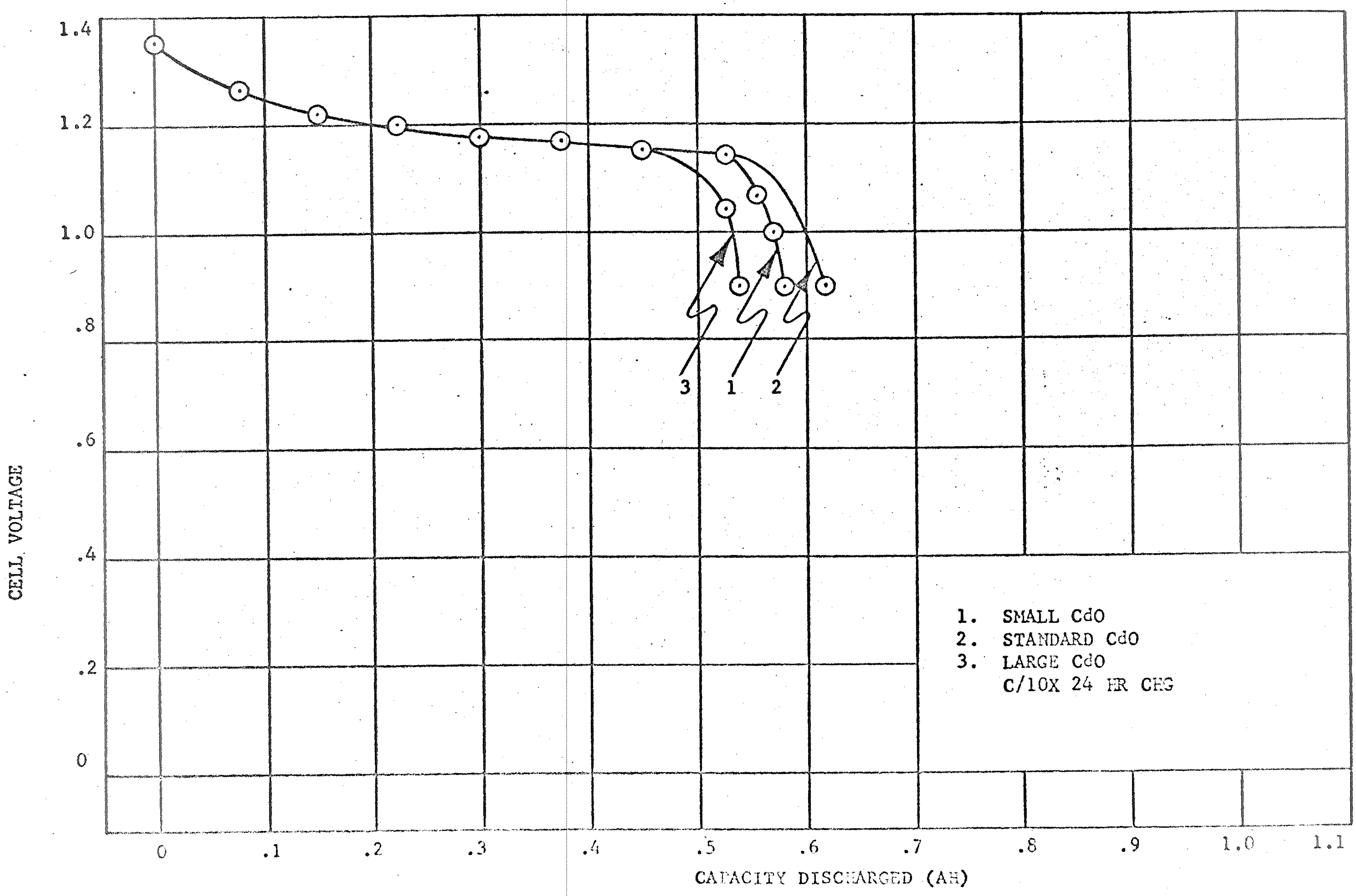

FIGURE 47 AVERAGE C/10 DISCHARGE CYCLE #2 POST CYCLING

4-3094

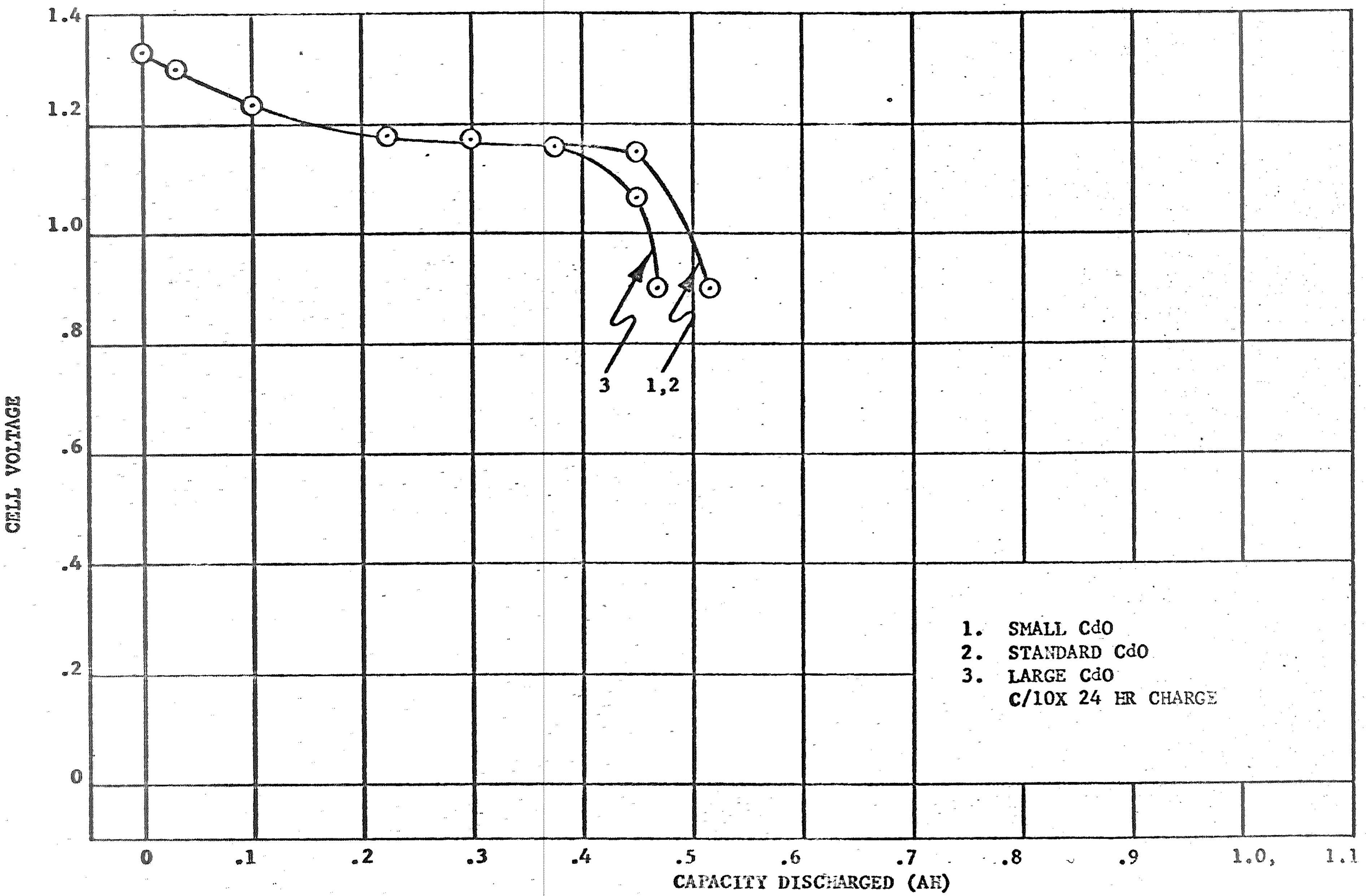

FIGURE 43 AVERAGE C/5 DISCHARGE CYCLE #2 POST CYCLING

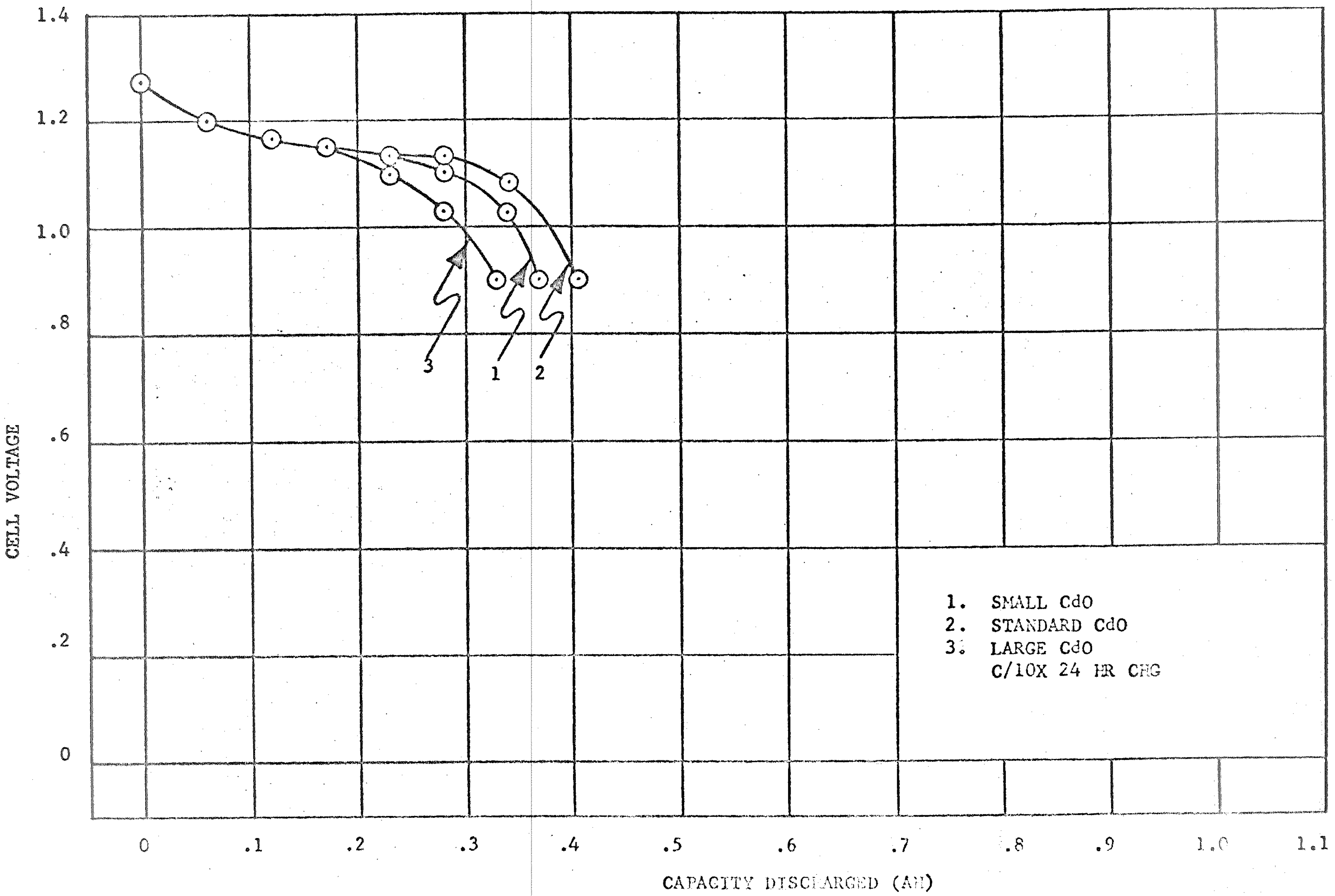

FIGURE 49 AVERAGE C/1 DISCHARGE CYCLE #2 POST CYCLING

4-3096

The post cycling capacity data indicate capacity retention ranging between 75 and 50% for Groups 4 and 6 and about 85% for Group 5. However, at all rates, the standard CdO (Group 5) exhibited greater capacity than the other cadmium oxides.

4. Final Evaluation

The final evaluation consisted of fabricating five electrodes from the apparently best material (standard particle size CdO) as shown by the preliminary work. They were constructed into negative limiting cells and tested as outlined below:

a. Two cycles each, at rates of C/10, C/5 and C/1

b. One week cycling on a 90 minute orbit at 50% depth of discharge (112 cycles).

c. Two cycles each at rates of C/10, C/5 and C/1.

d. Replace on cycle for one month.

In previous tests, nickel electrodes were wrapped in non-woven nylon separators. However, in this test, the nickel positive electrodes were wrapped in a cellulosic separator to more closely simulate conditions in a silver-cadmium cell and also to prevent any silver migration from the silver used as a conductive diluent in the negative for this longer life cycle test. The electrolyte was an aqueous solution of 38% KOH. This higher concentration is normally used in our silver-cadmium cells.

a. Pre-Cycle Testing

After activation, the cells were formed by charging at C/10 for 24 hours and discharging at C/5 to 0.9V. The average discharge capacities for the five cells are shown in Figure 50. Figures 51 and 52 show the two C/10 discharges, Figure 53 shows the second C/5 cycle, and Figures 54 and 55 show the two C/1 cycles. The average capacity results are summarized in Table XLVIII.

TABLE XLVIII. - AVERAGE PRE-CYCLING CAPACITIES

RATE	CAPACITY
C/5	1.10 Ah
C/10	0.96
C/10	0.90
C/5	0.84
C/1	0.65
C/1	0.63

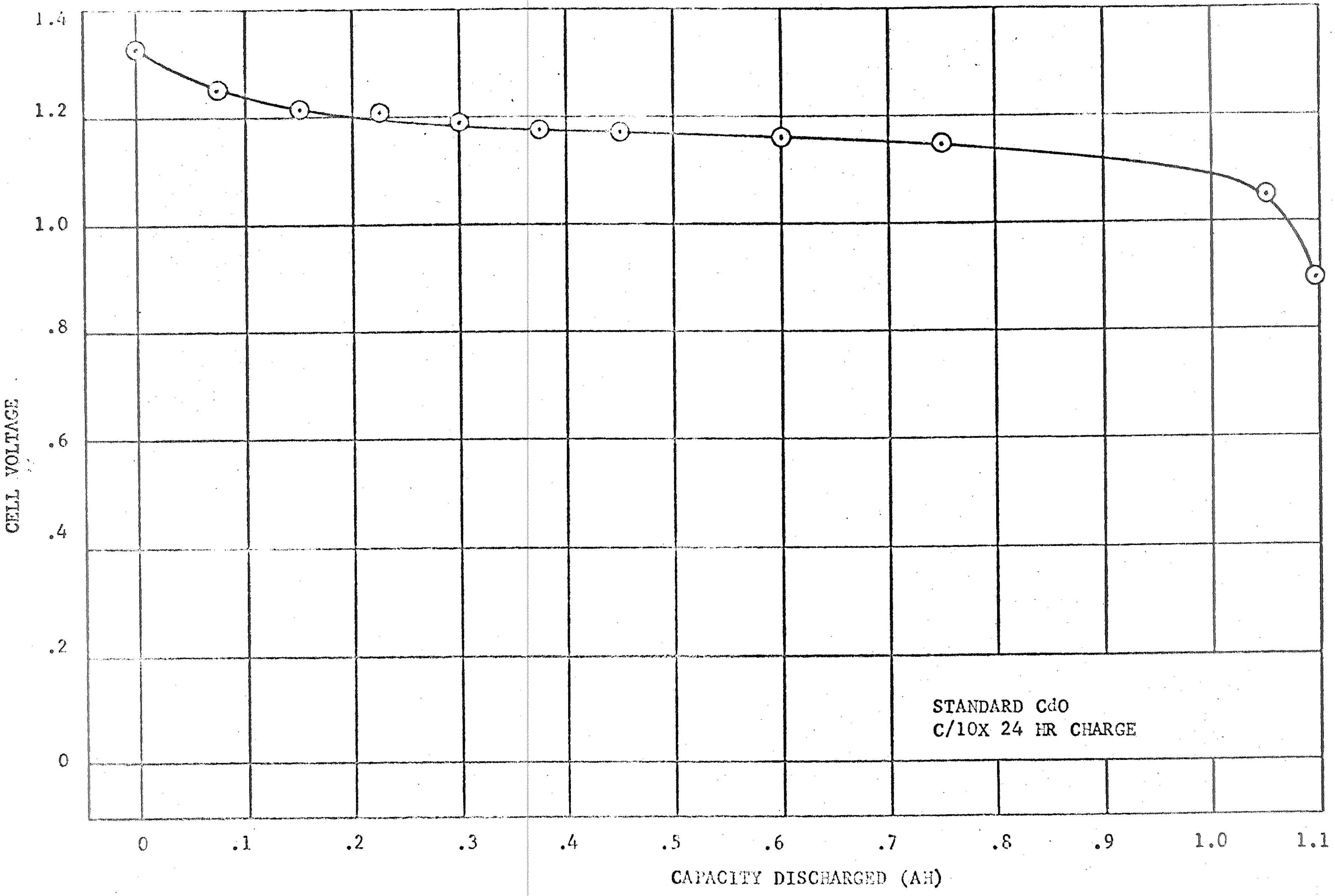

FIGURE 50 AVERAGE C/5 DISCHARGE CYCLE #1 PRE-CYCLING (FORMATION)

4-3097

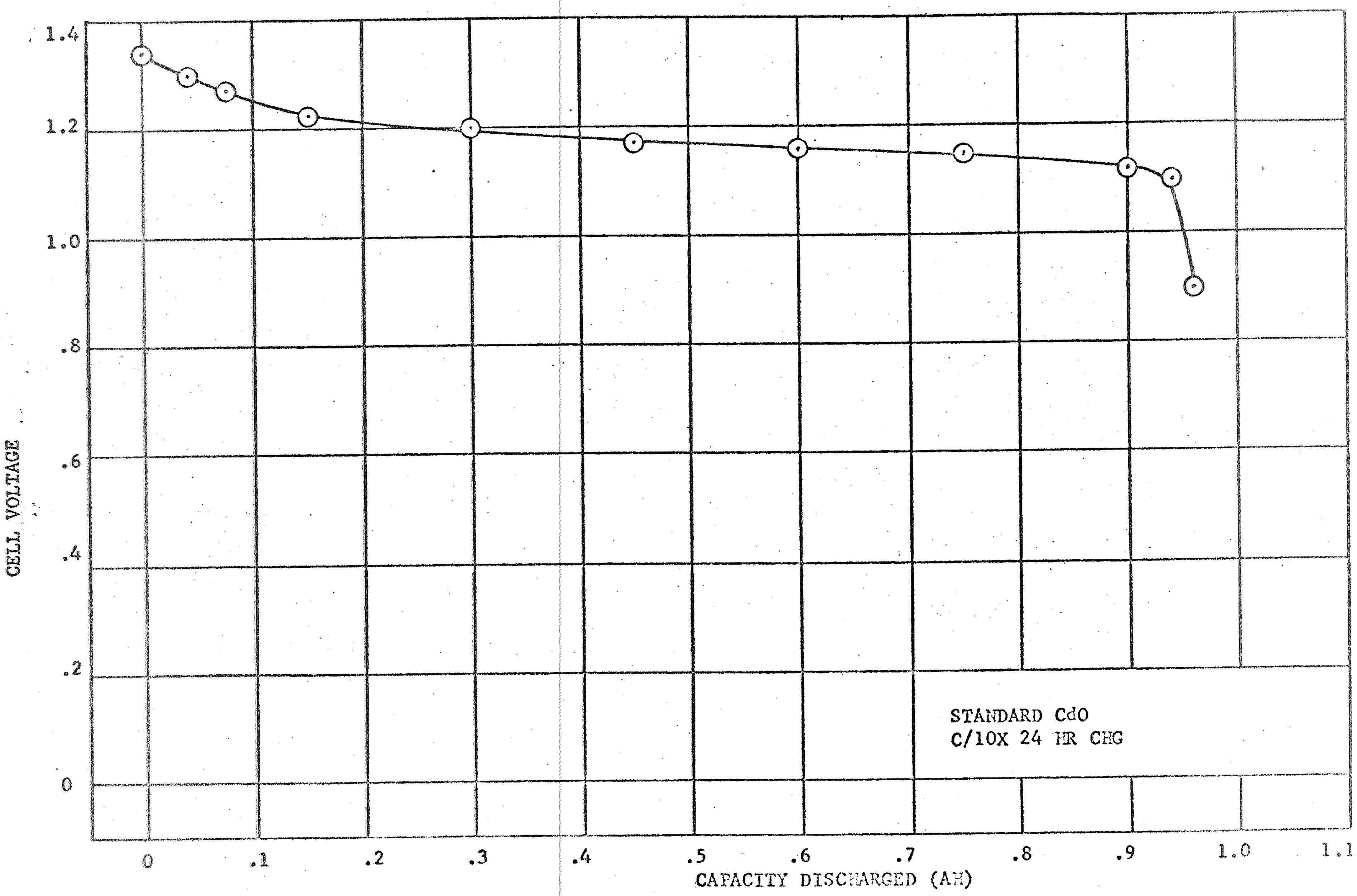

FIGURE 51 AVERAGE C/10 DISCHARGE CYCLE #1 PRE-CYCLING

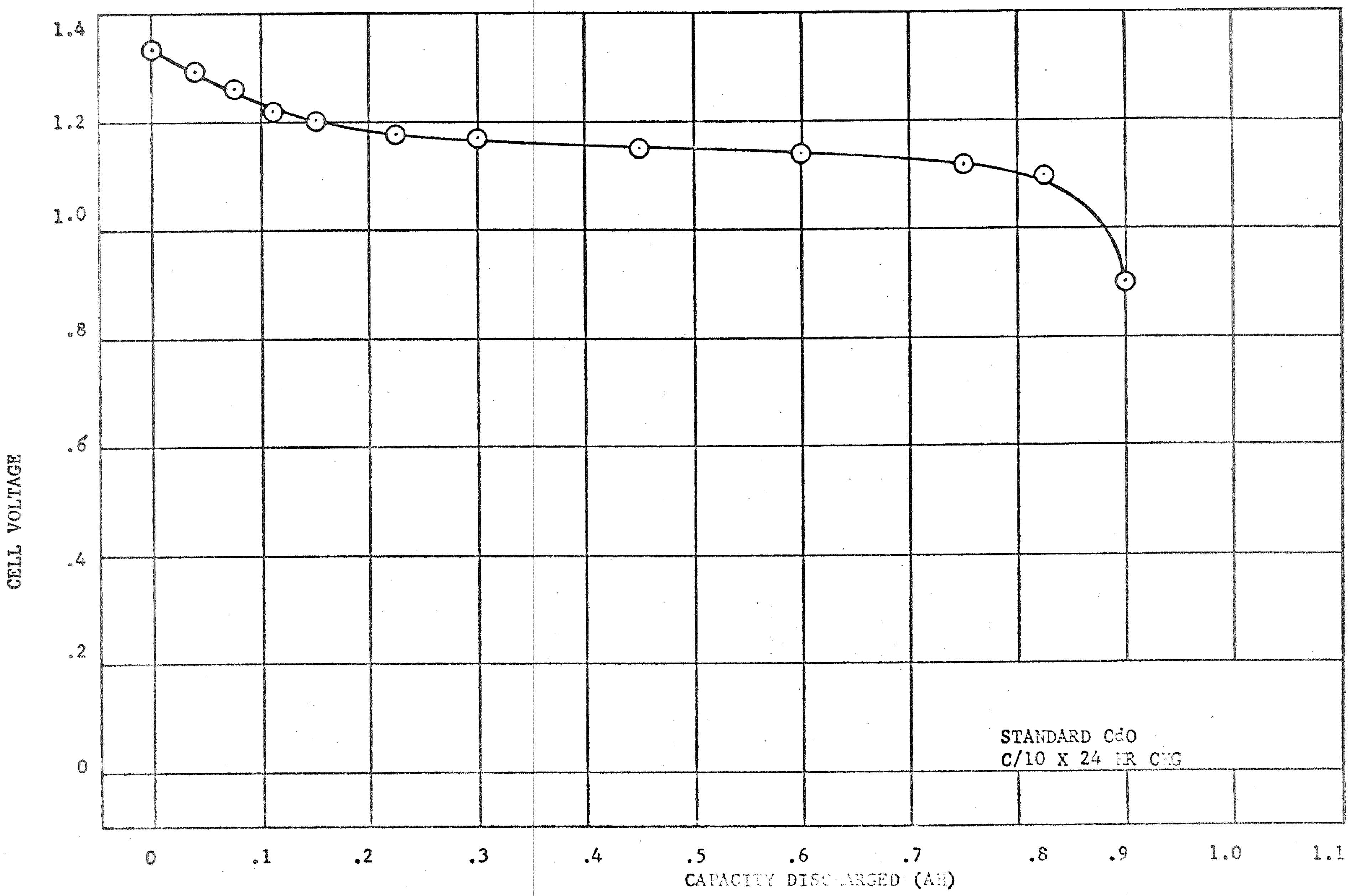

FIGURE 52 AVERAGE C/10 DISCHARGE CYCLE #2 PRE-CYCLING

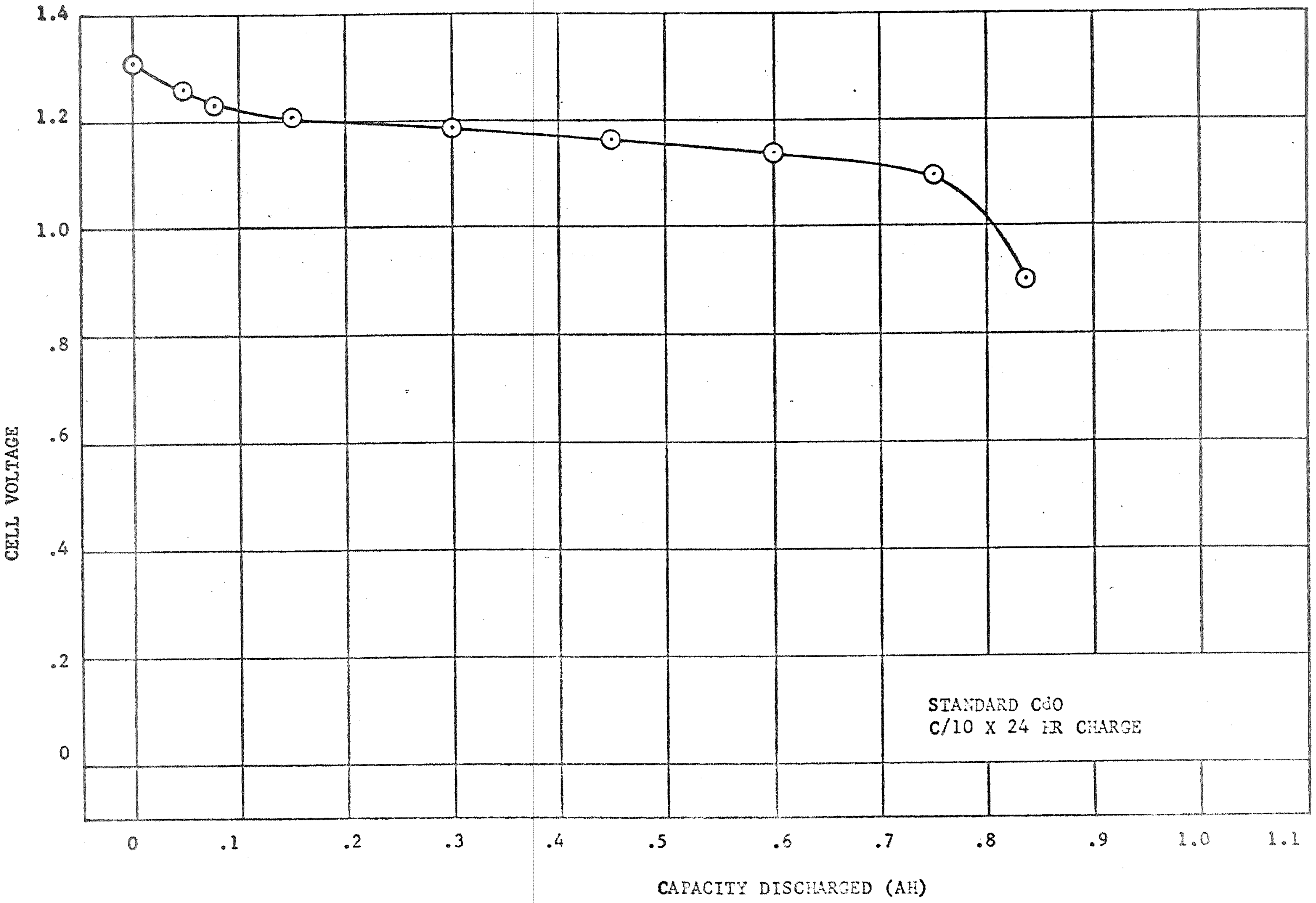

FIGURE 53 AVERAGE C/5 DISCHARGE CYCLE #2 PRE-CYCLING

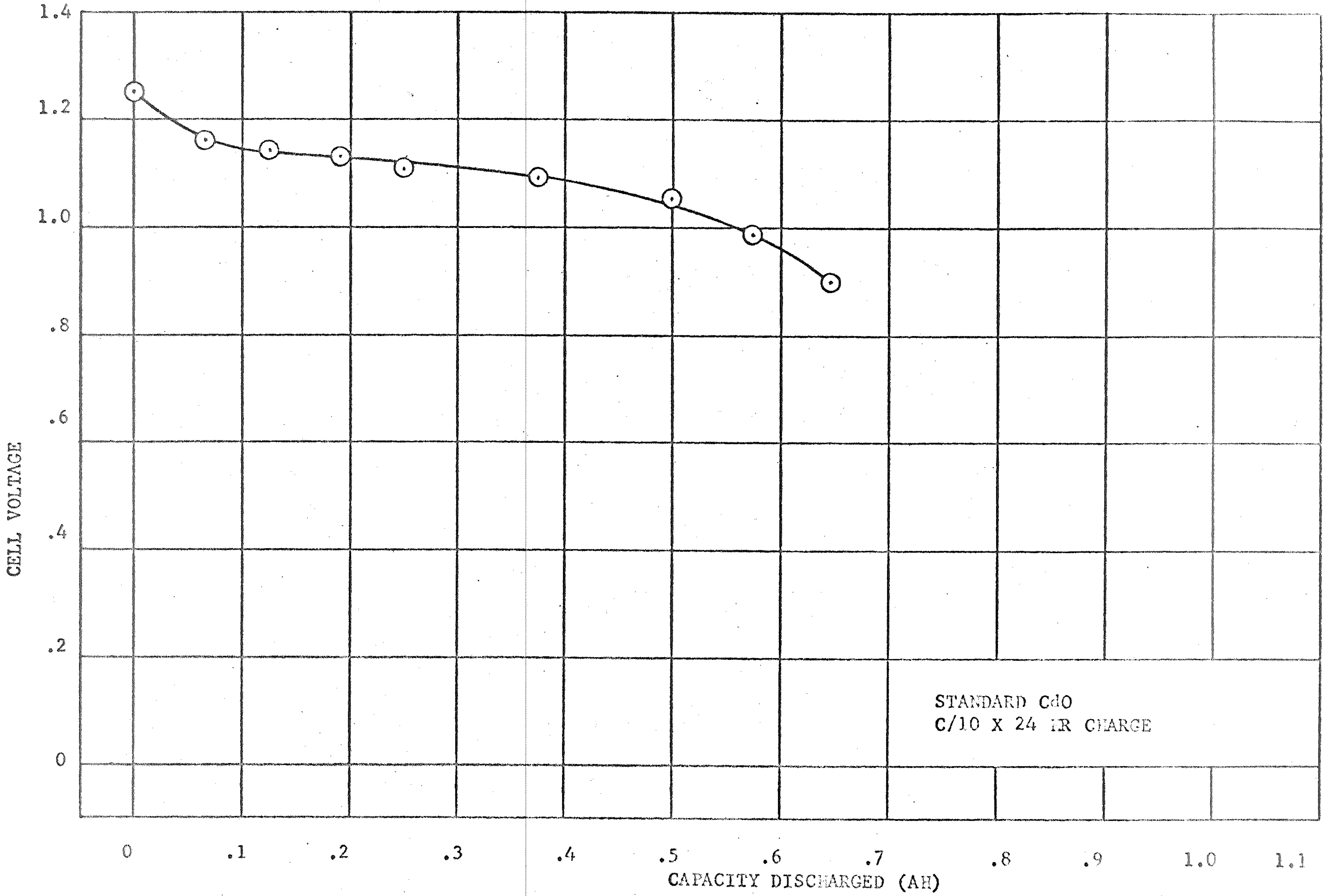

FIGURE 54 AVERAGE C/1 DISCHARGE CYCLE #1 PRE-CYCLING

4-3101

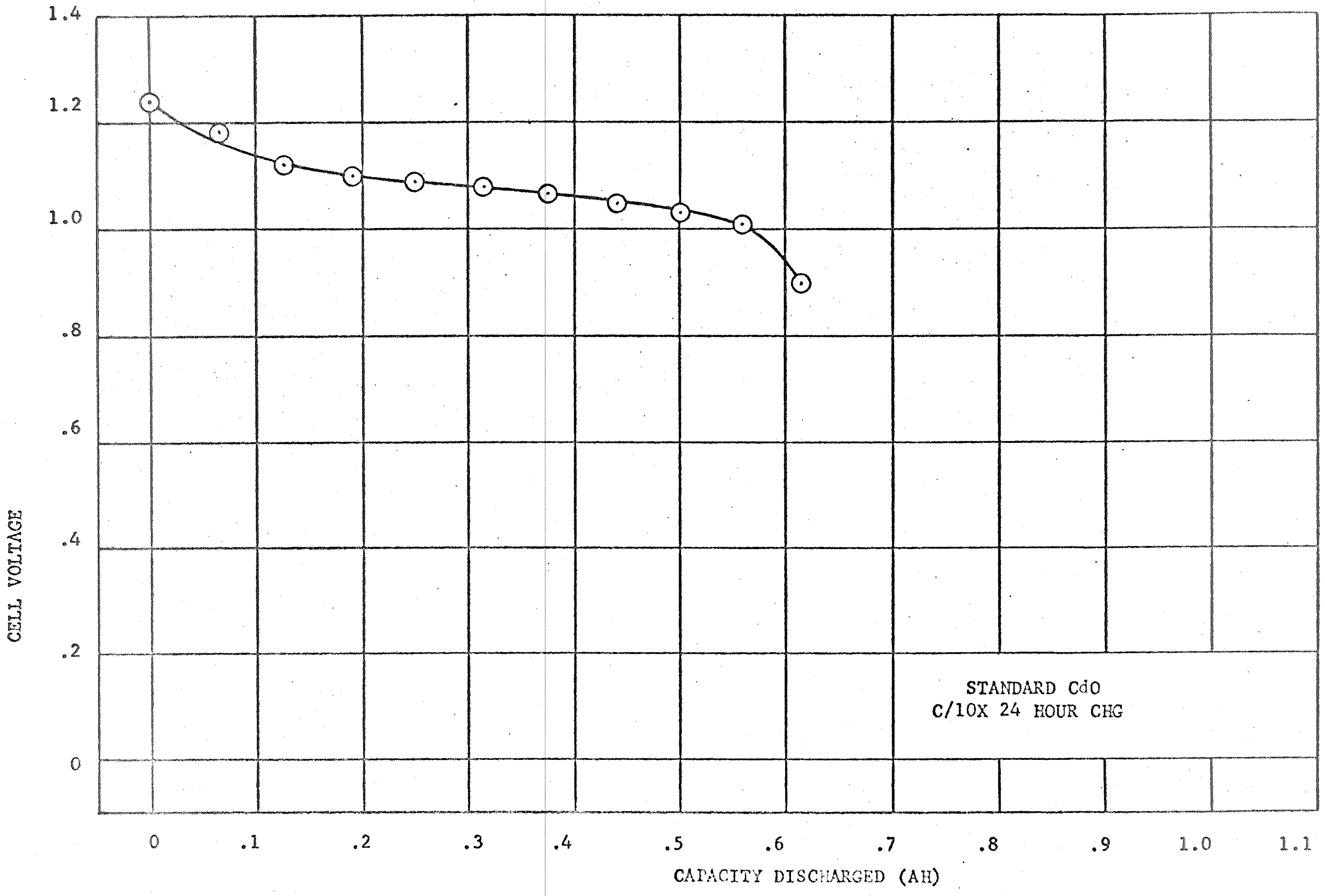

FIGURE 55. AVERAGE C/1 DISCHARGE CYCLE #2, PRE-CYCLING

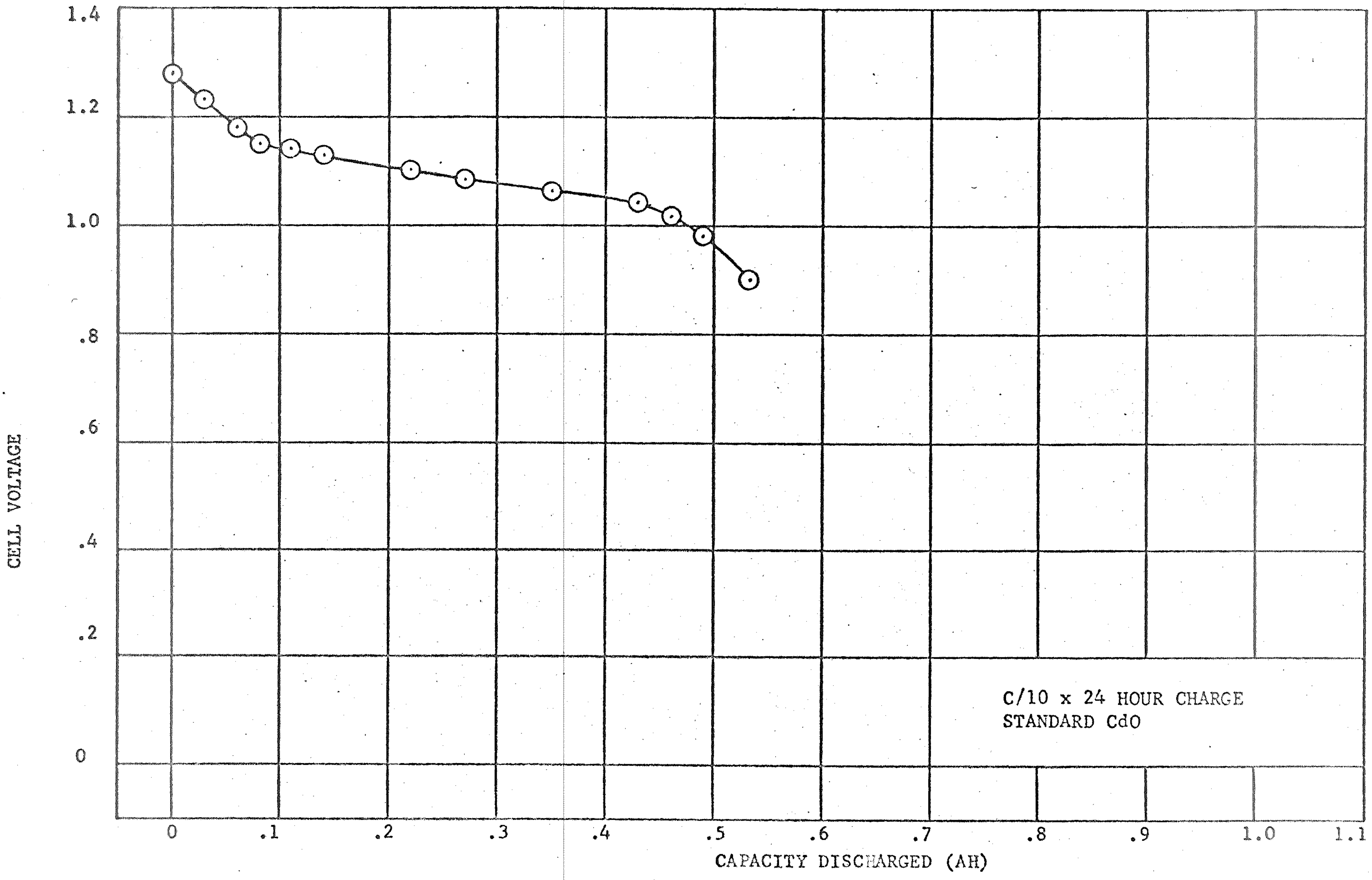

FIGURE 56. AVERAGE RESIDUAL CAPACITY DISCHARGE - CYCLE 113

4-3103

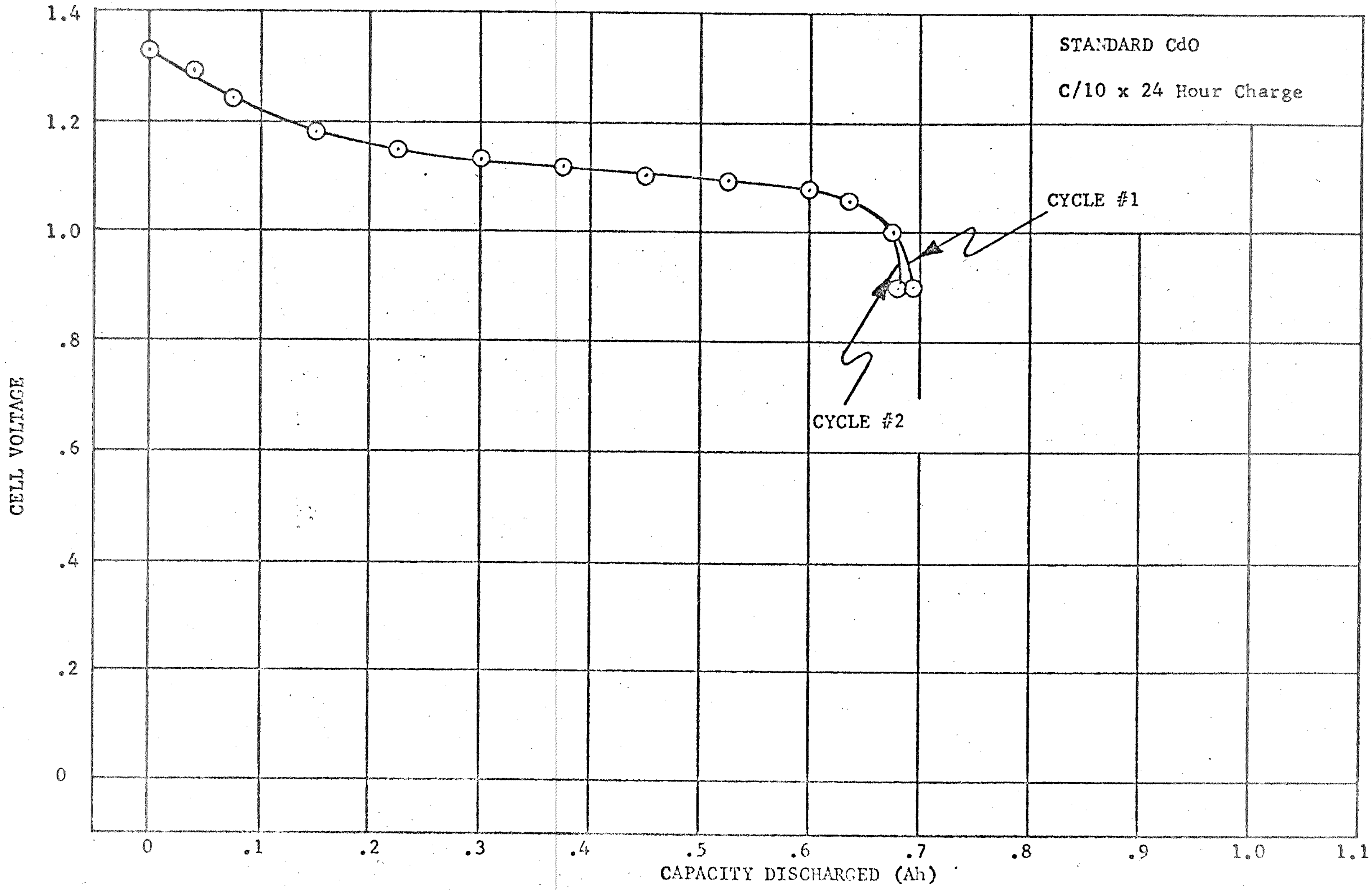

FIGURE 57 C/10 DISCHARGE, CYCLE 1 & 2, POST CYCLING

4-3147

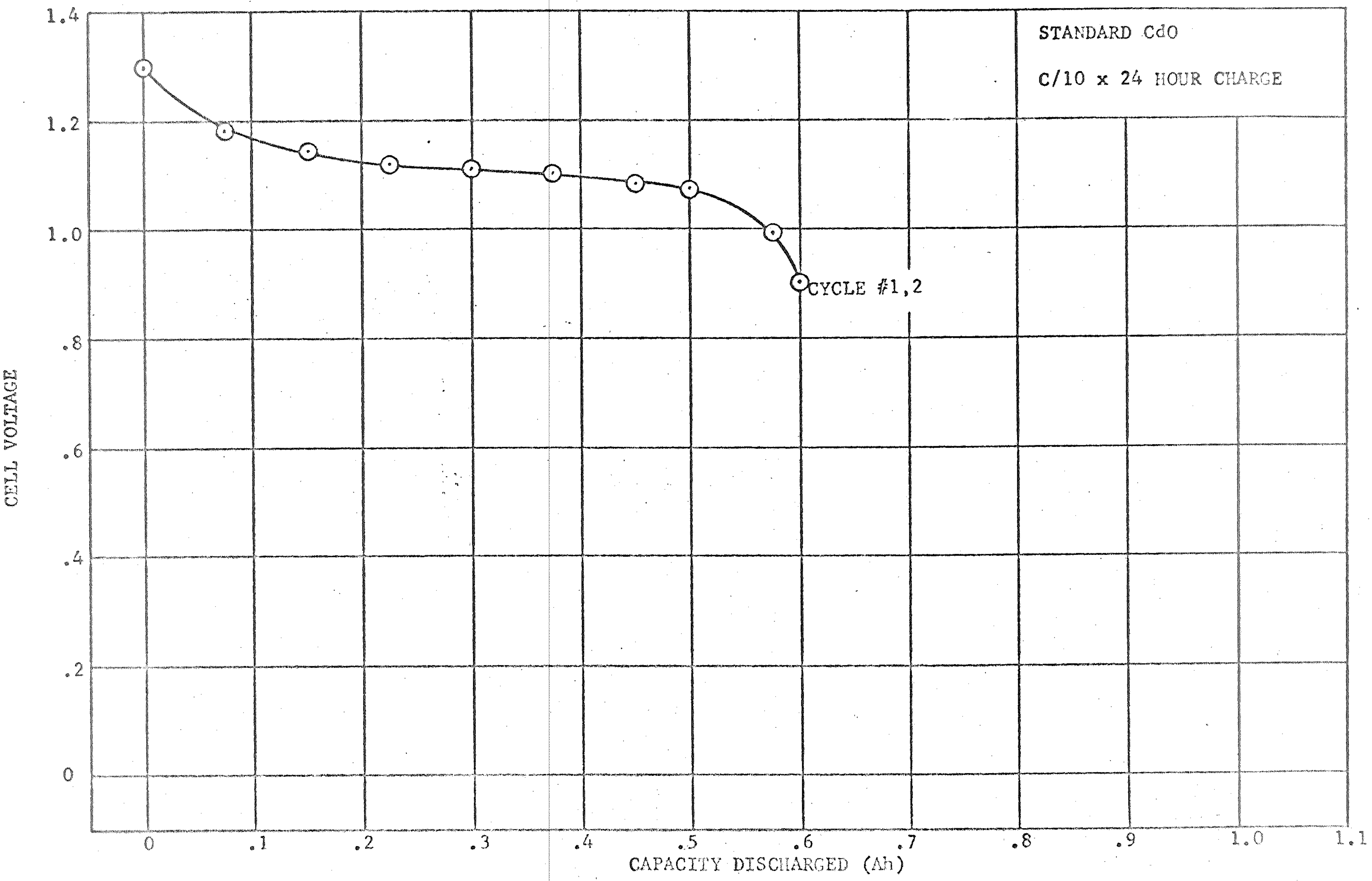

FIGURE 58 AVERAGE C/5 DISCHARGE, CYCLES 1 & 2, POST CYCLING

4-3148

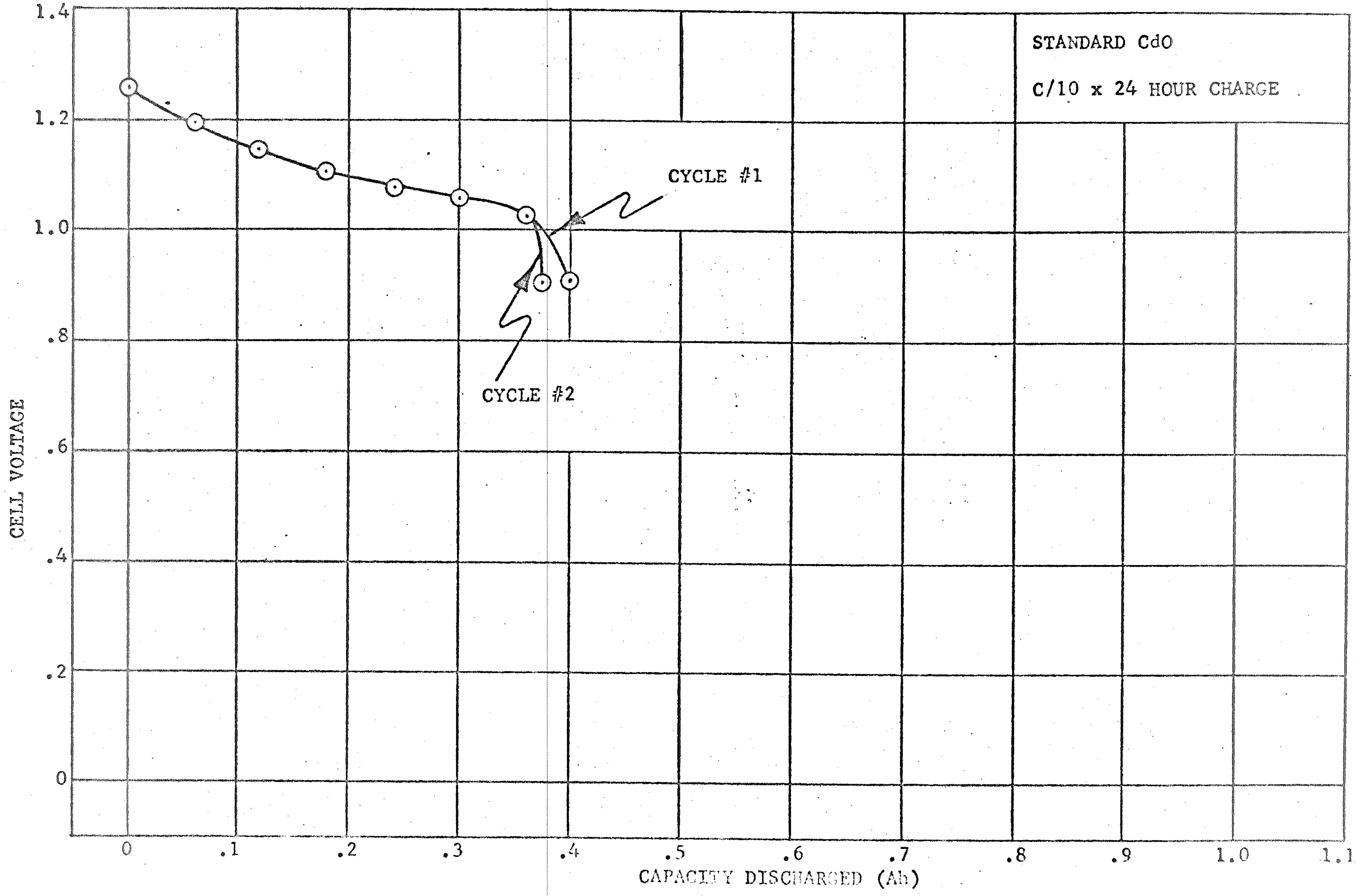

FIGURE 59 AVERAGE C/1 DISCHARGE, CYCLE 1 & 2, POST CYCLING

4-3149

b. Cycling

After completion of the pre-cycling tests, the cells were placed on a one-week cycle at 50% depth of discharge. The cycle consisted of a 30 minute discharge at the C/1 (0.6 A) rate and a 60 minute charge at 0.33 A. The rates were chosen based on the C/1 capacity data obtained in the pre-cycling tests.

Table XLIX shows end of discharge voltage versus cycle number.

TABLE XLIX. - END OF DISCHARGE VOLTAGE Vs CYCLE NUMBER

CYCLE	EODV*
1	1.10 V
16	1.07
32	1.07
48	1.07
64	1.07
80	1.07
96	1.07
112	1.07

* EODV= End of Discharge Voltage

The end of discharge voltages shown to be lower than the previous cells are apparently due to the increased cell impedance due to the use of the cellulosic separator and 38% KOH, as opposed to non-woven nylon and 34% KOH used previously. On cycle 113, the discharge was allowed to continue until the cells reached 0.9 V in order that total capacity be determined. The results are shown in Figure 56. The total capacity, after cycling, was 0.54 Ah compared to 0.63 Ah prior to cycling, or a capacity retention of 86% from the start of cycling.

c. Post Cycling Tests

After completion of cycling, the cells were subjected to two cycles at each of the following rates: C/10, C/5, C/1. The results of these tests are shown in Figures 57-59 and summarized in Table L.

TABLE L. - AVERAGE POST CYCLING CAPACITIES, STANDARD CdO

RATE	FIGURE	CAPACITY
C/10	57	0.70 Ah
C/5	58	0.60 Ah
C/1	59	0.40 Ah
C/10	57	0.68 Ah
C/5	58	0.60 Ah
C/1	59	0.37 Ah

The post cycling capacity data indicate a capacity retention of 75% for C/10 and C/5, and 60% for C/1 as compared to the pre-cycling capacity.

d. Additional Cycling

After the post cycling capacity determination, the cells were replaced on cycle and were allowed to remain on cycle for an additional 600 cycles. The cells completed the 600 cycles with and end of discharge voltage of 1.10 V.

A typical discharge curve for cycle 500 is shown in Figure 60.

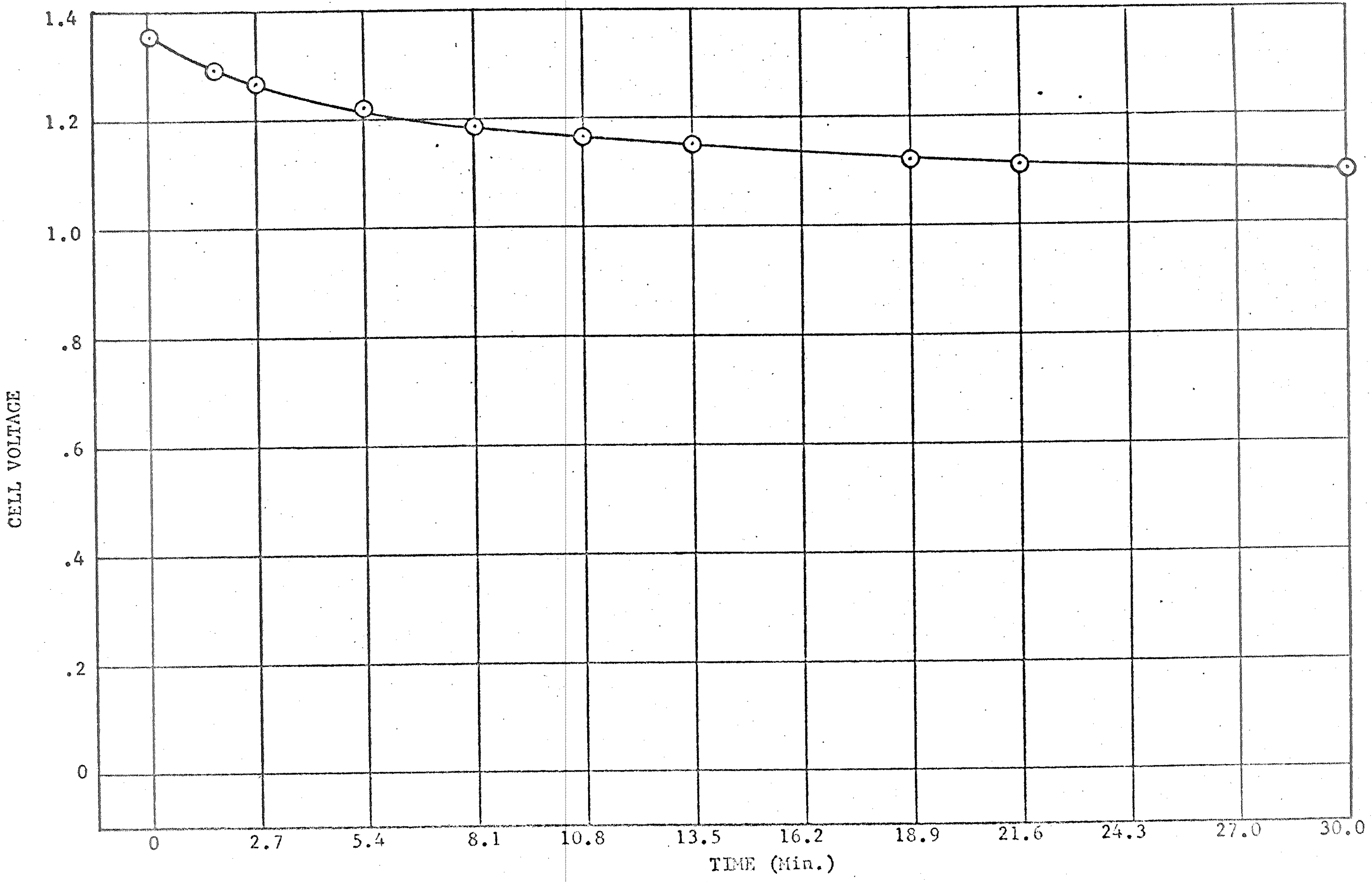

FIGURE 60 FINAL EVALUATION - STANDARD SIZE TEFLONATED CdO - CYCLE 500, AVG. DISCHARGE

III. CONCLUSIONS

The data accumulated during this intensive 26 month study lead to the following conclusions.

A. Pasted electrodes fabricated from mixtures of $Cd(OH)_2$ and CdO yielded electrodes with electrochemical utilization (21%) on high rate cycling. In addition, their physical integrity, after cycling, was so poor that a large percentage of material separated from the carrier (substrate) and fell off.

B. Sintered electrodes, those fabricated by impregnating a sintered silver plaque with $Cd(OH)_2$, showed moderate utilization (45%) on high rate cycling. However, because of the weight and volume of the silver sinter, their capacity per unit weight and volume was considerably less than for pressed type electrodes.

The low capacity per unit weight and volume make them impractical for use in silver-cadmium cells. Sealed silver-cadmium cells, fabricated with these electrodes, were negative limiting and lasted less than 20 cycles, with failure due to severe silver migration (Figure A-1).

C. Pressed electrodes of the standard type, $3CdO : 1Cd(OH)_2$, have a utilization of about 40% on high rate cycling. The electrodes have fair green strength and show minimal loss of material on cycling.

Further investigations indicated that utilization was neither a function of pressure nor a function of the amount of silver added as a conductive diluent.

Silver cadmium cells constructed with these electrodes have completed 342 cycles, at 50% depth of discharge, with end-of-discharge voltages of 1.07 volts.

D. Pressed electrodes of the teflonated $Cd(OH)_2$ type have high rate cycling utilizations of about 65%. In addition, the electrochemical utilization remains constant over a number of cycles, rather than steadily decreasing as do standard type pressed electrodes.

These electrodes have good green strength, and after cycling, show excellent adhesion to the substrate with no sign of material loss, blistering, or cracking.

Due to their high utilization and capacity retention, these electrodes can be made lighter by using less active materials, thus raising the energy density of silver-cadmium cells.

Silver-cadmium cells constructed with these electrodes have completed 382 cycles, at 50% depth of discharge, with end-of-discharge voltages of 1.07 volts.

E. Further investigations of teflonated cadmium electrodes have indicated that superior electrodes are produced when the teflonated material is cadmium oxide, as prepared in our laboratory, starting from a battery grade cadmium nitrate and mercury cell grade potassium hydroxide. The particle size of the starting $Cd(OH)_2$ should be controlled in order to produce electrodes with a high BET surface area.

In view of the data presented herein, we may conclude that the objective of this program, "the development of a non-magnetic cadmium electrode which is resistant to capacity fading", has been achieved.

APPENDIX I

FAILURE ANALYSIS REPORT

NASA Form 51221

FAILURE ANALYSIS REPORT

NASA CONTRACT NO.: NAS 3-11829

DATE: 10/31/69

REPORT NO.:

CELL IDENTIFICATION:

Lot No.
Cell No. 1
Test No. Teflonated $Cd(OH)_2$

TEST CONDITIONS:

Cycle Period 12 hrs.
Temp. 25 °C
Charge 11 hrs, 0.3 amps
Discharge 1 hrs., 2.5 amps

FAILURE CONDITIONS:

Cycles to failure 289
Date 10/30/69
Cause of failure silver migration
End of discharge voltage, last cycle 0.0 V

EXTERNAL INSPECTION:

a. Leakage None
b. OCV 1 hr. after test 0.0 V
c. Initial weight Not taken gms
Final weight N/A gms
Weight change N/A gms
d. Phenolphthalein Negative
e. Case inspection Good condition
f. Residual capacity 0 Ah

INTERNAL INSPECTION:

a. Active material in case Minimal
b. Pack wetness: Free KOH X ; moist ; dry
c. Migrated active material Some on separator
d. Terminals Good
Plate tabs Good
e. Negative pack capacity: As failed 2.3 Ah
After recharge 5.0 Ah
Positive pack capacity: As failed 0 Ah
After recharge 2.1 Ah
f. No. of plates: Positive 8 ; Negative 9

SEPARATOR INSPECTION
FROM TOP, (+) TERMINAL ON LEFT

POLARITY (+)

PLATE NO.	TYPE	TYPE	CONDITION	CONDITION
2	Dynel	Cellulose	Good	Good
4	↓	↓	↓	↓
6				
8				
10				
12				
14				
16				

SEPARATOR INSPECTION
FROM TOP, (+) TERMINAL ON LEFT

POLARITY (-)

PLATE NO.	TYPE	TYPE	CONDITION	CONDITION
1	Dynel	Pellon	Good	Good
3	↓	↓	↓	↓
5	↓	↓	↓	↓
7	↓	↓	↓	↓
9	↓	↓	↓	↓
11	↓	↓	↓	↓
13	↓	↓	↓	↓
15	↓	↓	↓	↓
17	↓	↓	↓	↓

Silver penetration through both separators

PLATE INSPECTION
FROM TOP, (+) TERMINAL ON LEFT

POLARITY (+)

PLATE NO.	CONDITION
2	Good - No material loss or cracking
4	↓
6	↓
8	↓
10	↓
12	↓
14	↓
16	↓

Remarks:

PLATE INSPECTION
FROM TOP, (+) TERMINAL ON LEFT

POLARITY (-)

PLATE NO.	CONDITION
1	Good - No material loss, blistering or crazing
3	↓
5	
7	
9	
11	
13	
15	
17	

Remarks:

FAILURE ANALYSIS REPORT

NASA CONTRACT NO.: NAS 3-11829

DATE: 10/31/69 REPORT NO.: ________

CELL IDENTIFICATION:

Lot No. ________ Cell No. 2 Test No. Teflonated Negs.

TEST CONDITIONS:

Cycle Period 12 hrs. Temp. 25 °C

Charge 11 hrs, 0.3 amps Discharge 1 hrs., 2.5 amps

FAILURE CONDITIONS:

Cycles to failure 277 Date 10/24/69

Cause of failure Silver migration

End of discharge voltage, last cycle 0.0 V

EXTERNAL INSPECTION:

a. Leakage Non

b. OCV 1 hr. after test 0.0 V

c. Initial weight Not taken gms

Final weight N/A gms

Weight change N/A gms

d. Phenolphthalein Negative

e. Case inspection Good condition

f. Residual capacity 0 Ah

INTERNAL INSPECTION:

a. Active material in case None

b. Pack wetness: Free KOH X ; moist ____ ; dry ____

c. Migrated active material on separator

d. Terminals Good

Plate tabs Good

e. Negative pack capacity: As failed 0.25 Ah

After recharge 4.7 Ah

Positive pack capacity: As failed 0 Ah

After recharge 3.34 Ah

f. No. of plates: Positive 8 ; Negative 9

SEPARATOR INSPECTION
FROM TOP, (+) TERMINAL ON LEFT

POLARITY (+)

PLATE NO.	TYPE	TYPE	CONDITION	CONDITION
2	Dynel	Cellulose	Good	Good
4	↓	↓	↓	↓
6	↓	↓	↓	↓
8	↓	↓	↓	↓
10	↓	↓	↓	↓
12	↓	↓	↓	↓
14	↓	↓	↓	↓
16	↓	↓	↓	↓

Remarks:

SEPARATOR INSPECTION
FROM TOP, (+) TERMINAL ON LEFT

POLARITY (-)

PLATE NO.	TYPE	TYPE	CONDITION	CONDITION
1	Dynel	Pellon	Good	Good
3	↓	↓	↓	↓
5	↓	↓	↓	↓
7	↓	↓	↓	↓
9	↓	↓	↓	↓
11	↓	↓	↓	↓
13	↓	↓	↓	↓
15	↓	↓	↓	↓
17	↓	↓	↓	↓

Remarks: Silver migration through both separators

PLATE INSPECTION
FROM TOP, (+) TERMINAL ON LEFT

POLARITY (+)

PLATE NO.	CONDITION
2	Good - No loss of active material
4	↓
6	↓
8	↓
10	↓
12	↓
14	↓
16	↓

Remarks:

PLATE INSPECTION
FROM TOP, (+) TERMINAL ON LEFT

POLARITY (-)

PLATE NO.	CONDITION
1	Good - No loss of active material
3	↓
5	↓
7	↓
9	↓
11	↓
13	↓
15	↓
17	↓

Remarks:

FAILURE ANALYSIS REPORT

NASA CONTRACT NO.: NAS 3-11829

DATE:

REPORT NO.:

CELL IDENTIFICATION:

Lot No.
Cell No. 3
Test No. Teflonated $Cd(OH)_2$

TEST CONDITIONS:

Cycle Period 12 hrs.
Temp. 25 °C
Charge 11 hrs, 0.3 amps
Discharge 1 hrs., 2.5 amps

FAILURE CONDITIONS:

Cycles to failure 175
Date 9/3/69
Cause of failure silver migration
End of discharge voltage, last cycle 0.0 V

EXTERNAL INSPECTION:

a. Leakage None
b. OCV 1 hr. after test 0.0 V
c. Initial weight Not taken gms
Final weight N/A gms
Weight change N/A gms
d. Phenolphthalein Negative
e. Case inspection Good condition
f. Residual capacity 0.0 Ah

INTERNAL INSPECTION:

a. Active material in case None
b. Pack wetness: Free KOH X ; moist ; dry
c. Migrated active material On separator
d. Terminals Good
Plate tabs Good
e. Negative pack capacity: As failed Not taken Ah
After recharge 7.4 Ah C/10 charge
Positive pack capacity: As failed 0 Ah 2.0 A charge
After recharge 5.7 Ah
f. No. of plates: Positive 8 ; Negative 9

SEPARATOR INSPECTION
FROM TOP, (+) TERMINAL ON LEFT

POLARITY (+)

PLATE NO.	TYPE	TYPE	CONDITION	CONDITION
2	Dynel	Cellulose	Good	Good
4	↓	↓	↓	↓
6	↓	↓	↓	↓
8	↓	↓	↓	↓
10	↓	↓	↓	↓
12	↓	↓	↓	↓
14	↓	↓	↓	↓
16	↓	↓	↓	↓

Remarks:

SEPARATOR INSPECTION
FROM TOP, (+) TERMINAL ON LEFT

POLARITY (-)

PLATE NO.	TYPE	TYPE	CONDITION	CONDITION
1	Dynel	Pellon	Good	Good
3	↓	↓	↓	↓
5				
7				
9				
11				
13				
15				
17				

Remarks: Silver Penetration through separators

PLATE INSPECTION
FROM TOP, (+) TERMINAL ON LEFT

POLARITY ( )

PLATE NO.	CONDITION
2	Good - No cracks or loss of active material
4	↓
6	
8	
10	
12	
14	
16	

Remarks:

PLATE INSPECTION
FROM TOP, (+) TERMINAL ON LEFT

POLARITY ( )

PLATE NO.	CONDITION
1	Good - No cracks or blisters or loss of active mtl.
3	↓
5	
7	
9	
11	
13	
15	
17	

Remarks:

FAILURE ANALYSIS REPORT

NASA CONTRACT NO.: NAS 3-11829

DATE: ________ REPORT NO.: ________

CELL IDENTIFICATION:

Lot No. ________ Cell No. 5 Test No. Teflonated Negs.

TEST CONDITIONS:

Cycle Period 12 hrs. Temp. 25 °C

Charge 11 hrs, 0.3 amps Discharge 1 hrs., 2.5 amps

FAILURE CONDITIONS:

Cycles to failure 255 Date 10/13/69

Cause of failure silver migration

End of discharge voltage, last cycle 0.0 V

EXTERNAL INSPECTION:

a. Leakage None

b. OCV 1 hr. after test 0.91

c. Initial weight Not taken gms

Final weight N/A gms

Weight change N/A gms

d. Phenolphthalein Negative

e. Case inspection Good condition

f. Residual capacity 0 Ah

INTERNAL INSPECTION:

a. Active material in case None

b. Pack wetness: Free KOH X ; moist ____ ; dry ____

c. Migrated active material on separator

d. Terminals Good

Plate tabs Good

e. Negative pack capacity: As failed 0 Ah

After recharge 5.7 Ah

Positive pack capacity: As failed 0 Ah

After recharge 4.4 Ah

f. No. of plates: Positive 8 ; Negative 9

SEPARATOR INSPECTION
FROM TOP, (+) TERMINAL ON LEFT

POLARITY (+)

PLATE NO.	TYPE	TYPE	CONDITION	CONDITION
2	Cellulose	Dynel	Good	Good
4	↓	↓	↓	↓
6	↓	↓	↓	↓
8	↓	↓	↓	↓
10	↓	↓	↓	↓
12	↓	↓	↓	↓
14	↓	↓	↓	↓
16	↓	↓	↓	↓

SEPARATOR INSPECTION
FROM TOP, (+) TERMINAL ON LEFT

POLARITY (-)

PLATE NO.	TYPE	TYPE	CONDITION	CONDITION
1	Dynel	Pellon	Heavy penetration both separators	
3			Condition of all separators good	
5				
7				
9				
11				
13				
15				
17	↓	↓		

PLATE INSPECTION
FROM TOP, (+) TERMINAL ON LEFT

POLARITY ( )

PLATE NO.	CONDITION
2	Good - No cracking, crazing or blistering
4	↓
6	↓
8	↓
10	↓
12	↓
14	↓
16	↓

Remarks:

PLATE INSPECTION
FROM TOP, (+) TERMINAL ON LEFT

POLARITY (-)

PLATE NO.	CONDITION
1	Good - No loss of material - no blistering
3	↓
5	
9	
11	
13	
15	
17	

Remarks:

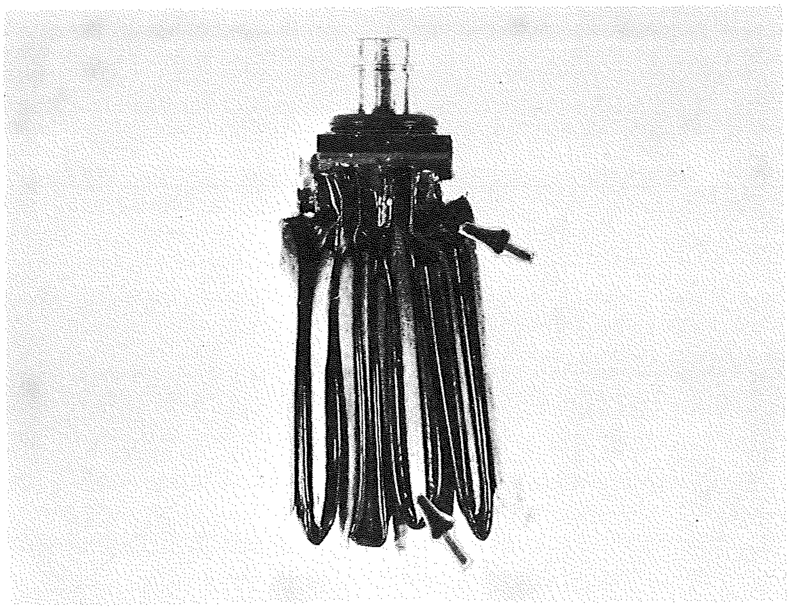

FIGURE A-1. SILVER-CADMIUM CELL SHOWING SEVERE SILVER MIGRATION

4-3180

APPENDIX II

ELECTRODE PROCESSING SPECIFICATIONS FOR TEFLONATED CADMIUM ELECTRODES

I. RAW MATERIAL SPECIFICATION

The raw materials used in the fabrication of the teflonated cadmium electrodes are:

1. Battery grade cadmium nitrate solution - specification attached.
2. Solvay mercury cell process potassium hydroxide - specification attached.
3. Silver powder, 11-16μ particle size - Handy & Harman Silpowder 150.
4. Teflon Emulsion - Dupont P-30 type.
5. Silver substrates - expanded silver, 99.9% fine silver. The substrates are 0.010" thick and have a mesh size of 0.093".

II. PREPARATION OF CADMIUM HYDROXIDE $Cd(OH)_2$

Battery grade $Cd(NO_3)_2$ solution is maintained at a concentration of 8.26N. Battery grade aqueous KOH is maintained at a concentration of 8.07N. To a given amount of the $Cd(NO_3)_2$ solution, a quantity of KOH solution, 2% in excess of the stoichiometric amount, is rapidly added (poured in all at once). The precipitate of Cd(OH) is washed with deionized water and filtered to remove the supernatant fluid containing the excess KOH. The precipitate is washed until the filtrate is neutral. The precipitate is then dried at 70°C. After drying, it is ground and passed through an 80 mesh screen. At this point, the material is analyzed for purity as described in Section III.

III. ANALYSIS OF CADMIUM HYDROXIDE

An amount of cadmium hydroxide is dried at 275°C for 24 hours. This converts the $Cd(OH)_2$ to cadmium oxide and removes any moisture. After drying, the CdO is cooled in a dessicator.

An accurately weighed amount of CdO is dissolved in dilute nitric acid. Cadmium hydroxide is re-precipitated by the addition of an excess of 5% KOH. Solid potassium cyanide (KCN) is added until the precipitate re-dissolves.

The cadmium is then determined by electroplating onto a platinum cathode. A minimum purity of 99.5% is required.

IV. PREPARATION OF ELECTRODE MIX

The electrode mix is made by weighing a portion of $Cd(OH)_2$. Silver powder, 11-16μ particle size, is added in the amount of 5 weight percent. Next, 5 weight percent of P-30 teflon emulsion (Dupont) is added. A minimum amount of distilled water is added and the mixture is thoroughly blended. The mixture is now dried at 70°C for 24 hours. After drying, the material is passed through a 20 mesh screen (similar to window screening). The mix is now teflon-bonded by firing at 275°C for 20 minutes. This bonded mix is then passed through an 80 mesh sieve.

V. ELECTRODE FABRICATION

The amount of material required for each electrode is calculated by the fabricator. One-half the required amount is weighed out to the nearest 0.01 gram. This material is evenly distributed using a spreader that just fits the mold cavity on the bottom of a cavity mold. The substrate is placed in the mold and the second half of the electrode mix is evenly distributed. The mold is closed and pressed at 7 tons/in^2 for 20 seconds to a density of 3.18 g/cc of $Cd(OH)_2$. The electrode is removed from the mold and any excess material is trimmed away. The electrodes are then stored in sealed plastic bags until they are ready to be assembled into cells.

VI. FLOW CHART

A flow chart for the entire operation is attached as Figure A-2.

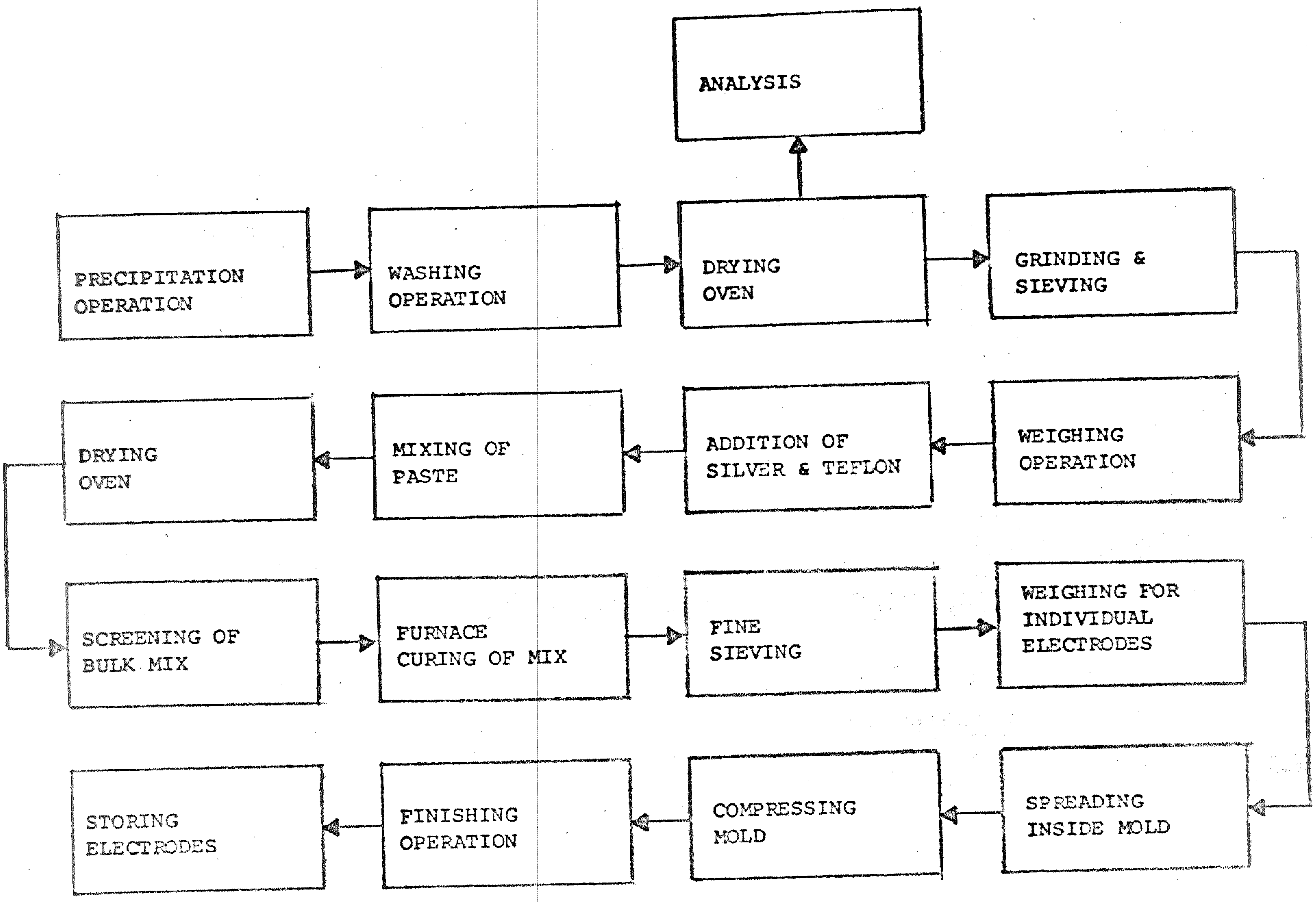

FIGURE A-2

FLOW CHART

TEFLONATED CADMIUM OPERATION

SPECIFICATION, POTASSIUM HYDROXIDE

(FOR ELECTROLYTE)

This material shall be Solvay Mercury Cell Process Potassium Hydroxide, Premium Grade, 45% Liquor having the following analysis:

KOH	45 - 46%
K_2CO_3	0.06% Max.
KCl	0.005% Max.
NaO	0.10% Max.
Fe	4 PPM Max.
Hg	1 PPM Max.
Turbidity	5 PPM Max.
$KClO_3$	None
Ni	None

Color, % White, Min, 98.0

Gulton Drawing No. A-5374

CHEMICAL PURITY SPECIFICATIONS

BATTERY GRADE CADMIUM NITRATE PURIFIED 85% SOLUTION - APPROX.

Clear, colorless solution, free from suspended matter or sediment

Specific Gravity: 1.90 at 120°F

Maximum Limits of Impurities on the Following:

Chloride	(Cl)	0.004%
Sulfate	(SO_4)	0.005%
Arsenic	(As)	0.001%
Copper	(Cu)	0.005%
Iron	(Fe)	0.002%
Lead	(Pb)	0.005%
Zinc	(Zn)	0.05%
Ammonia		0.01%
Free Acid Content, HNO_3		0.05% Min. 0.15% Max.
Total other impurities		0.1%

Note: Above limits of impurities are on a crystal basis as $Cd(NO_3)_2 \cdot 4H_2O$.

Gulton Drawing No.
A-551-13119

OFFICIAL DISTRIBUTION LIST
FOR BATTERY REPORTS

October, 1968/Revised December 3, 1970

National Aeronautics & Space Administration
Lewis Research Center
21000 Brookpark Road
Cleveland, Ohio 44135
Attn: G. M. Ault (MS 3-13)
V. Hlavin (MS 3-10)
Technology Utilization Office (MS 3-19)
Dr. L. Rosenblum (MS 302-1)
J. Toma (MS 302-1)
H. J. Schwartz (MS 309-1)
Dr. J. S. Fordyce (MS 309-1)
W. J. Nagle (MS 309-1)
D. G. Soltis (MS 309-1)
R. B. King (MS 302-1)
W. A. Robertson (MS 309-1)
J. E. Dilley (MS 500-309)
Library (MS 60-3)
Report Control (MS 5-5)

National Aeronautics & Space Administration
Washington, D. C. 20546
Attn: RPW/E. M. Cohn
SCC/A. M. Greg Andrus
MTG/Dr. R. C. Livingston
UT/Dr. E. N. Case
U/Technology Utilization Office

National Aeronautics & Space Administration
Goddard Space Flight Center
Greenbelt, Maryland 20771
Attn: Thomas Hennigan, Code 716.2
Gerald Halpert, Code 735
Joseph Sherfey, Code 735
Louis Wilson, Code 450

National Aeronautics & Space Administration
Langley Research Center
Instrument Research Division
Hampton, Virginia 23365
Attn: J. E. Zanks (MS 488)

National Aeronautics & Space Admin.
Geo. C. Marshall Space Flight Center
Huntsville, Alabama 35812
Attn: C. B. Graff (S&E-ASTR-EP)

National Aeronautics & Space Admin.
Manned Spacecraft Center
Houston, Texas 77058
Attn: William R. Dusenbury (EP-5)
W. E. Rice (EP-5)
Forrest E. Eastman (EE-4)

National Aeronautics & Space Admin.
Langley Research Center
Langley Station
Hampton, Virginia 23365
Attn: Harry Ricker (MS 474)

National Aeronautics & Space Admin.
Scientific & Technical Information
Center: Input
P. O. Box 33
College Park, Maryland 20740
(2 copies plus 1 reproducible)

National Aeronautics & Space Admin.
Ames Research Center
Pioneer Project
Moffett Field, California 94035
Attn: Arthur Wilber/A. S. Hertzog

National Aeronautics & Space Admin.
Ames Research Center
Moffett Field, California 94035
Attn: Jon Rubenzer
Code PBS (MS 244-2)

Jet Propulsion Laboratory
4800 Oak Grove Drive
Pasadena, California 91103
Attn: Dr. R. Lutwack (MS 198-220)
A. A. Uchiyama (MS 198-220)
D. Runkle (MS 198-220)

Department of the Army

U. S. Army Mobility Equipment R&D Center
MERDC
Fort Belvoir, Virginia 22060
Electro Technology Lab
Energy Conversion Research Division

Commanding General
U. S. Army Weapons Command
Attn: AMSWE-RDR, Mr. G. Reinsmith
Rock Island Arsenal
Rock Island, Illinois 61201

U. S. Army Research Office
Box CM, Duke Station
Durham, North Carolina 27706
Attn: Dr. Wilhelm Jorgensen

U. S. Army Research Office
Chief, R&D
Department of the Army
3D442, The Pentagon
Washington, D. C. 20546

U. S. Army Natick Laboratories
Clothing and Organic Materials Division
Natick, Massachusetts 01762
Attn: L. A. Spano

Commanding Officer
U. S. Army Electronics R&D Labs
Fort Monmouth, New Jersey 07703
Attn: Power Sources Division
AMSEL-KL-P

Army Materiel Command
Research Division
AMCRD-RSCM-T-7
Washington, D. C. 20315
Attn: John W. Crellin

Army Materiel Command
Development Division
AMCRD-DE-MO-P
Washington, D. C. 20315
Attn: Marshall D. Aiken

U. S. Army TRECOM
Fort Eustis, Virginia 23604
Attn: Leonard M. Bartone (SMOFE-ASE)

U. S. Army Mobility Command
Research Division
Warren, Michigan 48090
Attn: O. Renius (AMSMO-RR)

Harry Diamond Laboratories
Room 300, Building 92
Conn. Ave. & Van Ness St., N.W.
Washington, D. C. 20438
Attn: Nathan Kaplan

Department of the Navy

Office of Naval Research
Arlington, Virginia 22217
Attn: Director, Power Program, Code 473

Office of Naval Research
Department of the Navy
Arlington, Virginia 22217
Attn: H. W. Fox, Code 472

Naval Research Laboratory
4555 Overlook Avenue
Washington, D. C. 20360
Attn: Dr. J. C. White, Code 6160

Naval Ship R&D Center
Annapolis, Maryland 21402
Attn: J. H. Harrison, Code A731
R. J. Bowen, Code A731

Naval Air Systems Command
Department of the Navy
Washington, D. C. 20360
Attn: Code AIR-340C

Commanding Officer
U. S. Naval Ammunition Depot
Crane, Indiana 47522
Attn: D. Miley, Code QEWE

U. S. Naval Observatory
4301 Suitland Road
Suitland, Maryland 20390
Attn: R. E. Trumble, STIC, Bldg. 52

Naval Ordnance Laboratory
Silver Silver Spring, Maryland 20910
Attn: Philip D. Cole, Code 232

Naval Ship Engineering Center
Center Building, Prince Georges Center
Hyattsville, Maryland 20782
Attn: C. F. Viglotti, Code 6157D

Bureau of Naval Weapons
Department of the Navy
Washington, D. C. 20360
Attn: Whitewall T. Beatson, Code RAAE-52

Naval Ship Systems Command
Washington, D. C. 20360
Attn: Bernard B. Rosenbaum, Code 03422

Department of the Air Force

Aero Propulsion Laboratory
Wright-Patterson AFB, Ohio 45433
Attn: James E. Cooper, APIP-1

AF Cambridge Research Lab
Attn: CRFE
L. G. Hanscom Field
Bedford, Massachusetts 01731
Attn: Dr. R. Payne

AF Cambridge Research Lab
L. G. Hanscom Field
Bedford, Massachusetts 01731
Attn: Edward Raskind (Wing F), CREC

Headquarters, U. S. Air Force (AFRDR-AS)
Washington, D. C. 20325
Attn: Major G. Starkey

Headquarters, U. S. Air Force (AFRDR-AS)
Washington, D. C. 20325
Attn: Lt. Col. William G. Alexander

Rome Air Development Center, ESD
Griffis AFB, New York 13440
Attn: Frank J. Mollura (EMRED)

Space Systems Division
Los Angeles Air Force Station
Los Angeles, California 90045
Attn: HQSAMSO
(SMTAE/Lt. R. Ballard)

Other Government Agencies

National Bureau of Standards
Washington, D. C. 20234
Attn: Dr. W. J. Hamer

National Bureau of Standards
Washington, D. C. 20234
Attn: Dr. A. Brenner

Office, Sea Warfare System
The Pentagon
Washington, D. C. 20310
Attn: G. B. Wareham

U. S. Atomic Energy Commission
Auxiliary Power Branch (SNAP)
Division of Reactor Development
Washington, D. C. 20325
Attn: Lt. Col. George H. Ogburn, Jr.

Lt. Col. John H. Anderson
Advanced Space Reactor Branch
Division of Reactor Development
U. S. Atomic Energy Commission
Washington, D. C. 20325

Mr. Donald A. Hoatson
Army Reactors, DRD
U. S. Atomic Energy Commission
Washington, D. C. 20545

Bureau of Mines
4800 Forbes Avenue
Pittsburgh, Pennsylvania 15213
Attn: Dr. Irving Wender

Clearing House for Scientific &
Technical Information
5285 Port Royal Road
Springfield, Virginia 22151

Private Organizations

Aerojet-General Corporation
Chemical Products Division
Azusa, California 91702
Attn: William H. Johnson

Aeronutronic Division of Philco Corp.
Technical Information Services
Ford Road
Newport Beach, California 92663

Aerospace Corporation
P. O. Box 95085
Los Angeles, California 90045
Attn: Library Acquisition Group

Serospace Corporation
Systems Design Division
2350 East El Segundo Boulevard
El Segundo, California 90246
Attn: John G. Krisilas

A.M.F.
Attn: R. J. Mosny/M. S. Mintz
689 Hope Street
Stamford, Connecticut 06907

American University
Mass. & Nebraska Avenue, N.W.
Washington, D. C. 20016
Attn: Dr. R. T. Foley
Chemistry Department

Arthur D. Little, Inc.
Acorn Park
Cambridge, Massachusetts 02140
Attn: Dr. James D. Birkett

Atomics International Division
North American Aviation, Inc.
8900 DeSoto Avenue
Canoga Park, California 91304
Attn: Dr. H. L. Recht

Battelle Memorial Institute
505 King Avenue
Columbus, Ohio 43201
Attn: Dr. C. L. Faust

Bell Laboratories
Murray Hill, New Jersey 07974
Attn: U. B. Thomas/D. O. Feder

The Boeing Company
P. O. Box 3999
Seattle, Washington 98124
Attn: Sid Bross (MS 88-06)

Borden Chemical Company
Central Research Laboratory
P. O. Box 9524
Philadelphia, Pennsylvania 19124

Burgess Battery Company
Foot of Exchange Street
Freeport, Illinois 61032
Attn: M. E. Wilke, Chief Eng.

C & D Batteries
Division of Eltra Corporation
3043 Walton Road
Plymouth Meeting, Pennsylvania 19462
Attn: Dr. Eugene Willihnganz

Calvin College
Science Building
3175 Burton Street, S.E.
Grand Rapids, Michigan 49506
Attn: Prof. T. P. Dirkse

Communications Satellite Corporation
Comsat Labs
P. O. Box 115
Clarksburg, Maryland 20734
Attn: Mr. Robert Strauss

ChemCell Inc.
150 Dey Road
Wayne, New Jersey 07470
Attn: Peter D. Richman

Catalyst Research Corporation
6308 Blair Hill Lane
Baltimore, Maryland 21209
Attn: Mr. F. Tepper

Cubic Corporation
9233 Balboa Avenue
San Diego, California 92123
Attn: Librarian

Delco Remy Division
General Motors Corporation
2401 Columbus Avenue
Anderson, Indiana 46011
Attn: J. A. Keralla

Bellcomm, Inc.
955 Lenfant Plaza North, S.W.
Washington, D. C. 20024
Attn: B. W. Moss

Dynatech Corporation
17 Tudor Street
Cambridge, Massachusetts 02139
Attn: R. L. Wentworth

Eagle-Picher Industries, Inc.
Post Office Box 47
Joplin, Missouri 64801
Attn: E. P. Broglio

ESB Inc.
Post Office Box 11097
Raleigh, North Carolina 27604
Attn: Director of Engineering

Electromite Corporation
2117 South Anne Street
Santa Ana, California 92704
Attn: R. H. Sparks

Energy Research Corporation
15 Durant Avenue
Bethel, Connecticut 06801
Attn: M. Klein

ESB Inc.
Research Center
19 West College Avenue
Post Office Box 336
Yardley, Pennsylvania 19067
Attn: Librarian

Electrochemical & Water Desalination
Technology
13401 Kootenay Drive
Santa Ana, California 92705
Attn: Dr. Carl Berger

Electrochimica Corporation
1140 O'Brien Drive
Menlo Park, California 94025
Attn: Dr. Morris Eisenberg

E. I. DuPont Nemours & Co.
Engineering Materials Laboratory
Wilmington, Delaware 19898
Attn: J. M. Williams, Bldg. 304

Energetics Science, Inc.
4461 Bronx Boulevard
New Yor, NewYork 10470
Attn: Dr. H. G. Oswin

Elgin National Watch Company
107 National Street
Elgin, Illinois 60120
Attn: T. Boswell

Emhart Corporation
Box 1620
Hartford, Connecticut 06102
Attn: Dr. W. P. Cadogan

Engelhard Industries, Inc.
497 Delancy Street
Newark, New Jersey 07105
Attn: Dr. J. G. Cohn

Dr. Arthur Fleischer
466 South Center Street
Orange, New Jersey 07050

General Electric Company
R & D Center
Post Office Box 43
Schenectady, New York 12301
Attn: Dr. R. P. Hamlen

General Electric Company
Space Systems
Post Office Box 8555
Philadelphia, Pennsylvania 19101
Attn: K. L. Hanson, Room M-2700

General Electric Company
Battery Business Section
Post Office Box 114
Gainesville, Florida 32601
Attn: P. R. Voyentzie

General Electric Company
Research & Development Center
Post Office Box 8
Schenectady, New York 12301
Attn: Whitney Library

Dr. P. L. Howard
Centreville, Maryland 21617

General Telephone & Electronics Labs
Bayside, New York 11352
Attn: Dr. Paul Goldberg

Gould Ionics, Inc.
Post Office Box 1377
Canoga Park, California 91304
Attn: Dr. J. E. Oxley

Globe-Union, Inc.
Post Office Box 591
Milwaukee, Wisconsin 53201
Attn: Dr. E. Y. Weissman

General Electric Company
777 - 14th Street, N.W.
Washington, D. C. 20005
Attn: D. F. Schmidt

Gould-National Batteries, Inc.
Engineering & Research Center
2630 University Avenue, S.E.
Minneapolis, Minnesota 55418
Attn: D. L. Douglas

Gulton Industries
Battery & Power Sources Division
212 Durham Avenue
Metuchen, New Jersey 08840
Attn: D. J. Mager

Grumman Aerospace Corporation
OAO Project
Bethpage, Long Island, N. Y. 11714
Attn: S. J. Gaston (Plant 41)

Hughes Aircraft Corporation
Centinda Ave. & Teale Street
Culver City, California 90230
Attn: T. V. Carvey

G. & W. H. Corson, Inc.
Plymouth Meeting, Pennsylvania 19462
Attn: Dr. L. J. Minnick

Hughes Aircraft Corporation
Bldg. 366, M.S. 524
El Segundo, California 90245
Attn: M. E. Ellison

Hughes Research Laboratories Corp.
3011 Malibu, California 90265
Attn: T. M. Hahn

ITT Research Institute
10 West 35th Street
Chicago, Illinois 60616
Attn: Dr. H. T. Francis

Institute for Defense Analyses
R&E Support Division
400 Army-Navy Drive
Arlington, Virginia 22202
Attn: Mr. R. Hamilton

Heliotek
12500 Gladstone Avenue
Sylmar, California 91342
Attn: Dr. H. N. Seiger

Institute for Defense Analyses
R&E Support Division
400 Army-Navy Drive
Arlington, Virginia 22202
Attn: Dr. R. Briceland

International Nickel Company
1000 - 16th Street, N.W.
Washington, D. C. 20036
Attn: N. A. Matthews

Idaho State University
Department of Chemistry
Pocatello, Idaho 83201
Attn: Dr. G. Myron Arcand

John Hopkins University
Applied Physics Laboratory
8621 Georgia Avenue
Silver Spring, Maryland 20910
Attn: Richard E. Evans

Johns-Manville R&E Center
Post Office Box 159
Manville, New Jersey 08835
Attn: J. S. Parkinson

Leesona Moos Laboratories
Lake Success Park, Community Drive
Great Neck, New York 11021
Attn: Dr. A. Moos

Honeywell Inc.
Livingston Electronic Laboratory
Route 309
Montgomeryville, Pennsylvania 18936
Attn: Library

Lockheed Missiles & Space Company
Post Office Box 504
Sunnyvale, California 94088
Attn: R. E. Corbett
Dept. 62-25, Bldg. 157

Life Systems, Inc.
23715 Mercantile Road
Cleveland, Ohio 44122
Attn: Dr. R. A. Wynveen

Lockheed Missiles & Space Company
Department 62-30
3251 Hanover Street
Palo Alto, California 94304
Attn: J. E. Chilton

Lockheed Missiles & Space Company
Technical Information Center
3251 Hanover Street
Palo Alto, California 93404

Mallory Battery Company
South Broadway & Sunnyside Lane
Terrytown, New York 10591
Attn: R. R. Clune

P. R. Mallory & Company, Inc.
Northwest Industrial Park
Burlington, Massachusetts 01803
Attn: Dr. Per Bro

P. R. Mallory & Company, Inc.
Technical Services Laboratory
Indianapolis, Indiana 46206
Attn: A. S. Doty

P. R. Mallory & Company, Inc.
3029 E. Washington Street
Indianapolis, Indiana 46206
Attn: Technical Librarian

Marquardt Corporation
16555 Saticoy Street
Van Nuys, California 91406
Attn: Dr. H. G. Krull

Martin Company
Electronics Research Department
Post Office Box 179
Denver, Colorado 80201
Attn: William B. Collins (MS 1620)
Attn: M. S. Imanura (MS F8845)
J. Leuthard

McDonnell Douglas Astronautics Co.
5301 Bolsa Avenue
Huntington Beach, California 92647
Attn: Dr. G. Moe, Bldg. 11-3-12 (MS 12)
A. D. Tonelli, Bldg. 22 (MS 17)

Melpar
Technical Information Center
7700 Arlington Boulevard
Falls Church, Virginia 22046

North American Rockwell
Autonetics Division
Post Office Box 4181
Anaheim, California 92803
Attn: R. F. Fogle, GF18

Metals and Controls Division
Texas Instruments, Inc.
34 Forrest Street
Attleboro, Massachusetts 02703
Attn: Dr. J. W. Ross

Midwest Research Institute
425 Volker Boulevard
Kansas City, Missouri 64110
Attn: Physical Science Laboratory

North American Aviation, Inc.
12214 Lakewood Boulevard
Downey, California 90241
Attn: Burton M. Otzinger

North American Aviation, Inc.
Rocketdyne Division
6633 Canoga Avenue
Canoga Park, California 91304
Attn: Library

North American Aviation Co.
S&ID Division
Downey, California 90241
Attn: Dr. James Nash

Oklahoma State University
Stillwater, Oklahoma 74075
Attn: Prof. William L. Hughes
School of Electrical Engineering

Power Information Center
University City Science Institute
3401 Market St., Rm. 2107
Philadelphia, Pennsylvania 19104

Prime Battery Corporation
15600 Cornet Street
Santa Fe Springs, Calif., 90670
Attn: David Roller

Portable Power Sources Corp.
166 Pennsylvania Avenue
Mount Vernon, New York 10552
Attn: L. Schulman

RAI Research Corporation
225 Marcus Boulevard
Hauppauge, L.I., New York 11787

Philco Corporation
Division of the Ford Motor Company
Blue Bell, Pennsylvania 19422
Attn: Dr. Phillip Colet

Philco-Ford Corporation
Power & Control Eng. Dept, MS R26
3939 Fabian Way
Palo Alto, California 94303
Attn: Mr. D. C. Briggs

Radio Corporation of America
415 South Fifth Street
Harrison, New Jersey 07029
Attn: Dr. G. S. Lozier
Bldg. 18-2

Southwest Research Institute
P. O. Drawer 28510
San Antonio, Texas 78228
Attn: Library

Sonotone Corporation
Saw Mill River Road
Elmsford, New York 10523
Attn: A. Mundel

Thomas A. Edison Research Laboratory
McGraw Edison Company
Watchung Avenue
West Orange, New Jersey 07052
Attn: Dr. P. F. Greiger

Texas Instruments, Inc.
P. O. Box 5936
Dallas, Texas 75222
Attn: Dr. Isaac Trachtenberg

Stanford Research Institute
19722 Jamboree Boulevard
Irvine, California 92664
Attn: Dr. F. R. Kalhammer

TRW Systems, Inc.
One Space Park
Redondo Beach, California 90278
Attn: Dr. Herbert P. Silverman (R-1/2094)
Dr. W. R. Scott (M-2/2154)

TRW, Inc.
23555 Euclid Avenue
Cleveland, Ohio 44117
Attn: Librarian (TIM 3417)

Tyco Laboratories, Inc.
Bear Hill
Hickory Drive
Waltham, Massachusetts 02154
Attn: Dr. Jose Giner

Unified Sciences Associates, Inc.
2925 E. Foothill Boulevard
Pasadena, California 91107
Attn: Dr. S. Naiditch

Union Carbide Corporation
Development Laboratory Library
P. O. Box 6056
Cleveland, Ohio 44101

Union Carbide Corporation
Parma Laboratory
Post Office Box 6116
Parma, Ohio 44130
Attn: Dr. Robert Powers

University of California
Space Science Laboratory
Berkeley, California 94720
Attn: Dr. C. W. Tobias

University of Pennsylvania
Electrochemistry Laboratory
Philadelphia, Pennsylvania 19104
Attn: Prof. John O M. Bockris

University of Toledo
Toledo, Ohio 43606
Attn: Dr. Albertine Krohn

Westinghouse Electric Corporation
Research and Development Center
Churchill Borough
Pittsburgh, Pennsylvania 15235
Attn: Dr. C. C. Hein/Dr. A. Langer

Whitakker Corporation
3850 Olive Street
Denver, Colorado 80207
Attn: L. K. White

Yardney Electric Corporation
82 Mechanic Street
Pawcatuck, Connecticut 02891
Attn: Director of Engineering